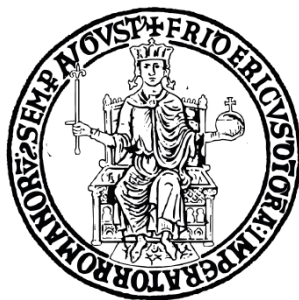


UNIVERSITÀ DEGLI STUDI DI NAPOLI FEDERICO II

Scuola Politecnica e delle Scienze di Base

Dipartimento di Ingegneria Chimica, dei Materiali e dei Prodotti Industriali

XXXIII° Ciclo del Dottorato in Ingegneria dei Prodotti e dei Processi Industriali



## **SMART PROCESS MONITORING OF MACHINING OPERATIONS**

Coordinatore:

Prof. Ing. Andrea D'ANNA

Candidato:

Ing. Salvatore CONTE

Tutors:

Prof.ssa Ing. Dorian M. D'ADDONA

Prof. Ing. Roberto TETI

ANNO ACCADEMICO 2020 / 2021

## INDEX

1. INTRODUCTION	pag. 1
2. STATE OF THE ART	pag. 4
2.1. Industry 4.0	pag. 8
2.2. Sensor Monitoring in Manufacturing	pag. 11
2.3. Optimization Processing in Manufacturing	pag. 15
2.4. Decision-Making in Manufacturing via AI	pag. 19
3. ARTIFICIAL INTELLIGENCE TECHNIQUES	pag. 24
3.1. Neural Network	pag. 28
3.1.1. Supervised and Unsupervised Neural Network	pag. 36
3.1.2. Backpropagation Algorithm	pag. 39
3.1.3. Self-Organizing Map (SOM)	pag. 41
3.2. Bees Algorithm	pag. 44
4. ACTIVITY ON GRINDING OPERATIONS	pag. 51
4.1. Tool Condition Monitoring via Acoustic Emission	pag. 55
4.1.1. Case study	pag. 55
4.1.2. Neural Network Models (Supervised)	pag. 62
4.2. Tool Condition Monitoring via Impedance	pag. 70
4.2.1. Case study n°1	pag. 71
4.2.2. Neural Network Models for case study n°1 (Supervised)	pag. 73
4.2.3. Case study n°2	pag. 75
4.2.4. Neural Network Models for case study n°2 (Unsupervised)	pag. 78
5. ACTIVITY ON CUTTING TESTS	pag. 81
5.1. Image analysis via Bees Algorithm	pag. 83
6. CONCLUSIONS	pag. 92
7. REFERENCES	pag. 96

# 1. INTRODUCTION

The world has experienced exponential growth in digitalisation and connectivity over the last twenty years. Many sectors have begun this process of change, including manufacturing. This evolution is often known as Industry 4.0 [1]. The fourth industrial revolution is a reality now. The first revolution began in the steam engine days, then came electricity, while the third industrial revolution is characterised by the entry of computers into the industrial world. The fourth revolution is the process that uses network technologies to enable communication between machines. The world has moved from a mass-market to mass customisation, which is only possible thanks to increased automation. From this market demand, the solution found to increase product customisation speed is communication between machines and remote control of the system.

Key Enabling Technologies (KETs) play a key role in Industry 4.0. The European Commission defines them as: *"knowledge intensive and associated with high R&D intensity, rapid innovation cycles, high capital expenditure and highly skilled employment. They enable process, goods and service innovation throughout the economy and are of systemic relevance. They are multidisciplinary, cutting across many technology areas with a trend towards convergence and integration. KETs can assist technology leaders in other fields to capitalise on their research efforts"* [2].

Therefore, they have the function of creating agile, fast processes that offer the possibility of seizing opportunities quickly, promoting growth through targeted and consequent actions and, last but not least, 'enabling' the skills and competences of users by making them evolve. Bearing in mind the exponential growth that technology is experiencing, it is not easy to compile a satisfactory list over time [3]. One possible list is as follows:

- Advanced Manufacturing, such as Collaborative Robotics and Mechatronics, which collaborate with people with whom they share spaces to pursue common goals, these technologies can recognise human presence and dialogue both machine to machine and machine to human, they are also easily reprogrammable [4].
- Additive Manufacturing, as the 3D printer can now printed many finished products, consists of using digital designs that allow the creation of three-dimensional objects thanks to the use of layered materials. This technology is beneficial when complicated and expensive products have to be made with one or more materials, obtaining a unique and ready-to-use product [5].

- Augmented reality consists of extending reality with virtual reality by making a great deal of additional information accessible when needed. Therefore, this technology superimposes virtual reality on physical reality [6].
- Rapid prototyping allows the simulation of a designed object or service, which is iteratively implementable, making it easier and faster over time. This helps to generate a competitive advantage over time. It, therefore, makes it possible to anticipate the market, which is increasingly fast-paced and turbulent [7].
- Internet of Things (IoT) is an orchestration of tools, data collection and industrial processes. Therefore, it consists of inserting measurement sensors into industrial processes that enable the collection of data, to be analysed and normalised, to perform actions that will generate new business models in terms of margins or business cases [8].
- Cloud computing, has the role of enabling other technologies and makes available and usable services and software. Such as buying licences on a per-user, per-use or per-time basis. It also makes it possible to store collected data without having to use corporate hardware [9].
- Cybersecurity is a technology that protects the company from cyber-attacks on the data it stores, such as personal data or intellectual property [10].
- Big Data has the role of processing all the data collected in a distributed way on different machines. These processes must manage the enormous amount of data produced at other points of contact, classify the different variety of data, both structured and unstructured, and finally deal with the flow of data at speed with analytical capabilities that allow a specific competitive advantage [11].
- Artificial Intelligence, refers to the design of algorithms that allow the machine to learn and support production by generating self-learning feedback, allowing it to intervene in a predictive manner. Predicting the future concerning information already known is strategic to anticipate malfunctions or sudden and reliable actions [12].

Artificial intelligence certainly plays an essential role among the enabling technologies of Industry 4.0. Today, Artificial Intelligence is much more than a promise; in fact, it is entering factories in a very overbearing way. Starting from the information contained within our data that can be collected, Artificial Intelligence allows this information to be fed into applications that support or complement humans to improve their processes, whether they are quality or production processes [13].

A concept at the heart of Artificial Intelligence is Machine Learning. Machine Learning works like this: I do not know the relationship between input and output, and the algorithm finds this relationship. To make a simple analogy, think of how a child learns how to walk. The child learns by acquiring as input the images of its parents walking. The function is unknown to the child, but its neural network allows it to understand how to apply it to obtain the desired output: walking. This reasoning is

applicable to any mathematical function. For example, if I have as input 2, 3, 4, 5, and as output 4, 9, 16, 25, our brain recognises the function that regulates input and output: Exponentiation. The name of this type of learning is Supervised Learning. The name derives from the fact that the algorithm has as elements to solve the input and output data, so the supervising of the algorithm is the output results. In the case in which input and output are continuous data, belonging to a linear function, the problem is classifiable as "regression". If input and output are discrete, it speaks of "classification" problems. Thanks to this type of solution, it is possible to predict or recognise specific characteristics of a problem. In this case, it is talking about the optimisation of processes with chip removal as a characteristic. Each technique is best suited to the type of problem.

For this reason, different algorithms are useful depending on the problem. This thesis's objective is to explore the applications of artificial intelligence in the world of manufacturing. Therefore, there will be many bibliographical references for new research in this area. The thesis will explore the prediction and classification potential of supervised and unsupervised artificial neural networks. In particular, I will apply and implement neural networks with the best characteristics to understand dressing processes' performance for abrasive wheels. These tests aim to study sensory monitoring and understand the effectiveness of monitoring by the sensor system used. The same objective is the aim of the second part of the thesis, where it will show the innovative possibility of the Bees Algorithm to classify and measure wear in orthogonal cutting operations. Returning to the beginning of this introduction, this research is in line with the context of Industry 4.0.

The ability to intelligently control processing is the short-term goal of the manufacturing industry. The following thesis work addresses these issues by focusing on processes involving the removal of excess material. The optimisation of machining is fundamental because there are many benefits: reduction of costs [14], reduction of waste and consequent reduction of environmental impact [15–17], increase in tool life [18–20], qualitatively superior end products [21–23]. The optimisation process is not only limited to a change in process parameters but also to a system that allows decisions to be taken more quickly. Automatic decision-making is the ultimate goal of most technologies used to optimise processes.

## 2. STATE OF THE ART

The world of industry has undergone profound changes over the last 15 years. The advent of new digital technologies and the growing demand for remote control of production activities has led to a change in the concept of industry and enterprise. At the same time, the manufacturing sector has also been involved in this process of change. Sites that only deal with individual specifications of the producible parts are often responsible of the production. Other sites take care of the quality control, others of the assembly, not forgetting the administrative offices of a company. In the course of this chapter, it will address the journey into the changing industry and manufacturing world. In particular, it will focus on some aspects of this process. Scientific production on the topics mentioned will be under the magnifying glass. Specifically, it will try to understand which the tools make possible the remote control in manufacturing processes. Sensory monitoring will then be the subject of study with the latest work on the subject and a bit of history related to scientific production. Afterwards, the focus will be on the optimisation of manufacturing processes. The final objective will be to talk about scientific production linked to automatic decision making thanks to the support of artificial intelligence. The next step is to talk about the methods that have led to that context and that allow control. The data acquired by the analysed method are then destined to an analysis that will lead to the best choice based on the results of the optimisation by artificial intelligence techniques. The logical path is the one just illustrated, and it utilizes a careful and detailed bibliometric analysis of the various topics. The first step in this sense is the bibliometric study related to Industry 4.0. In the specifically sub-paragraph dedicated to this topic there will be a discussion related to it.

The research work related to Industry 4.0 is 11'991 on the indexed Scopus database. The time is 2012-2021. In the works mentioned, there are, therefore "in the press" works. The distribution of works over the period is visible in Table 1 and Fig. 1. The trend is exponential with an apparent increase in production in recent years. The countries that produced the most documents are Germany (17%), Italy (11%) and the United States (6%), as shown in Table 2 and Fig. 2. As can be seen in the next paragraph, it is easy to understand the primacy of Germany. As far as the area of interest of the works related to Industry 4.0 is concerned, the area where there are more documents is Engineering (27%), followed by Computer Science (26%). Table 3 and Fig. 3 show the results of this aspect.

Table 1. Number of documents related to “Industry 4.0” per year [source: SCOPUS]

Year	Documents
2012	2
2013	31
2014	93
2015	208
2016	547
2017	1154
2018	2144
2019	4385
2020	3312
2021	115

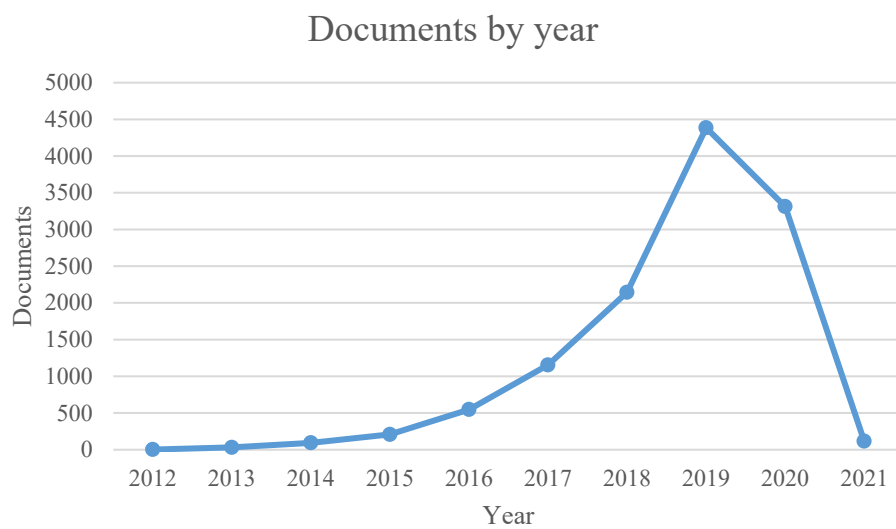


Fig. 1 - Trend in scientific production related to “Industry 4.0” in the period 2012-2021 [source: SCOPUS]

Table 2. Number of documents related to “Industry 4.0” per country [source: SCOPUS]

Country	Documents
Germany	2002
Italy	1295
United States	748
China	745
United Kingdom	626
Spain	536
Russian Federation	505
India	466
Brazil	424
Indonesia	399
France	390
Portugal	360
Austria	338
Poland	317
Czech Republic	245
Other	2595

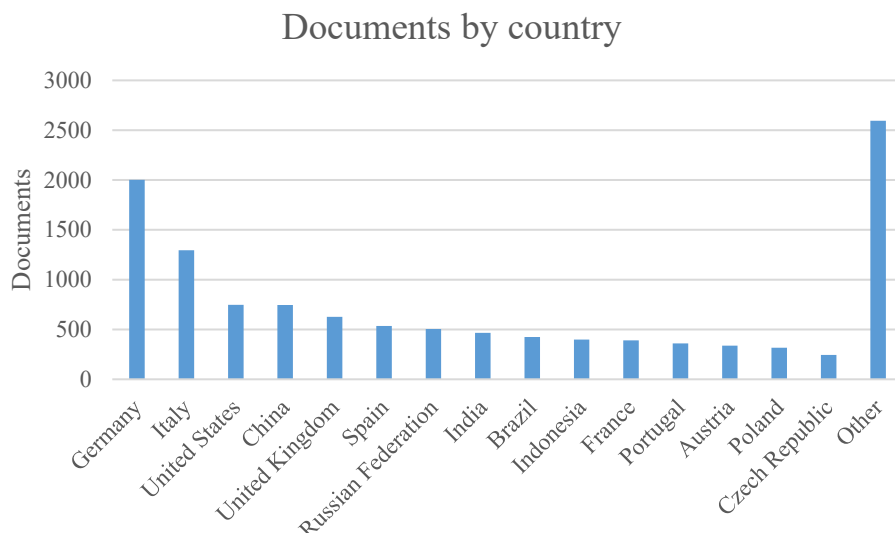


Fig. 2 - Histogram of scientific production linked to “Industry 4.0” related to the various countries [source: SCOPUS]

Table 3. Number of documents related to “Industry 4.0” per subject area [source: SCOPUS]

Subject area	Documents
Engineering	7085
Computer Science	6666
Business, Management and Accounting	1806
Decision Sciences	1709
Mathematics	1622
Physics and Astronomy	1330
Social Sciences	1102
Materials Science	1094
Energy	789
Environmental Science	566
Chemical Engineering	454
Economics, Econometrics and Finance	408
Medicine	286
Chemistry	270
Earth and Planetary Sciences	240
Agricultural and Biological Sciences	156
Biochemistry, Genetics and Molecular Biology	145
Arts and Humanities	109
Psychology	71
Multidisciplinary	26
Pharmacology, Toxicology and Pharmaceutics	25
Health Professions	19
Neuroscience	11
Immunology and Microbiology	7
Nursing	4



## Documents by subject area

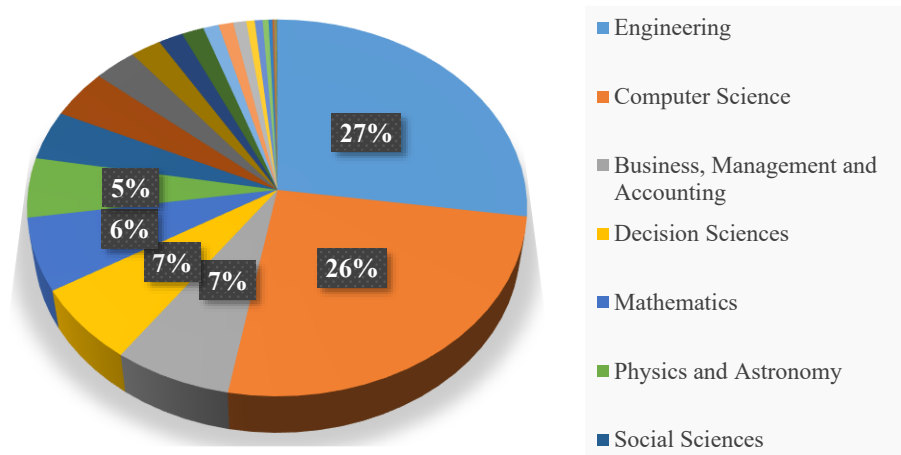


Fig. 3 - Pie chart showing the percentages of scientific work related to Industry 4.0 in the various subject areas  
[source: SCOPUS]

## 2.1. INDUSTRY 4.0

In the beginning of 2010s, the German manufacturing industry must respond to the pressures caused by intense global competition on product quality and production costs. Labour costs are high, and industries have experienced a period of suffering due to the relocation of production facilities to other states. Manufacturing companies have, therefore become virtual places where companies have combined all their key competencies. The virtualisation of the production process has ensured rapid operations between companies and provided real-time access to product and production information. This process of company relocation is known as Industry 4.0 [24].

The Industry 4.0 concept introduces new development and service concepts under the banner of a digital transformation, thanks to a technological mix of automation, information, connection and programming that are leading to a change in technological and cultural paradigms involving the manufacturing system in all its forms.

The suffix 4.0 corresponds to the stages of an exact evolution. The transition to the fourth industrial revolution is taking companies towards a new dimension called bimodal because it made up of an ecosystem of physical and virtual resources. Industry 4.0 in recent years has also become a new dimension of communication and business, just as digital transformation is progressively changing customs and habits, triggering a cultural revolution on a global scale [1].

The historical analysis of the industrial evolution (Fig. 4) that follows will provide a better understanding of how it has come to this point, not only in Germany but also throughout the industrial world.

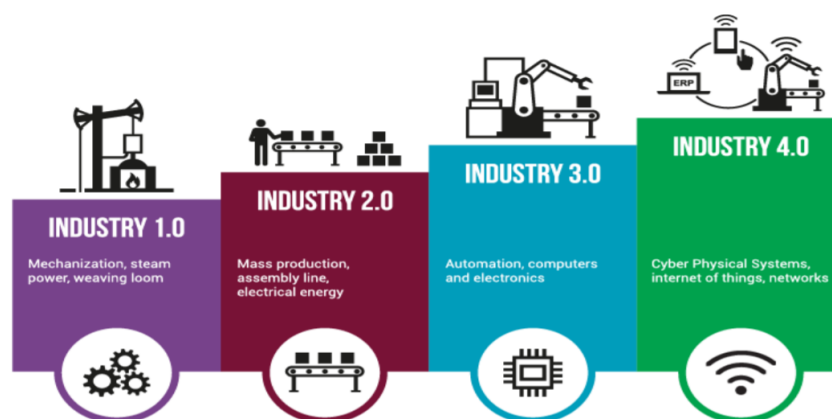


Fig. 4 - Industry Evolution [25]

*Industry 1.0* (1784) corresponds to a revolution in manufacturing concerning the use of energy: the invention of the steam engine allows factories to abandon mills and introduce mechanisation of production in the name of more incredible speed and power [1].

*Industry 2.0 (1870)* represents the second generation of energy, linked to the use of electricity first and then of oil, which allows increasing the levels of mechanisation and production further. It is thanks to this renewed power that the assembly line that inaugurates the era of mass production is progressively established in manufacturing [1].

*Industry 3.0 (1970)* sums up the entry of the first-generation ICT into the factory: IT and electronics further increased levels of automation not only in the production field but also (and above all) organisation. Infrastructures are diversified, and new processes are launched which, under the banner of progressive digitalisation, diversify and facilitate people's work by improving the quality of production [1].

*Industry 4.0 (2011)* represents a new revolution in the way of manufacturing products and organising work. How? Thanks to new production models that are increasingly automated and interconnected, intelligent and communicating assets and products, traceability and traceability of processes leading to a collective, shared and collaborative information management at the supply chain level, new service logics under the banner of cloud and mobility. All this is connectable on the latest generation Internet (Industrial Internet), capable of bringing in and out of factories more information, more integration, more interaction and more efficiency renewing processes and systems but also bringing new rules of communication and service. New generation software on the one hand and Big Data Management on the other, this is how production manages to achieve mass customisation. The continuous evolution of technologies is diversifying the 4.0 declination on several levels and operational areas associated with the use of Artificial Intelligence and all the digital drifts, Blockchain included [1].

A working group used the term Industry 4.0 for the first time in 2011 at the Hannover Trade Fair in Germany. The term indicates a project hypothesis and it included a set of recommendations for the implementation of the Industry Plan 4.0 to the German Federal Government in 2012. The name is a new term that has given the start to a reinterpretation of our technological history [1]. The German Federal Government's idea was to refer to the current trend towards intelligent products and production processes. Associated with the term Industry 4.0 are other keywords such as “Fourth Industrial Revolution”, “Intelligent Factory”, “Smart Factory”, “Internet of Things (IoT)” and, indeed, “Cyber-Physical System (CPS)”. The transition to Industry 4.0 has, therefore become a priority for many professionals and researchers. It is changing industries by promoting communication and integration of industrial information [26]. The importance of this industrial revolution is such that it has economic, social and ecological repercussions [27–29].

When it comes to Smart Industry, it proposed to divide technology clusters into three levels:

- **SMART PRODUCTION:** new production technologies create interaction between all production-related assets, fostering collaboration between people, machines and systems.
- **SMART SERVICES:** new generation governance of IT and technical infrastructures helps to manage and oversee systems, exploiting the logic of maximum integration between all players in the supply chain, including customers.
- **SMART ENERGY:** new power supply systems and a focus on monitoring energy consumption make infrastructures more efficient, cheaper and more ecological [1].

Modern digital engineering techniques made possible the virtualisation of the production process of industrial realities. Of fundamental importance is the use of Cyber-Physical-Systems, systems capable of interacting continuously with the physical system in which they operate [30,31]. This type of advanced communication between the machines has replaced the dialogue between the workers [24].

Industry 4.0 promotes the idea of unsupervised factories and global involvement with a dense network of links between companies around the globe through supply chains and sensor networks. Another objective of Industry 4.0 is to overcome the problem of national product demand. Many companies produce parts that have no market at home but are in demand abroad. The idea of being able to transfer their products, both physical and IT, abroad is one of the cornerstones of the fourth industrial revolution. An example could be the 3D printing technology that leads to an unlimited design for spare parts systems. The success of Industry 4.0 lies precisely in the possibility of data sharing and analysis using new, more effective methods [1,32–34].

Industry 4.0 is not only a process of industrial transformation but also a process of change in our society. Economy, education, commerce and many other aspects of our society will be involved in this change. Nevertheless, the industry remains the protagonist of this change. Several large players, particularly in terms of production facilities, dominate the market. Nevertheless, thousands of production plants from all over the world are interested in working together to produce products, in line with the Industry 4.0 philosophy [32].

## 2.2. SENSOR MONITORING IN MANUFACTURING

Industry 4.0 is the industrial revolution based on remote control and decentralisation of the production process [1]. The control of manufacturing processes in real-time is fundamental for remote control. The objective to realize can only be achievable through a system that provides real-time production or processing conditions. Sensor systems assume a crucial role in machining processes [35–37]. This section focused on the study of sensor monitoring.

In the scientific literature, you can find articles dating back to the 60s and 70s dealing with the topic of sensory monitoring. To be more precise in these works, it talks about the use of sensors to monitor the progress of processes [38–42]. The technologies are not the same as they are today, but the progress of research would then focus on these aspects. Fig. 5 shows the progress of research in this sector. In the period from the 1980s to 30th October 2020, there are 26'689 published documents on the subject. While until the 2000s, on average, products were around 200 units per year, since 2000, there has been a marked increase in production, particularly since 2014, following the development of Industry 4.0. The influence of Industry 4.0 on this sector is obvious by analysing scientific production divided by country. If the United States of America and China are in the lead with production percentages of 22.3% and 21.4% respectively, it is not surprising to see Germany in the third position with 9.3% of all scientific production related to sensor monitoring in the manufacturing world. In Fig. 6, it is possible to see scientific production by country. Scopus is the source for this analysis. The documents considered are various: scientific articles, conference proceedings, books, contributions in book chapters.

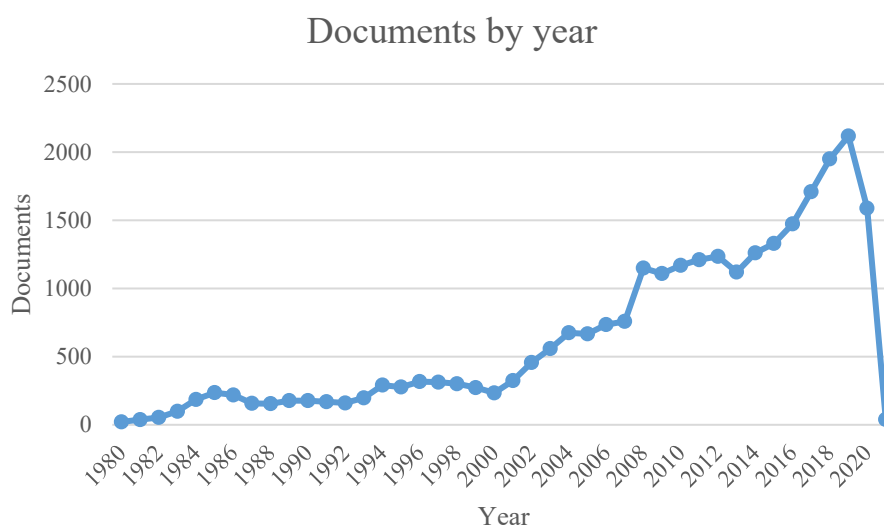


Fig. 5 - Trend in scientific production related to “Sensor Monitoring in Manufacturing” in the period 1980-2021  
 [source: SCOPUS]

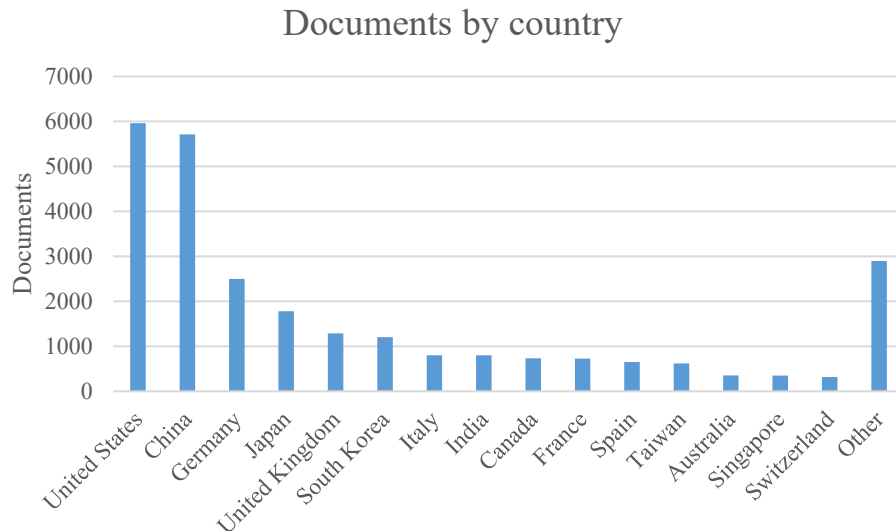


Fig. 6 - Histogram of scientific production linked to “Sensor Monitoring in Manufacturing” related to the various countries [source: SCOPUS]

Table 4. Number of documents related to “Sensor Monitoring in Manufacturing” per country [source: SCOPUS]

Country	Documents
United States	5959
China	5712
Germany	2500
Japan	1778
United Kingdom	1290
South Korea	1203
Italy	802
Other	7445

In cognitive science, sensory perception is the process of obtaining knowledge or understanding of sensory information. This work is much more complicated than was imagined in the 1950s. At that time, people predicted that it would take about ten years to build a sensory machine. This goal is still far from being achieved. The passive perception was initially developed by R. Descartes [35]. However, now this is a theory that has largely lost its momentum. The theory of active perception stems from extensive research into a misunderstanding of the senses. The most surprising is the work of Gregory [43,44]. This theory, experiments increasingly supported it, can be thought of as describing (in the brain) the "dynamic" relationship between senses the surrounding environment, all of which conform to the linear concept of experience. For more information on the impact of active perception theory on science and technology, see [45]. Traditionally, there are two methods related to the measurement techniques in monitor machining operations: direct methods and indirect methods. In the direct method, the actual number of variables, such as measuring tool wear. In this case, examples of direct measurement are visual inspection using cameras, radioisotopes, laser beams

Ing. Salvatore Conte

and resistance. Many direct methods can only be used as laboratory techniques [35,37]. This is mainly due to practical limitations caused by contact problems during machining, lighting and the use of cutting fluids. However, direct measurement has high accuracy. It has been widely used in research laboratories to support the study of basic measurable phenomena in the machining process. Indirect measurement methods permit the measurement of auxiliary quantities such as cutting force components. The actual number come from empirically determined correlations. The indirect method is less accurate than the direct method, but it is also less complicated and more suitable for practical applications. Contrary to traditional tool status detection, this method continuously monitors the processing process through sensing equipment to quantify process performance or use sensors to provide information for process optimization. Fig. 7 summarizes the commonly used sensors in online measurement [35].

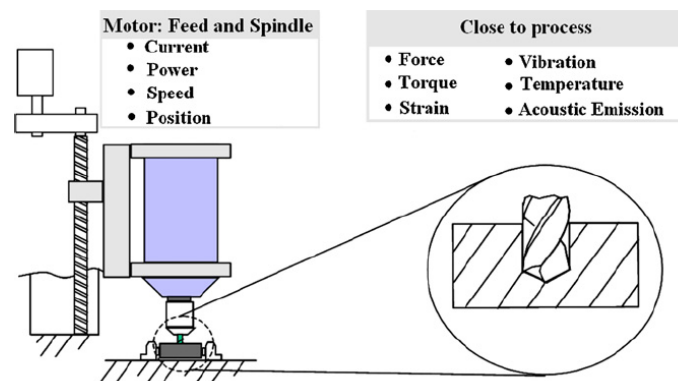


Fig. 7 - Measurable phenomena for online sensor monitoring [35]

The development of intelligent monitoring programs can significantly increase productivity and reduce tool costs, and optimize tool life by implementing a condition-based tool replacement strategy (i.e., replace tools only when the service life is approaching). Instead of a conservative time-based tool replacement strategy (replace the tool after a predetermined time, regardless of the actual wear of the tool), they can help reduce the risk of damage to the machine and workpiece by responding quickly when there is a damage on the tool. From the perspective of zero-defect manufacturing, this will help improve the performance of the manufacturing process and support the reliable automation of the manufacturing system through intelligent system adaptation [46,47]. Axinte and Gindy [48] tried to correlate the working conditions of the broaching machine with the output signals of multiple sensors: AE, vibration, cutting force and broaching machine hydraulic pressure. In [49], they evaluated the use of the TCM spindle power signal in milling, drilling and turning. This method is successful for continuous drilling and turning, but shows lower sensitivity for discontinuous milling. Teti and Baciú [50] applied an intelligent monitoring system based on audible sound energy to identify the status of tools in the process of aluminium alloy and mild steel band saws. Lee et al. [51]

Ing. Salvatore Conte

proposed a real-time tool breakage monitoring system for milling, which is based on the measurement of the cutting force indirectly measured by the feed drive AC motor current, and its sensitivity is sufficient to identify tool breakage. Ryabov et al. [52] developed online tool geometry measurement system based on laser displacement meter. Lee and Kim et al. [53] established a vision system to detect small diameter tap breaks, and this indirect process monitoring method can hardly detect small diameter tap breaks, such as AE, torque and motor current. In [54], they proposed an online drill bit wear estimation method based on the spindle motor power signal during drilling. In [55], Gandarias et al. analyzed and compared cost-effective tool breakage detection methods by conducting experiments on an ultra-precision micro-milling machine. Govekar et al. [56] use the filtered AE spectral components to classify the chip format. Teti et al. [57] applied the spectrum estimation of WPT and cutting force signals to chip form recognition. Venuvinod et al. [58] use various sensors to obtain stable chip morphology clusters under changing dry cutting conditions through a geometric transformation of control variables: they are designed to identify chip entanglement, chip size (including continuity) and chip shape. Andreasen and De Chiffre [59] developed and tested a laboratory system that automatically detects chip breaking through frequency analysis of cutting forces. Azouzi and Guillot [60] used cutting parameters and two cutting force components to estimate surface finish and dimensional deviation online. Chen et al. [61] used statistical methods to correlate surface roughness and cutting force in face milling operations. Abouelatta and Madl [62] developed a turning surface roughness prediction method based on cutting parameters and tool vibration FFT analysis. Salgado et al. [63] use singular spectrum analysis to decompose vibration signals in order to predict surface roughness during processing. Axinte et al. [64] tried to establish a correlation between the processed surface quality, geometric accuracy, burr formation, chatter marks and surface abnormalities after broaching, and the output signals of multiple sensors (AE, vibration, cutting force). The former is effective in detecting slight surface abnormalities such as plucking, laps and smudges. Kwak and Song [65] used AE signal analysis to identify grinding burns during cylindrical plunge grinding. Zhou et al. [66] introduced a systematic approach to design and implement an integrated intelligent monitoring system with a modular and reconfigurable structure to monitor power, vibration, temperature, and drive and spindle pressure for condition monitoring in flexible manufacturing units, Fault diagnosis and maintenance plan. The development and growth of precision machining applications to a wide field of mechanical products (from medical devices to automotive drivetrain, power systems and aerospace) due to the demand for higher performance, better energy-efficient and more complex products have pushed the “commercialization” of precision machining. This requires highly reproducible processes despite work material properties variability, tool wear, thermal distortion, etc., and has called for the increased use of sensors in precision machining [35].



## 2.3. OPTIMIZATION PROCESSING IN MANUFACTURING

The optimization of manufacturing processes is an important topic. Optimizing processes means improving product quality, reducing production time, reducing costs, reducing environmental impact. These reasons have led to a very consistent scientific production. From the Scopus database, considering the time interval 1980-2021, 54'757 documents are counted among scientific articles, conference proceedings, reviews, books, book chapters. Fig. 8 shows the trend of scientific production. As in the case of scientific production related to "sensor monitoring", the impact of Industry 4.0 is visible on the curve shown in Fig. 8. In fact, from 2014 there is a sharp increase in production.

Fig. 9 instead shows the scientific production divided by nations. Table 5 have the data for the realization of the histogram of Fig. 9. The country with more outstanding scientific production is China with 26.2%. China is before the United States, with 16.7% of global production, while India is in third position with 8.8%.

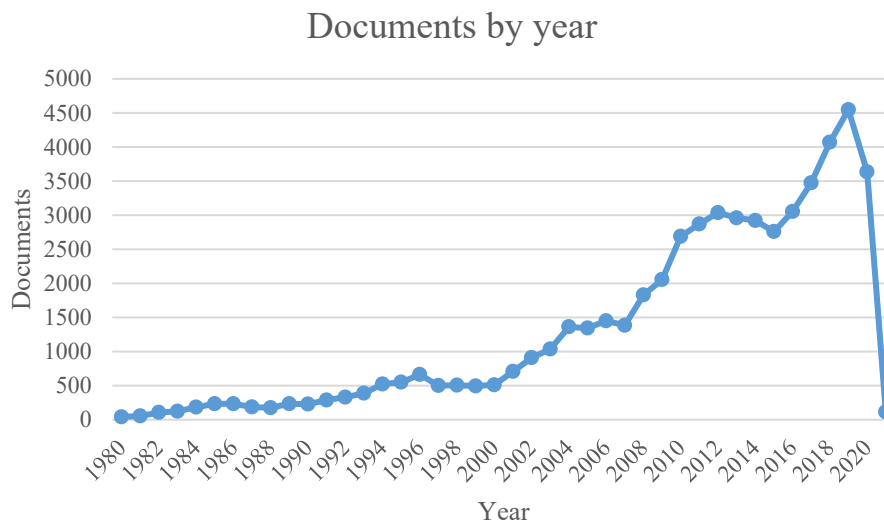


Fig. 8 - Trend in scientific production related to “Optimization process in Manufacturing” in the period 1980-2021

[source: SCOPUS]

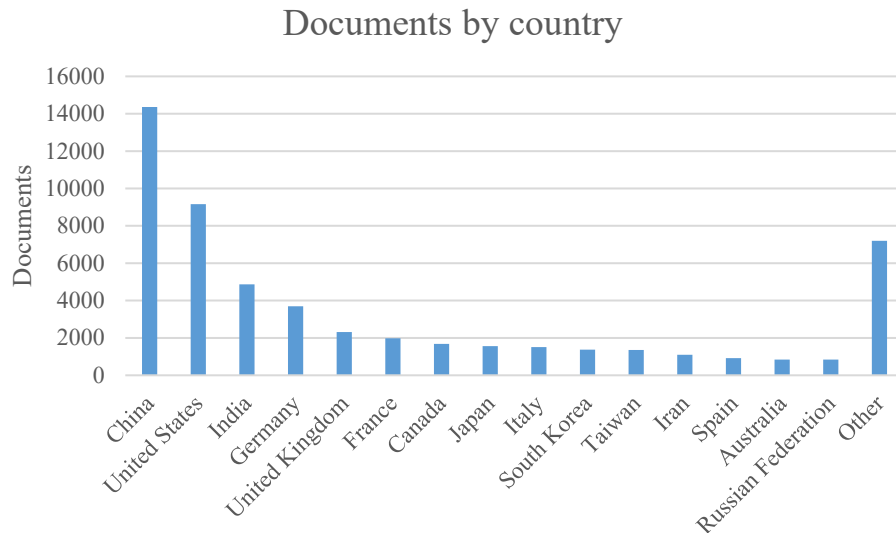


Fig. 9 - Histogram of scientific production linked to “Optimization process in Manufacturing” related to the various countries [source: SCOPUS]

Table 5. Number of documents related to “Optimization process in Manufacturing” per country [source: SCOPUS]

Country	Documents
China	14362
United States	9163
India	4864
Germany	3698
United Kingdom	2316
France	1980
Canada	1685
Other	16689

The focus of production optimization is increasingly shifting from mass production to mass customization. Due to competitive business conditions, production planning and scheduling of this production system are critical [67]. Short production time for orders, high reliability of delivery time, low inventory, high flexibility [68] and right cost-time conditions are associated with manufacturing value streams [69]. They are becoming key production goals, which can be achieved mainly through appropriate multi-object production optimization [67,70].

The introduction of modern technology with the support of the Industry 4.0 concept has changed things [71]. The production process requires complex, innovative and revolutionary solutions to new challenges, especially in the field of multi-object production optimization [67]. Method and algorithm of production system optimization as a user manual introduces the design of production facilities [72]. Application solutions can realize the basic ideas of theory, algorithm and system support [73]. Researchers have proposed various methods for performance analysis of production systems, based on the algorithms and methods used to evaluate the production system optimization [74].

In the Industry 4.0 environment, more and more product customization require these systems to handle a more significant number of product variants and smaller batches. Therefore, manufacturing systems are becoming more and more complex to deal with these uncertain situations [68].

Using a dedicated production system to process parts has been and will continue to be a viable manufacturing method. However, in some cases, this type of system is not feasible due to changes in product types, customer requirements, workpiece materials or design specifications. In a highly competitive manufacturing environment, choosing a production system is a crucial issue for all component-manufacturing companies. Improper selection may negatively affect the overall performance of the manufacturing system, such as productivity, cost and quality of manufactured components [75].

Performance evaluation permits to measure the impact of requirements or product design changes or design changes on the behaviour of the manufacturing system. The motivation behind performance evaluation is to analyse and compare different manufacturing systems or implement strategic decisions to improve the performance of manufacturing systems. Before evaluating system performance, a set of performance indicators must be selected. There are two basic categories to indicate manufacturing indicators:

- Production performance indicators;
- Manufacturing costs.

Indicators that indicate production performance include productivity (throughput), factory capacity, equipment uptime ratio and manufacturing lead-time. High manufacturing costs for a company include labour and material costs, the cost of producing products, and the cost of operating a piece of given equipment [75].

Hon [76] introduced five general indicators for performance evaluation, namely time, cost, quality, flexibility and productivity. Time measurement: average batch time, average delivery time, conversion time, cycle time, machine downtime, average turnover time, delivery on time, settings Time, beat time, throughput time. Cost measurement: indirect cost, scrap cost, installation cost, tooling cost, total quality cost, unit labour cost, unit manufacturing cost, unit material cost and construction in progress.

Data collection permits to measure performance in existing systems. Analysis or computer simulation models allow the process of evaluating the system in the design phase or evaluating system performance due to policy changes. For many years, many companies have been using simulation to aid their decision-making process. An evaluation model is a model used to estimate the performance of a manufacturing system for a given set of decisions and system parameters. These models are based

on stochastic processes, probability and simulation model techniques made a significant contribution to the modelling and analysis of the production line [75].

Jain and Smith [77] used an extended method to evaluate the performance indicators of similar sites on the production line. In their paper, concatenation, merge and split topologies are studied. Patchong and Willaeyts [78] is another paper that has attracted widespread attention, in which each parallel machine is replaced by an equivalent single machine at each station on the production line. Then, existing methods can derive the performance indicators of the original system. Cao and Ho [79] realized the disturbance analysis method of the discrete event dynamic system based on only one sample trajectory of the system, which was used to estimate the system throughput. In that study, the manufacturing system consists of a set of serial single workstations with limited storage capacity. This analysis is limited to infinite perturbations and does not work with the changes in discrete parameters (such as buffer size).

The other aspect of process optimization is energy reduction and sustainability of the manufacturing world. The new challenge of sustainable processing is to use the triple bottom line framework [80] to achieve overall sustainable structuring, simplification and reduction of complexity; this strategy may be an opportunity for continuous improvement to move manufacturing towards excellence. This means that as a core competitive concept, sustainability should be considered to optimize the processing process. In this process, material efficiency, low energy consumption and periodic metabolism can help alleviate metabolic cracks and improve product quality life [80–82].

## **2.4. DECISION-MAKING IN MANUFACTURING VIA AI**

The process of automation of manufacturing production processes passes through decision-making. The decision-making process is the result of cognitive and emotional processes, which determine the selection of a line of action among different alternatives. In everyday life, decisions are made continuously. In some cases, decisions are automatic, while in other cases, making a decision can be a longer, more demanding and complicated process. The decision, on the part of an individual, involves voluntary and intentional behaviour that follows reasoning. Usually, the decision made in order to solve a problem. In psychological terms, however, there is a specific difference between deciding and solving a problem. In problem-solving, our decision-making act is always linked to the objective it wants to achieve, while in decision making the decision-making act is a reasoning of choice of the most appropriate alternative within a series of options [83]. Therefore, in formal terms, the decision-making process can be considered as the result of mental processes (cognitive and emotional), which determine the selection of a line of action among different alternatives. Each decision making produces a final choice. Making decisions usually requires the evaluation of at least two options that differ from different characteristics and elements. Selecting one option at the expense of another requires the person to carry out an overall assessment of the different alternatives, using specific research and information processing methods and decision-making strategies. In most cases, making decisions means reasoning under conditions of uncertainty: it cannot predict with certainty the future outcome of the possible alternatives available, but at best, it can only estimate the probability of such outcomes. Therefore, decision-making is linked closely to probabilistic reasoning. By "probabilistic reasoning", it means inductive inferential reasoning that allows us to estimate the probability that a given event under certain conditions can be realised.

With regard to theoretical models in the field of decision-making psychology, there are two different approaches: the normative approach and the descriptive approach. The normative approach focuses on the theory of rational choice. According to this theory, in conditions of uncertainty and risk, individuals represent themselves the options of choice in terms of expected utility. In other words, every possible alternative corresponds to a possible attainable state of the world, which is associated with a corresponding probability value that it can actually be realised. According to Von Neumann and Morgenstern [84], those who make a choice rationally evaluate the utility corresponding to their choice and the probability that it will be realized [83]. According to normative and rational choice theories, human beings reason in terms of probabilistic and expected utility and applies the rules of statistics in a precise way. In this sense, the way opens to the descriptive approach within decision-

making models. Along the same lines, the studies of Kahneman and Tversky [85,86] found that people do not think in statistical and rational terms, but would use so-called heuristic strategies. In particular, Kahneman and Tversky [85,86] studied decision-making processes under conditions of uncertainty and risk; their experiments showed that during decision-making processes under conditions of uncertainty and risk there are often systematic errors and cognitive bias that violate the assumptions of rational choice theory. Such systematic errors, acting in a precise direction and particular circumstances, are predictable, and by deepening the functioning of cognitive processes in decision-making, it is possible to identify their causes.

With the enormous growth of Big Data, mostly from the Internet of Things equipment, the use of Artificial Intelligence and IoT has an impact on the Decision-Making Process. Artificial Intelligence has had a long and troubled history. Since the 1950s, there have been alternating periods of super optimism and dark periods. Today, Artificial Intelligence has reached a certain maturity and much technology from cars to call centres, smartphones to IT systems, primarily enabled by IoT used AI. The Internet of Things is contributing to an exponential growth in data describing the physical world. Moreover, this massive amount of data supports Artificial Intelligence. Through a range of names such as deep learning, autonomous vehicles, cognitive computing, robotics, algorithms and more, Artificial Intelligence and IoT together offer, promise to revolutionise all aspects of IT, business and society [87].

Decision-making in the world of manufacturing via AI plays an essential role in automating production processes and processes. As previously done for other topics, there is a bibliometric research on decision-making in the manufacturing world. This time space-time is from 1990 to 2021. 8'455 is the number of documents produced in this interval. In addition, in this case, the advent of Industry 4.0 has an impact on scientific production with a marked increase in the number of documents produced, as in Fig. 10. In the manufacturing decision-making sector, the countries that invest the most in research are still the United States (21.4%) and China (15.9%). Fig. 11 shows the results in the histogram, which summarises the values in Table 6.

Recently, dynamic business scenarios have put forward different demands on the decision-making process, and these demands must be supported by discovering information and knowledge. Therefore, managers need to make more precise decisions based on current strong demand and dynamic market moments, thereby bringing competitive advantages to organizations that can use the information they possess [42].

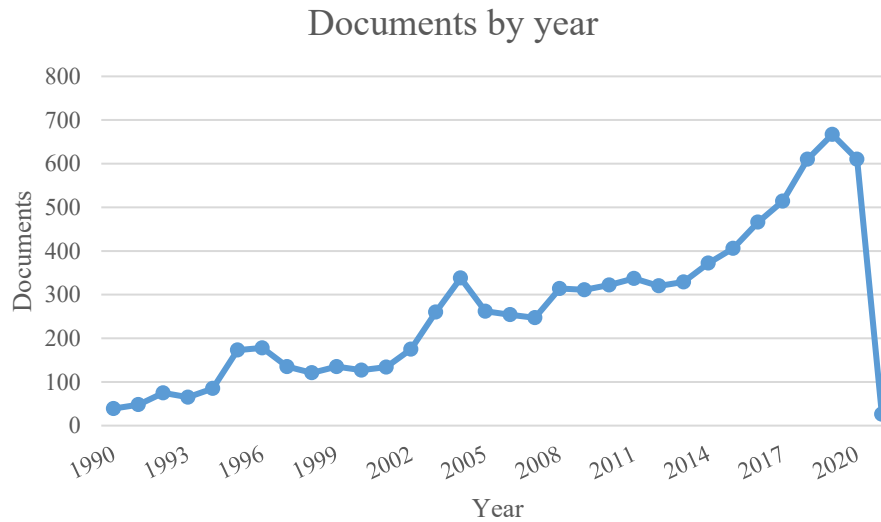


Fig. 10 - Trend in scientific production related to “Decision-Making in Manufacturing” in the period 1990-2021  
[source: SCOPUS]

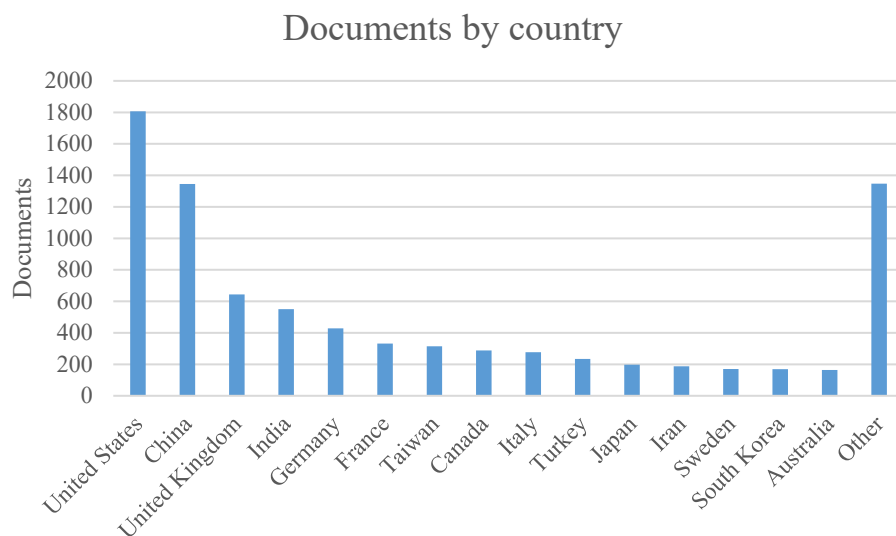


Fig. 11 - Histogram of scientific production linked to “Decision-Making in Manufacturing” related to the various countries [source: SCOPUS]

Table 6. Number of documents related to “Decision-Making in Manufacturing” per country [source: SCOPUS]

Country	Documents
United States	1807
China	1345
United Kingdom	644
India	550
Germany	428
France	332
Taiwan	315
Other	3034

The increase in the number and diversity of IoT devices is an essential part of big data, which can realize knowledge extraction and make decisions based on data. Analysis based on big data sets has entered the manufacturing industry and can make better decisions. From the perspective of Industry 4.0, collecting, processing and evaluating data from different sources enables real-time decision-making, thereby providing greater flexibility and agility in the value chain [88]. The data generated by production systems and products can optimize equipment and equipment management. Decisions are not manual but based on mathematical and computational models developed through the generated data. Similarly, it can improve production efficiency, so that customers can obtain high-quality products and services and obtain high satisfaction. As a result, the results of the entire production chain tend to improve significantly because there are better decisions that benefit not only customers but also the entire value chain [89]. In this case, system reliability will become an essential aspect of smart manufacturing in different ways. For example, production costs due to defective products and spare parts inventory are a direct and essential aspect of reliability gains for all organizations. By adopting system reliability research, real-time prognostic information and preventive maintenance measures can be provided [88]. Concerning the latest applications in the field of decision-making in manufacturing via artificial intelligence, there are some works reported below. Burggräf et al. [90] studied how AI-supported decision-making can improve production management with a performance assessment methodology. Han et al. [91] use the technology of reconfigurable manufacturing systems to do a reconfiguration decision-making systems with the data acquisition system based on Internet of Things technology. Lv et al. [92] consider parameters as efficiency, processing quality, resource consumption and environmental emissions for optimization of production in machining processes. They use a multi-objective decision-making to select the best option for the system and apply their model to machining process of spindle sleeve. Yu et al. [93] propose an efficient intelligent decision-making method based on multi-source heterogeneous data fusion in manufacturing. Another multi-criteria decision-making is proposed by Tran et al. [94]. In their paper, the decision-making criteria use entropy weight Grey-TOPSIS method to drilling process on CFRP. In the field of grinding, Zheng et al. [95] proposed a grey target decision-making method based on uniform effect measurement to realize intelligent optimization of process parameters. Yurdakul used a decision-making tool to selection between machine tool alternatives. The decision-making tool is based on hierarchical decision structures [96]. Other kind of decision-making tool use in manufacturing. An example is the work of Bozdağ et al. [97]. They use a tool based on fuzzy technology to supporting computer integrated manufacturing. Kannan et al. [98] used a multi criteria decision-making method based on fuzzy technology too. Their work has the goal to find the best programming approach for order allocation and supplier selection in a green supply chain. Another



topic related to decision-making in manufacturing is to finding the best configuration to have energy efficiency optimization. A model to do this was proposed by Dietmair and Verl [99]. Chakraborty proposed, instead, various kind application of MOORA method for decision making in manufacturing environment [100].

### 3. ARTIFICIAL INTELLIGENCE TECHNIQUES

We call ourselves "Homo sapiens" because our wisdom is so important to us. For thousands of years, we have been trying to understand our thinking. The field of artificial intelligence (AI) is further developed: it not only tries to understand but also tries to build intelligent entities [101]. Artificial intelligence is one of the latest fields of science and engineering. Artificial intelligence is a discipline belonging to computer science that studies the theoretical foundations, methodologies and techniques. That allows the design of hardware systems and software program systems capable of providing the computer with performances that, to an ordinary observer, would seem to be of exclusive relevance to human intelligence [102]. In 1956, a conference held at Dartmouth College in New Hampshire in 1956 at which some of the leading figures in the emerging field of computation dedicated to the development of intelligent systems took part: John McCarthy, Marvin Minsky, Claude Shannon and Nathaniel Rochester. At McCarthy's initiative, a team of ten people was to create in two months a machine capable of simulating every aspect of human learning and intelligence [101]. In the same conference, McCarthy introduced the expression of artificial intelligence, which indelibly marked the actual birth of this discipline and gave it its nature [103]. The scientific production on the subject of artificial intelligence is very high. On Scopus Database, there are 424'662 registered documents produced from 1956 to 2021, including in press works. The values shown in this chapter date back to 30th October 2020. Since the 1990s, the trend in scientific production has been exponential in terms of artificial intelligence. With the advent of Industry 4.0, it can see a greater slope of the curve of the documents produced for every single year, as shown in Fig. 12.

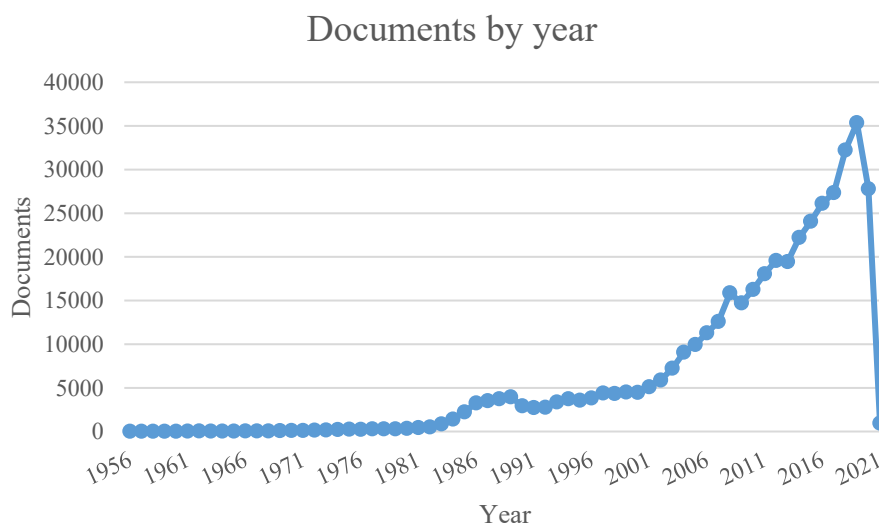


Fig. 12 - Trend in scientific production related to "Artificial Intelligence" in the period 1956-2021 [source: SCOPUS]

Table 7. Number of documents related to “Artificial Intelligence” per subject area [source: SCOPUS]

Subject area	Documents
Computer Science	276366
Mathematics	115337
Engineering	112256
Medicine	41477
Biochemistry, Genetics and Molecular Biology	21269
Physics and Astronomy	19602
Other	152106

### Documents by subject area

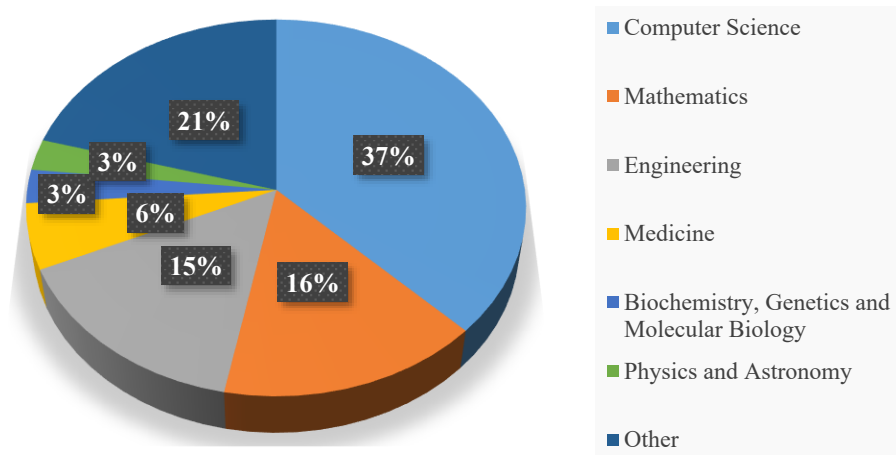


Fig. 13 - Pie chart showing the percentages of scientific work related to Artificial Intelligence in the various subject areas [source: SCOPUS]

### Documents by country

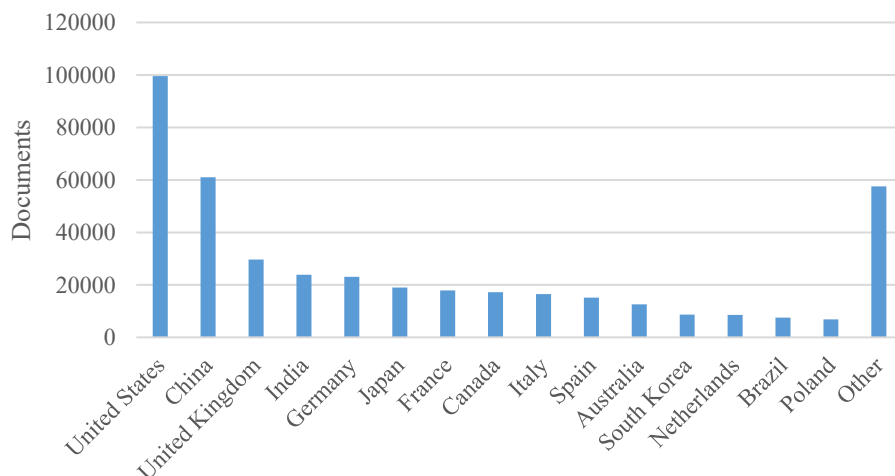


Fig. 14 - Histogram of scientific production linked to “Artificial Intelligence” related to the various countries [source: SCOPUS]

Table 8. Number of documents related to “Artificial Intelligence” per country [source: SCOPUS]

Country	Documents
United States	99569
China	61022
United Kingdom	29670
India	23880
Germany	23070
Japan	18975
France	17913
Other	150563

Table 7 and Fig. 13 show in which areas there are the documents dealing with artificial intelligence. As you can see, the areas of scientific production are not only related to computer science or engineering. The applications of artificial intelligence are now multiple and many countries used them, as shown in Fig. 14 and Table 8. The United States hold the primacy with 23.4% of the total scientific production. The United States is ahead of the China (14.3%) and the United Kingdom (6.9%). It is interesting to see the applications of artificial intelligence in the manufacturing sector. For this reason, research has related to the Scopus database. This time the period of search goes from 1980 to 2021. In addition, in this case, the data of the search is 30th October 2020. Therefore, in the calculation of the scientific production there are also the works in press. 12'871 is the total number of works present on Scopus. In Fig. 15, it is possible to notice the progress of scientific jobs related to the applications of artificial intelligence in manufacturing. Interestingly, at the end of the '80s, the scientific community was very productive in this field and then increased again around 2000. The most significant increase as often happened during these bibliometric analyses is associated with the appearance of the Industry 4.0 phenomenon. It led to an almost exponential increase in scientific production with about 1047 works in 2019 alone.

Table 9. Number of documents related to “Artificial Intelligence in Manufacturing” per country [source: SCOPUS]

Country	Documents
United States	2499
China	1776
United Kingdom	804
India	692
Germany	685
Japan	502
Canada	409
Other	5504

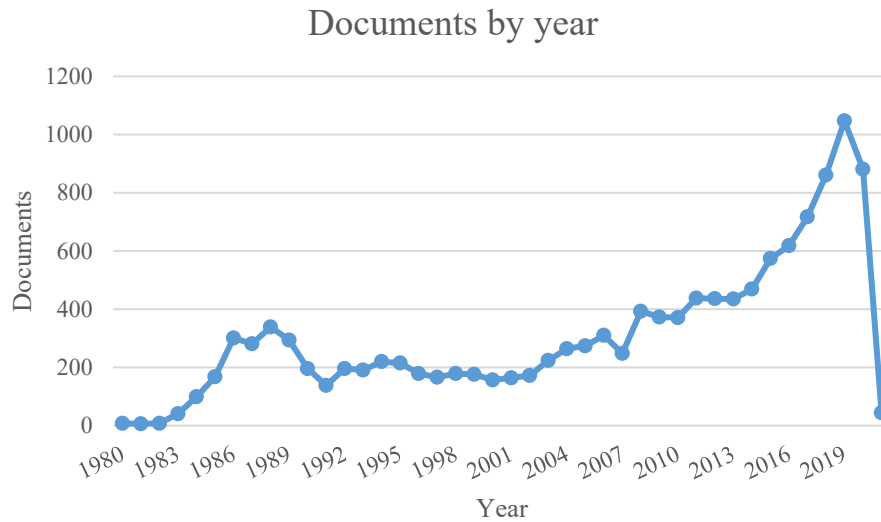


Fig. 15 - Trend in scientific production related to “Artificial Intelligence in Manufacturing” in the period 1980-2021  
[source: SCOPUS]

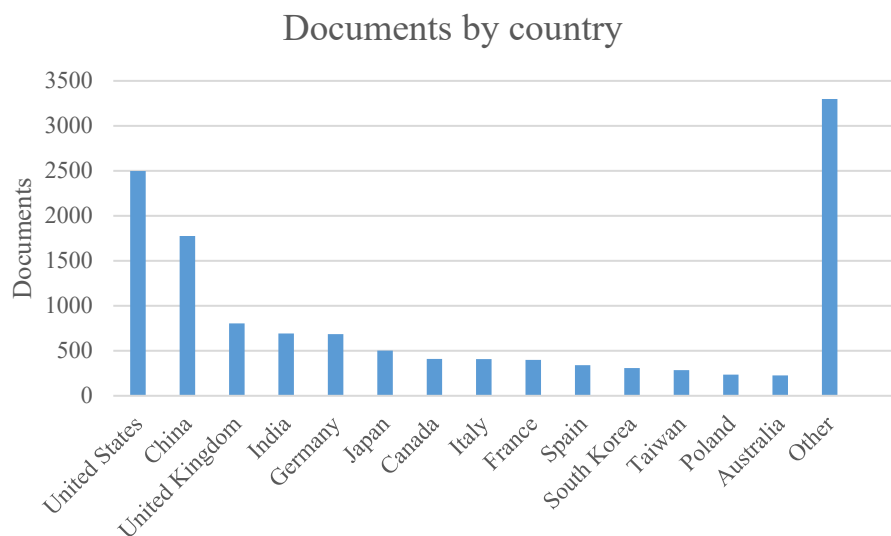


Fig. 16 - Histogram of scientific production linked to “Artificial Intelligence in Manufacturing” related to the various countries [source: SCOPUS]

As previously shown, also concerning artificial intelligence applications in manufacturing the countries that produce the most documents are the United States (19.4%), China (13.8%) and the United Kingdom (6.2%). Fig. 16 and Table 9 show these results. In the course of this chapter will be shown the artificial intelligence techniques used during the PhD project. It will be possible to learn more about the techniques used, and there will be state of the art on the application of the same techniques in the manufacturing sector.

### 3.1. NEURAL NETWORK

Artificial neural networks are an artificial intelligence technique that simulates the behaviour of biological neurons. While a biological neuron consists of the nucleus, axon and synapse, the artificial neuron has a nucleus that can be assimilated to a series of algorithms and inputs and outputs [104]. There are billions of neurons (nerve cells) in the nervous system [105]. A neuron consists of a cellular body and many-branched extensions, called dendrites, through which the neuron receives electrical signals from other neurons. Each neuron also has a filamentous extension called an axon, whose length can vary from about 1 cm to a few metres. At the end, the axon branches out forming terminals through which other cells receive electrical signals. There is a space between a terminal of an axon and the receiving cell. The signals exceed this space through chemicals called neurotransmitters. The connection point between terminal and dendrite is called the synapse [106]. A neuron "activates", i.e. it transmits an electrical impulse along its axon when there is a difference in electrical potential between the inside and outside of the cell. The electrical impulse causes the release of a neurotransmitter from the axon terminals, for example, which in turn can influence other neurons. The human brain is a complex, non-linear, parallel computer. Although it consists of specific processing elements (neurons), it can perform complex computations, such as recognition, perception and motion control, many times faster than the fastest of today's computers. The brain can modify the connections between neurons based on experience, i.e. it can learn. There is no centralised control in the brain, in the sense that the various areas of the brain work together, influencing each other and contributing to a specific task. Finally, the brain is fault-tolerant, i.e. if a neuron or one of its connections is damaged, the brain continues to function, albeit with slightly degraded performance. In particular, the performance of the brain process gradually degrades as more and more neurons are destroyed [105]. Therefore, in order to artificially reproduce the human brain, it is necessary to create a network of straightforward elements that is a distributed, massively parallel structure, capable of learning and therefore of generalising. Typically, the artificial neuron has many inputs and only one output. Each input is associated with a  $W$  weight. The  $W_i$  weights are real numbers that reproduce synapses. If  $W_i > 0$ , the channel is called excitatory, if  $W_i < 0$ , the channel is inhibitory. The absolute value of weight represents the strength of the connection. The weight assigned to the neuron represents the influence of this input on the calculation of the network output. If the weight assigned to neuron 1 ( $W_1$ ) is greater than the weight assigned to neuron 2 ( $W_2$ ), then the input from neuron 1 has a more significant impact on the network output than from neuron 2 [104]. The body of the neuron have two parts. One part named the network input of the neuron, which shows the part of the calculation performed by the neuron body. This part is usually marked as  $Z$  on the network diagram.

The sum of each input of the neuron multiplied by the corresponding weight, and finally, the deviation is added, which is the linear part of the calculation (Eq. 1).

$$Z = W_1 \cdot I_1 + W_2 \cdot I_2 + W_3 \cdot I_3 + B_1 \quad (\text{Eq. 1})$$

The output, i.e. the signal with which the neuron transmits its activity to the outside, calculated by applying the activation or transfer function (Eq. 2) to the weighted sum of the inputs.

$$O = \sigma(Z) \quad (\text{Eq. 2})$$

There are many activation functions for the network. Their usage depends on various factors, such as well-behaved intervals (unsaturation), how fast the arguments of the function change when they change, and your preference. Let us look at one of the most commonly used activation functions; it is called the sigmoid (Eq. 3) [104,105].


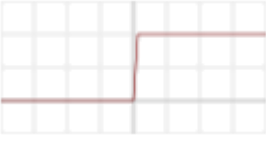
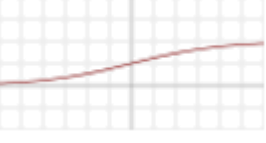
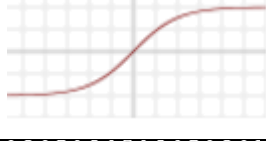
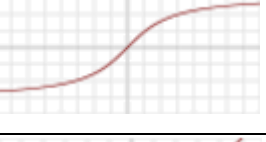
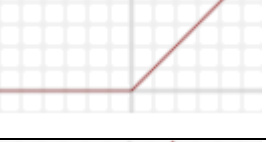
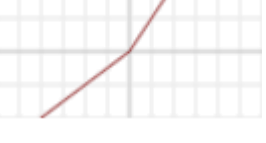
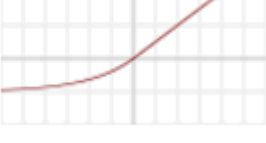
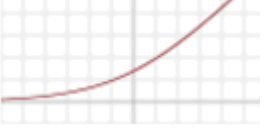
$$\sigma(Z) = \frac{1}{1+e^{-Z}} \quad (\text{Eq. 3})$$

The sigmoid function (sometimes called the logistic function) performs best on the interval  $\{-1, 1\}$ . Outside this interval, it will quickly saturate, which means that its value does not change with its argument. This is why network input data is usually normalized on the interval  $\{-1, 1\}$ . Some activation functions perform well on the interval  $\{0, 1\}$ , so the input data is normalized accordingly on the interval  $\{0, 1\}$  [104]. Table 10 shows the most significant activation functions.

The most commonly used method to train a neural network is to present a set of examples (training sets) at the entrance to the network. The answer given by the network for each example provide a comparison with the desired answer, the difference (error) between the two is evaluated and, based on this difference, and the weights are adjusted. This process is repeated over the entire training set until the network outputs produce an error below a predetermined threshold [106].

Each synapse corresponds to an interconnection weight, which modifies the signal of the emitting neuron. The interconnection weights are fundamental because they are the only elements of the neural network able to memorize information. Therefore, they are responsible for the learning capacity of the neural model. The interconnection weights and the transfer function of the neuron itself determines the outputs. The latter chosen during the project and generally cannot be modified, while the weights are changed according to a "training rule" that takes into account the input and output values. During the training, i.e. the exposure of the network to examples, this rule obtains the correction values of the weights based on specific parameters, which in turn vary as a result of the exposure to the examples [105].

Table 10. Most important activation functions [104]

Name	Plot	Equation
Identity		$f(x) = x$
Binary step		$f(x) = \begin{cases} 0 & \text{for } x < 0 \\ 1 & \text{for } x \geq 0 \end{cases}$
Logistic		$f(x) = \frac{1}{1 + e^{-x}}$
TanH		$f(x) = \tanh(x) = \frac{2}{1 + e^{-2x}} - 1$
ArcTan		$f(x) = \tan^{-1}(x)$
Rectified Linear Unit		$f(x) = \begin{cases} 0 & \text{for } x < 0 \\ x & \text{for } x \geq 0 \end{cases}$
Parameteric Rectified Linear Unit		$f(x) = \begin{cases} \alpha x & \text{for } x < 0 \\ x & \text{for } x \geq 0 \end{cases}$
Exponential Linear Unit		$f(x) = \begin{cases} \alpha(e^x - 1) & \text{for } x < 0 \\ x & \text{for } x \geq 0 \end{cases}$
SoftPlus		$f(x) = \ln(1 + e^x)$

The learning phase of a network necessarily precedes that of use. During the training phase, the network modifies specific characteristics, following an appropriate rule, based on a set of examples given in advance. The learning rule is not a property of the network: in fact, the same rule can be used for different structures, and different algorithms can be used on the same network [105,106].



Learning consists of the repeated presentation of a series of vectors, also called training patterns. The modification of the synaptic  $W_{ji}$  values of the network calculated after each presentation of a single pattern or only at the end of the presentation of all the training patterns. Once the learning phase has been complete, the synaptic values are record, and it is possible to study the network response on test vectors. The test phase consists of the presentation of new input patterns and the calculation of the network activation nodes without modifying the weights [105].

In the following sub-paragraphs, various types of neural networks will be shown, which are subdivided according to the learning process by the network.

In 1943, McCulloch and Pitts created a neural network model based on algorithms [107]. They are considered the fathers of artificial neural networks [104]. Only in 1958, however, did Rosenblatt create the perceptron [108]. Perceptron is an algorithm for pattern recognition of binary classification [109].

As far as scientific production is concerned, artificial neural nets are the protagonists in about 265'930 documents produced from 1958 to 2021. The results extrapolated from the Scopus database have the following data: 30th October 2020. Work-related to artificial neural networks has increased in terms of documents produced in the second half of the 2000s. In Fig. 17, you can see an apparent increase after 2013. In addition, in this case, there is an impact of Industry 4.0 in scientific production.

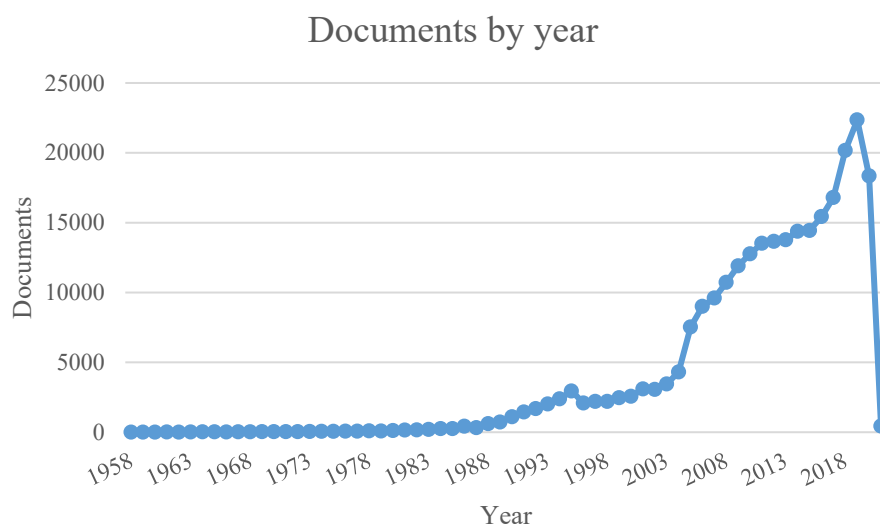


Fig. 17 - Trend in scientific production related to “Artificial Neural Network” in the period 1958-2021  
 [source: SCOPUS]

As regards the distribution of scientific publications, the country that produces the most are the United States (27.8%). They are ahead of the China (14.3%) and India (7.2%), as shown in Table 11 and Fig. 18. As regards the areas in which neural networks most used in science, it finds medicine (17%) and engineering (15%). However, there are many applications, and this demonstrated by the percentage of the other uses, which are 37% of the total documents produced. In Fig. 19 and Table 12, it is possible to see the results about the bibliometric research concerning the application of artificial neural networks in different areas.

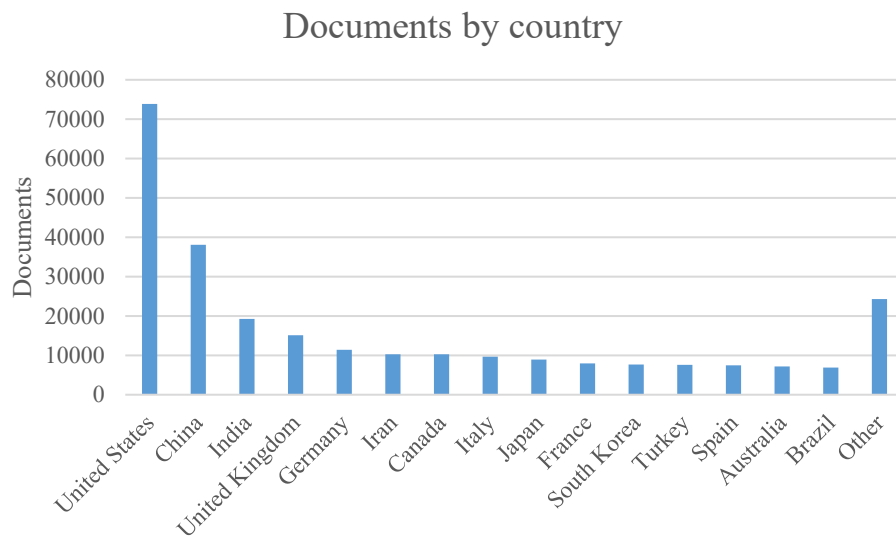


Fig. 18 - Histogram of scientific production linked to “Artificial Neural Network” related to the various countries  
[source: SCOPUS]

Table 11. Number of documents related to “Artificial Intelligence” per country [source: SCOPUS]

Country	Documents
United States	73878
China	38078
India	19250
United Kingdom	15111
Germany	11392
Iran	10286
Canada	10277
Other	87658

## Documents by subject area

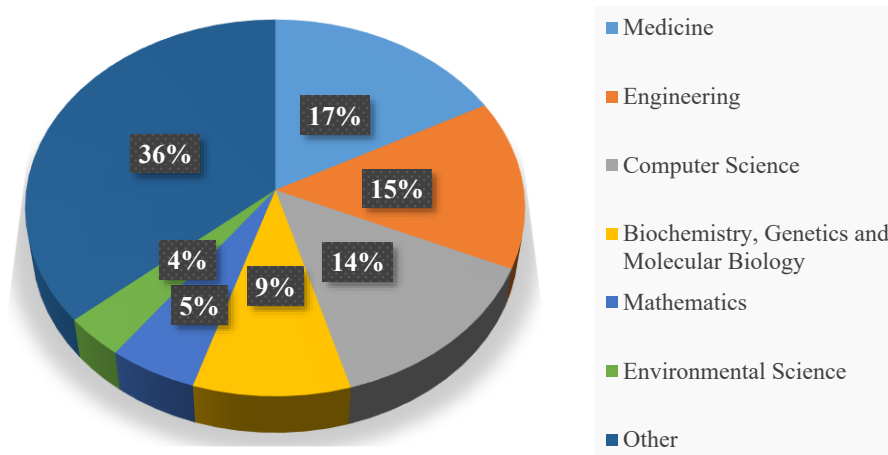


Fig. 19 - Pie chart showing the percentages of scientific work related to Artificial Neural Networks in the various subject areas [source: SCOPUS]

Table 12. Number of documents related to “Artificial Neural Network” per subject area [source: SCOPUS]

Subject area	Documents
Medicine	82576
Engineering	69981
Computer Science	66888
Biochemistry, Genetics and Molecular Biology	44845
Mathematics	25221
Environmental Science	17141
Other	175036

As regards the scientific production linked to the use of artificial neural nets in the manufacturing sector, from 1980 to 2021, there are 7'051 documents produced. As already repeated previously, there is an increasing trend in production, in particular from 2014 to today. In general, in 2010 scientific production increased by about 217% compared to the number of documents produced previously. In addition, in this case, the countries that have more scientific documents on the application of artificial neural networks are the United States (16.6%), China (15.2%) and India (14.8%). However, a significant percentage (17.7%) also reserved for all the other countries in the world. Synonymous with a reasonably widespread application at a global level as far as the manufacturing sector is concerned. The results of this analysis are in Fig. 20, Fig. 21 and Table 13.

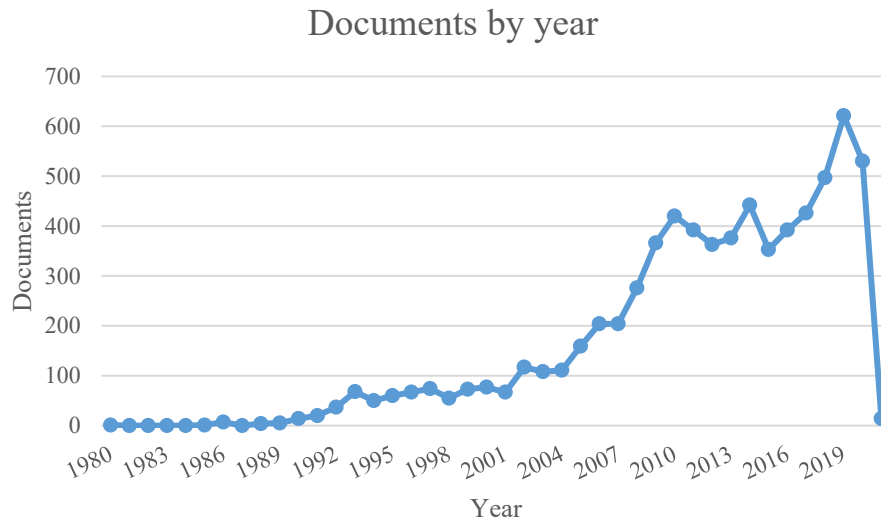


Fig. 20 - Trend in scientific production related to “Artificial Neural Networks in Manufacturing” in the period 1958-2021 [source: SCOPUS]

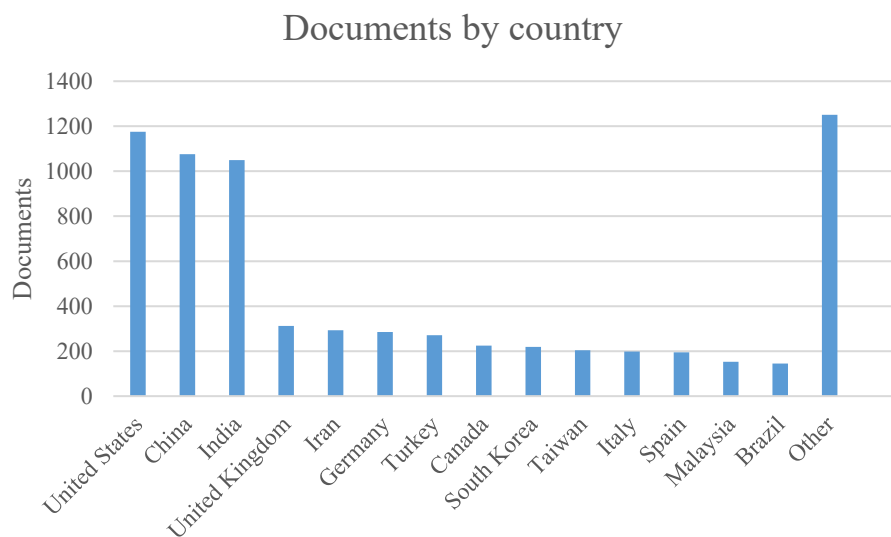


Fig. 21 - Histogram of scientific production linked to “Artificial Neural Networks in Manufacturing” related to the various countries [source: SCOPUS]

Table 13. Number of documents related to “Artificial Neural Networks in Manufacturing” per country [source: SCOPUS]

Country	Documents
United States	1175
China	1076
India	1049
United Kingdom	312
Iran	293
Germany	285
Turkey	271
Other	2590

The applications of artificial neural networks are manifold in the manufacturing sector. Petkar et al. [110] use artificial neural networks to analyse the behaviour in cold forging of AISI 1010 steel. Instead, Kalombo et al. [111] use artificial neural networks to estimate the fatigue life of an aluminium alloy 1055 MCM conductor. Khorasani and Yazdi [112] utilize the artificial neural network to develop dynamic surface roughness monitoring system in milling operations. Zhao et al. [113] use neural network to study the effects of welding parameters on tensile strength of ultrasonic spot welded joints of aluminium to steel. The applications of them related to prediction too. Hanief et al. [114] model and predict cutting forces during the turning of red brass with artificial neural networks. Wiciak-Pikuła et al. [115] use them to predict tool wear during aluminium matrix composite milling. Instead, Saoudi et al. [116] use artificial neural networks to predict mechanical properties of welded steel X70 pipeline. Chowdhury et al. [117] use artificial neural network to minimize the geometric inaccuracies resulting in the part during the additive manufacturing process. Hesser and Markert [118] utilize artificial neural networks to tool wear monitoring of a retrofitted CNC milling machine. Mikołajczyk et al. [119] predict tool life in turning operations using neural networks. D'Addona et al. [120] utilize neural network to predict tool wear and pattern-recognition with DNA-based computing. Zerti et al. [121] use artificial neural networks to predict machining performance in hard turning of martensitic stainless steel AISI 420. In that case, the team utilize the artificial neural networks with response surface methodology. It is not the only case of combination of different artificial intelligence techniques. Laouissi et al. [122] use artificial neural networks in combination with response surface methodology and genetic algorithm to optimize cutting parameters in turning of gray cast iron using coated and uncoated silicon nitride ceramic tools. Ghosh et al. [123] use a mix technique with genetic algorithm and particle swarm optimization to optimize surface roughness in keyway milling. Another recent work with the mix technique is the Bensingh's paper. Bensingh et al. [124] use artificial neural networks with particle swarm optimization to optimize injection molding process of a bi-aspheric lens. Venkata Rao and Murthy [125] utilize artificial neural network in combination with response surface methodology and support vector machine to optimize tool vibration and surface roughness in boring of steel. Artificial neural networks are used in micro mechanical operations too [126]. Automatize image analysis uses the technique of ANN too. An example is the Mikołajczyk et al. paper [127]. In this case, the team use artificial neural networks to automatize image analysis of cutting edge wear.

### 3.1.1. SUPERVISED AND UNSUPERVISED NEURAL NETWORK

In the previous paragraph, it discussed how artificial neurons emit signals according to the sigmoid activation function based on three parameters: input signals, input weight and bias. In this chapter, it will use this knowledge to begin to understand the differences between the various types of artificial neural networks. To begin this process, it should start by talking about the straightforward neural network, known as the perceptron. This network is so simple that it contains only one outgoing neuron. However, it contains the critical behaviours found in today's neural networks. Perceptrons show how artificial neurons process information and how neural networks optimize weights in each connection to learn. This aspect is fundamental to understand the substantial difference between the various types of networks. The division between supervised and unsupervised networks lies in the mechanism by which they learn information. Thanks to their simplicity, perceptrons have minimal applications and can only deal with relatively simple problems. The perceptron uses supervised training to learn, which means you must provide a set of inputs and their matching outputs. The perceptron works through the input and calculates the output-if it is incorrect, the weight adjusted until the correct answer is obtained. Therefore, learning is an iterative process, which means that each weight must be adjusted and changed repeatedly to find the most suitable combination [128].

$$W_{new} = W_{old} + \alpha \cdot (desired - output) \cdot input \quad (\text{Eq. 4})$$

In Eq. 4,  $W_{new}$  and  $W_{old}$  are the weights of a single connection.  $\alpha$  is the learning rate. This value indicates how fast the network adapts and it is between 0 and 1. The other parameter are *desired* (desired value/correct value), *output* and *input* are the value in output and input of the network [129]. Learning is an iterative process, and the weights can still adjust. As a result, it must use the activation function to calculate the new output and determine whether it is satisfactory. If the distance is not close enough, it must repeat the above process until the new output matches our expected output. This is the basis of neural network learning. When there are several layers, it talks about multilayer perceptron. It has at least three layers of nodes. The layers are input layer, hidden layer, and output layer. A feature of multilayer perceptron is to use nodes with non-linear functions. This with the exception of the input layer [108]. Now it is appropriate to distinguish between supervised and unsupervised learning.

Supervised learning is a machine learning model used to study the task of mapping input data to output data based on sample input and output pairs. Its task is to infer functions from labelled training data, which consists of a set of training models. In this learning system, the external source stimulates

the delivery network through a set of feedback. For the feedback stimulation, the output has been confirmed in advance, and during the entire process of execution, the output effect is always related to the required information [101]. When some iterations are performed, the slope descent rule uses the error between the actual output and the target information to normalize the connection weights in order to obtain the closest match between the target signal (+) and the actual output signal (-) until Accumulate the error so far, and then down to update the weight, as shown in Fig. 22. Therefore, supervised learning relies on the fact that the real class of the data is known [130,131].

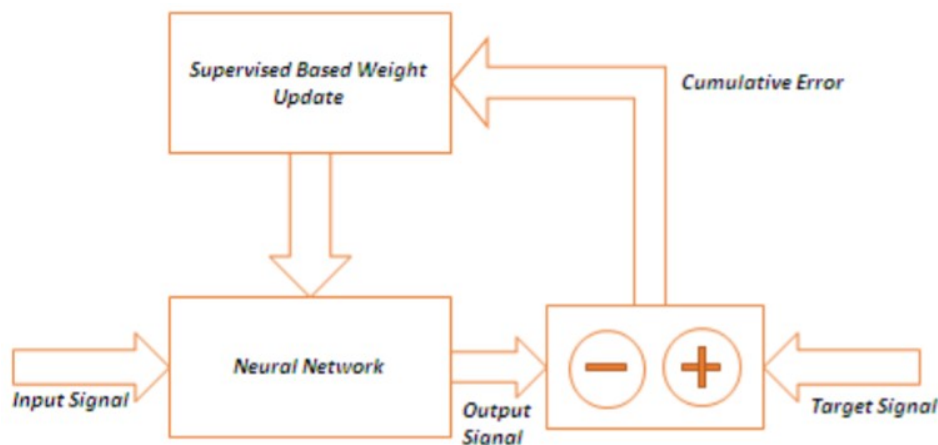


Fig. 22 - Supervised learning model [130]

In order to solve some of the problems in supervised learning, the following steps are expected:

- Select training data;
- Collect teaching materials;
- Define the input data graph of the training function;
- Control the configuration of post-training functions and consistent post-training algorithms;
- Complete the design and run the learning algorithm on the collected training data;
- Estimate the correctness of the learning task [101,130].

Unsupervised learning represents how the network learns to represent specific input designs through a method that reproduces the numerical arrangement of the overall set of input designs or patterns. Machine learning is responsible for inferring functions to define hidden structures based on unlabelled data. This is just a learning algorithm; it does not contain any tags for supervised learning/training. In this algorithm, a large amount of data and features are provided for each observation, but the required output is not provided [132]. Usually based on some inherent characteristics of the image (such as colour, size, shape, etc.), unsupervised learning (such as clustering) is used to divide the

Ing. Salvatore Conte

image into two groups or clusters. Fig. 23 describes the training network connection. Since there is no external basis to provide information to the network, it is also called self-organizing or adaptive learning algorithm. It depends on local facts and internal mechanisms. The system acquires knowledge on its own by learning and familiarizing with information in the input data [130].

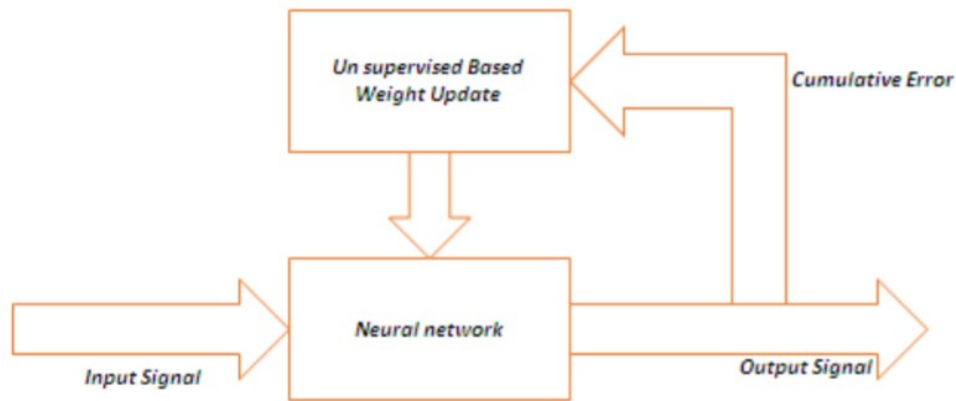


Fig. 23 - Unsupervised learning model [130]

The system provides to the training graphics and input patterns, and the system arranges them into categories or clusters as data. In the input layer stage, the system provides to a set of training patterns or data too; the network correlation weight adjusted according to a specific competition between nodes in the output layer, and the node with the highest value will be the successful candidate. Clustering and association algorithms use mainly the unsupervised learning. The main challenge associated with unsupervised learning is responsible for discovering hidden structures in unlabelled data [128,130,132]. Algorithms for unsupervised learning include:

- Clustering: it is the process of aligning a group of entities so that entities in similar groups (called clusters) are similar to each other than entities in other groups (called clusters).
- Anomaly detection: In the field of data mining, anomaly detection can also be described as outliers, noise, deviation, novelty, and anomaly, which is the identification of items, notes or events that do not fit the expected design. Alternatively, other items in the data set [130].

The primary purpose of unsupervised learning is to find the possible structure inherent in the input data. The next sub-paragraphs will show the concept of backpropagation for supervised neural networks and Self-Organizing Maps for unsupervised neural networks. Among the unsupervised neural networks, there are also algorithms such as the Diabolo Network [133], the Deep Belief Network [134], Hebbian Learning [135] and the Generative Adversarial Network [136].



### **3.1.2. BACKPROPAGATION ALGORITHM**

One of the most widely used ways to enable a network to learn is supervised learning, which involves presenting the network with the corresponding output for each training example. Usually, the weights initialised with random values at the beginning of the training. Then, one by one, the examples forming the training set presented. For each example presented, the error made by the net is calculated, i.e. the difference between the desired output and the actual output of the net. The error used to adjust the weights. The process is usually repeated by re-submitting to the net, in random order, all the examples of the training set until the error committed on the whole training set (or the average error on the training set) is below a predetermined threshold [137].

After the training, the network tested by checking its functioning with the examples not used during the training phase. The purpose of the test phase is, therefore, to evaluate the ability of the neural network to generalise. It will say that the network has learnt, i.e. it is able to provide answers also for inputs never presented to it during the training phase. The performance of a neural network depends strongly on the set of examples chosen for the training. These examples must therefore be representative of the reality that the network must learn and in which it will be used. The training is, in fact, an ad hoc process, depending on the specific problem dealt with [137]. The artificial neural network based on the back-propagation learning algorithm has been widely used successfully, to solve a wide range of real-world problems affecting different application areas [138–141].

The multilevel non-recurring network model based on the back-propagation supervised learning algorithm has become, in a short time, the most widely used in real-world applications of feature vector recognition and classification. Theoretically, there is no limitation to the number of intermediate stages to be set, however, in most of the problems faced with the use of multilevel networks rarely more than two hidden levels have been used. The neural network of the back-propagation type consists of fully interconnected layers. The main problem in training is how to modify the connection weights to reduce the output error. The back-propagation algorithm solves this problem by back propagating the output error, through the connections of the previous stages, until the input level reached. The value of the back-propagation error is used to calculate a local error that is used to modify the incoming connection weights in the current level [129].

Before starting the learning process, small random values assigned to the connection weights. In this way, problems with a saturation of neuron outputs avoided at an early stage of training.

The primary mechanism of back-propagation learning consists of the following steps (Fig. 24):

- Propagate forward, through all stages of the network, the input example in order to calculate the vector of the actual outputs;
- Determine the local error in the output stage and the increment to be added to the incoming connection weights;
- Back-prop the local error calculated in the output stage, through all the hidden levels up to the input level, in order to calculate the increment to be added to the connection weights;
- Repeat the previous steps, iteratively throughout the whole training set, until the global error reaches the minimum value [137].

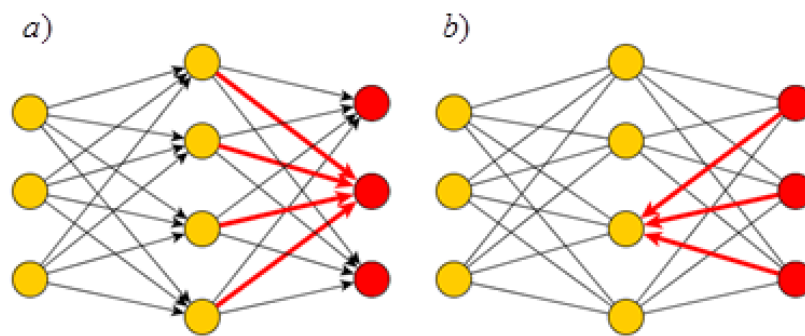


Fig. 24 - Error in Back Propagation: a) forward propagation of signals; b) backward propagation in the opposite of the same bonds as in a) [142]

### 3.1.3. SELF-ORGANIZING MAP (SOM)

The only way a layered network through back-propagation training can produce desired outputs is, as seen, through a series of samples, where the corresponding outputs known for each input. Nothing similar can happen in a biological neuronal network, where the outputs of the neurons have no way to compared with "correct" numerical quantities if this makes any sense.

Instead, there is an artificial model that is not based on this mechanism, but rather on a process of neuronal self-organisation based on experience (non-supervised training), known by the acronym SOM (Self-Organising Map), also called Kohonen's maps, from the name of those who developed from 1980 to 2000 [143,144]. A vital feature of this model is its neuron map architecture, in which the organisational structure emerges spontaneously in the form of a two-dimensional topological arrangement.

The Self Organizing Maps are the result of studies carried out by Tuevo Kohonen, head of the Neural Network Centre at the University of Technology in Helsinki [144]. SOMs have been developed since 1982 [143]; they represent the most common artificial neural network algorithm in the unsupervised learning category. Unlike supervised learning networks, in which the operator chooses the examples with which to carry out the training assigning both input and output vectors, unsupervised learning networks receive only vectors in the input phase.

In this type of networks, there are two levels, called X and Y (Fig. 26), of which the first is the input one and the second is the classification one. There are two types of connections, those from level X to level Y, which it will call W, and those between the units of the classification level, the side connections, which are not total, but organised in a scheme that can be either one-dimensional or two-dimensional (grid) in which each unit is connected only to its neighbours. These connections are fixed and are not taught-in. Therefore, it can conclude that each unit of level Y receives stimuli both from the units of level X above and from its direct neighbours. Each neuron has a transfer function similar to the ramp function shown in Fig. 25.

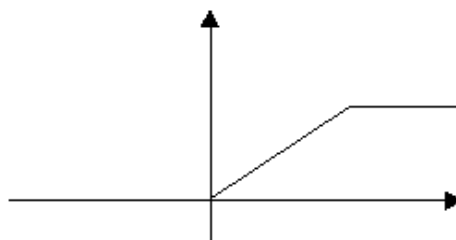


Fig. 25 - The transfer function of a neuron of a SOM network [144]

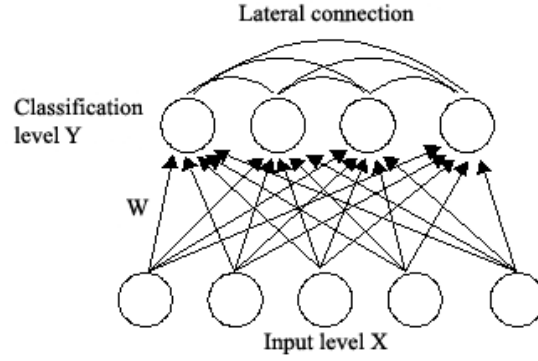


Fig. 26 - Architecture of SOM [144]

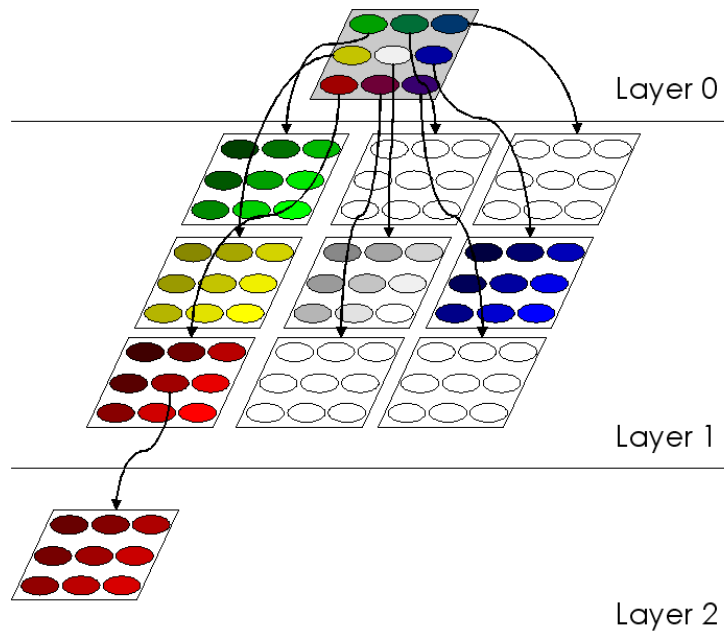


Fig. 27 - Layers in SOM [145]

Learning takes place in various stages. In the beginning, each of the input neurons initialised with the corresponding input data. Then each of the neurons of the classification level calculates its Euclidean distance from the input example, measured in the input configuration space. It then results as a multidimensional distance, which to be precise has as many dimensions as the neurons of the first level. The generic distance  $D_j$  between neurons is calculated according to the Eq. 5 [144].

$$D_j = \sqrt{\sum_{i=0}^{NX} (x_i - w_{i,j})^2} \quad (\text{Eq. 5})$$

$NX$  is the number of incoming connections. Since the unit that has the shortest distance to the input (Best matching Unit: BMU) must be rewarded, the value of the unit is set to complement one of the

distances. BMU is the Layer 2 in Fig. 27. At this point, a competition phase begins to make sure that only one neuron is the winner and thus better represents the input. In this phase, each unit reinforces itself linearly and at the same time inhibited by all the others squared, to avoid too strong inhibitions. In the end, only one neuron will emerge victoriously. Consequently, the weights of the winner and of its neighbours updated, as it wants the network to organise itself so that neighbouring units represent similar input classes (Fig. 27). In their more straightforward form, SOM networks have a fundamental flaw: they tend to create few extensive classes. Since the initial distribution of weights is random, the first example given will create a new class. A second example will have a good chance of being more similar to the pre-existing class than to a random combination of weights, and will therefore be placed in the first class already created.

For this reason, it is good to introduce a sort of neuron consciousness, so when one unit wins too much, it tends to give way to the other units. In the end, therefore, the various units will win fairly. In order to implement this situation, the Eq. 5 is edit, subtracting a correction factor proportional to the frequency of winning the unit:

$$D_j = D_j - \gamma \cdot \left(\frac{1}{NY} - F_j\right) \quad (\text{Eq. 6})$$

where  $\gamma$  is the unit consciousness factor and  $F_j$  is the frequency of the unit's winning frequency. This placed at the beginning equal to  $1/NY$  (where  $NY$  is the number of units of classification  $Y$ ) and calculated as follows:

$$\begin{cases} F_w = F_w + (0.1 \cdot (1 - F_w)) & \text{for winner} \\ F_j = F_j + (0.1 \cdot F_j) & \text{for others} \end{cases} \quad (\text{Eq. 7})$$

The learning phase of a SOM network is organised in epochs. Each epoch corresponds to a complete scan of all examples. Repeating several learning periods leads to an optimal network configuration [143]. In order to achieve better behaviour, it is best to ensure that the network has a high degree of freedom at the beginning, whereas towards the end it should be gradually reduced. This can achieve with a new factor  $\delta$ , which should multiply by the learning rate  $e$ , the consciousness factor  $\gamma$  and by the size of the neighbourhood of each unit. This regrowth factor  $\delta$  can be express as:

$$\delta = \frac{\text{epochs number} - \text{epoch} + 1}{\text{epochs number}} \quad (\text{Eq. 8})$$

This function gradually decreases from 1 at the beginning to almost 0 at the end. At the beginning the values that constitute an example must be renormalized, so that their sum is equal to 1 [146].

### 3.2. BEES ALGORITHM

The bees algorithm (BA) is a method that allows optimizing the search for specific values through a code that simulates the search behaviour of bees. The algorithm was developed by Prof. Pham [147] and optimized with his student Dr Castellani [148]. It is part of that category of bio-inspired artificial intelligence techniques implemented to optimize processes. More specifically, it is one of the techniques called Particle Swarm Optimization (PSO). PSOs replicate the behaviour of particle systems for optimization and research processes. The particles, in this case, are bees, but they can be ants, flocks of birds, shoaling and schooling of fish.

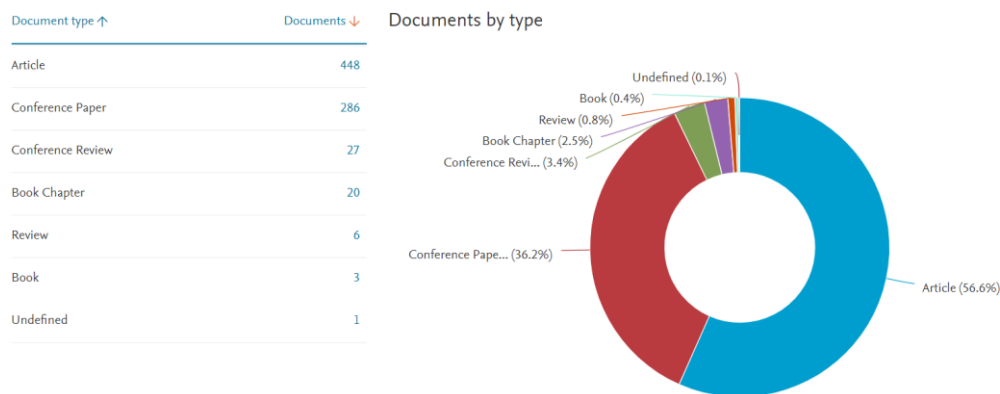


Fig. 28 - Documents by type using metadata for “Bees Algorithm” keyword [source: SCOPUS]

From a search in the Scopus database, 791 documents are dealing with the topic Bees Algorithm. From the same database, thanks to *Biblioshiny for Bibliometrix* [149], it knows that every year 5.48 documents are produced, each of which has an average of 13.27 citations. Of the documents produced 448 are articles published in magazines, three books, 20 book chapters, 286 conference papers, seven reviews and 27 conference reviews (Fig. 28). Of all these documents 207 were produced in the two years 2018-2020, about 26% of the entire production calculated over the period from 2006 to 2020. It is possible to notice how this technique is associated with words such as *optimization* (288 times), *genetic algorithm* (106 times), *PSO* (91 times), *artificial intelligence* (89 times), *evolutionary algorithms* (82 times) and *swarm intelligence* (74 times). These results (Table 14) suggest the use of the technique associated with other artificial intelligence methods. To confirm this, among the most cited articles, there is the work of Pham and Packianather that talk about the optimization of neural networks for the identification of wood defects via BA [150,151]. Another work that sees the use of mixed techniques is Sundararaj's 2019 work in which he uses BA coupled with the ant algorithm for optimal task assignment in mobile cloud computing [152].

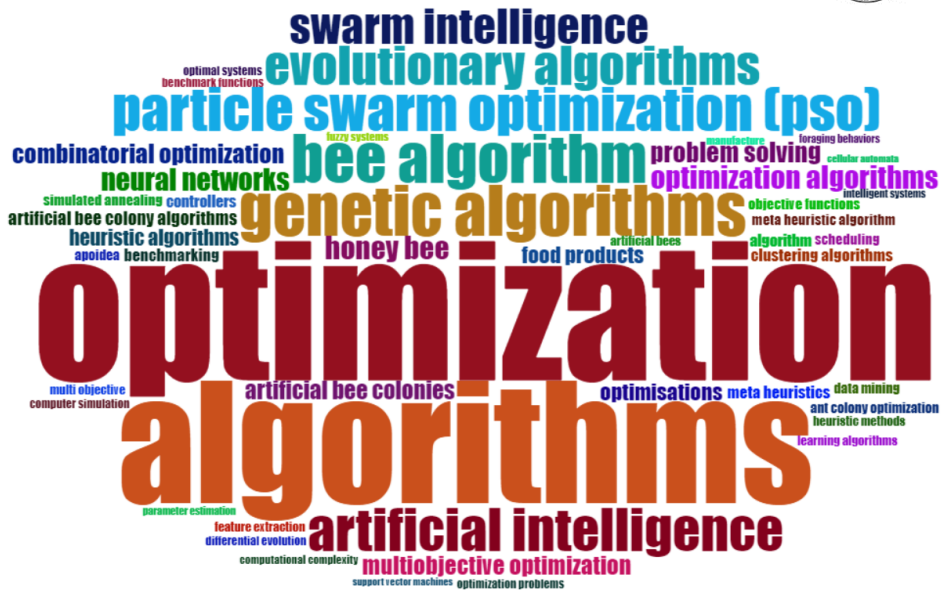


Fig. 29 - Word cloud realized with *Biblioshiny* using metadata for “Bees Algorithm” keyword [source: SCOPUS]

Table 14. Most used keywords using metadata for “Bees Algorithm” [source: SCOPUS]

TERMS	FREQUENCY
Optimization	288
Algorithms	252
Genetic Algorithms	106
Particle Swarm Optimization (PSO)	91
Artificial Intelligence	89
Evolutionary Algorithms	82
Swarm Intelligence	74
Honey Bee	48

## Documents by subject area

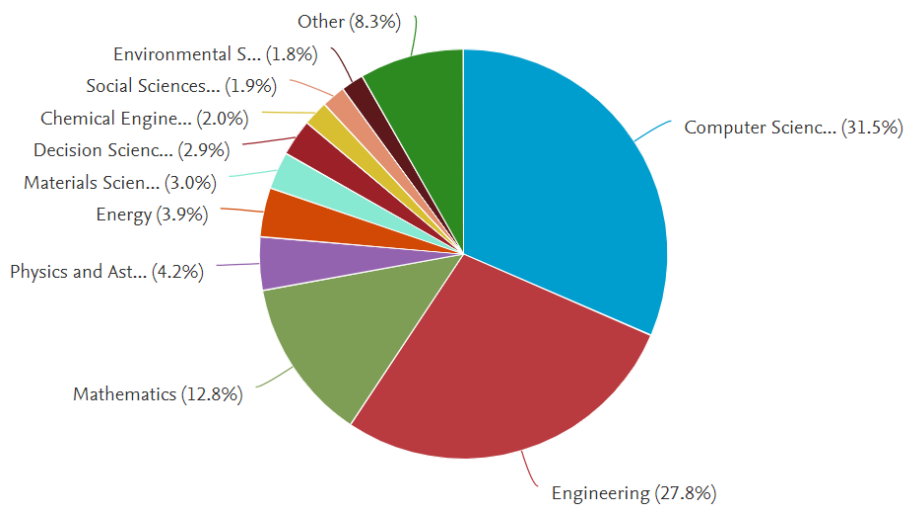


Fig. 30 - Percentage of documents by subject area for “Bees Algorithm” keyword [source: SCOPUS]

Particularly interesting are the research fields in which the BA is used. 31.5% of the productions fall in Computer Science, 27.8% in Engineering, 12.8% in Mathematics, but there are also other fields such as Physics and Astronomy (4.2%) or Social Sciences (1.9%). Fig. 30 shows these results. Therefore, it is possible to find as an application of the BA a model that foresees the pattern synthesis of linear antenna arrays [153], or the comparison between BA and genetic algorithm for location-allocation of earthquake relief centres [154]. There are other like work concerning robotic disassembly sequence planning where the BA has been used to reduce the disassembly time [155], or even applications in the medical field such as the selection of the most appropriate parameters for the classification of the type of breast cancer [156]. Another exciting fact that results from the bibliometric analysis of the works containing the BA are that of the geographical distribution that sees 66 different countries that have produced at least one work on the subject. The country with the highest production is Iran with about 180 products, followed by the UK with 106 products and Malaysia with 91 works. Fig. 31 shows the results of this research.

#### Documents by country or territory

Compare the document counts for up to 15 countries/territories.

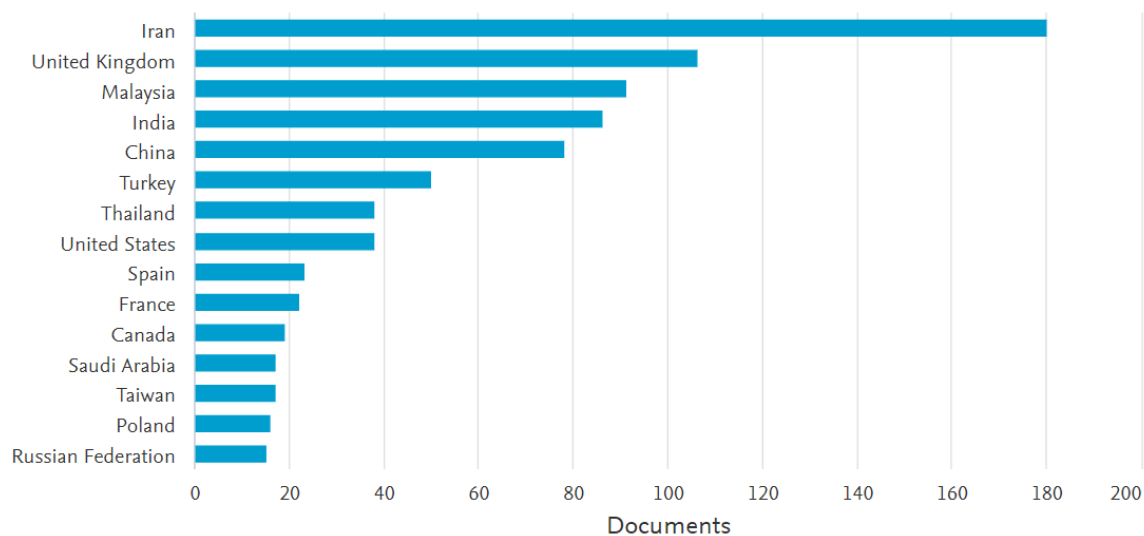


Fig. 31 - Number of documents by country or territory for “Bees Algorithm” keyword [source: SCOPUS]

As far as the use of BA in manufacturing is concerned, there are about 4.9% of total works. The first works date back to 2007 and are all produced by Prof. Pham's group. These jobs used the BA to schedule jobs for a machine [157,158] and to find the best gearbox configurations [159]. Another application of the BA is the study to determine crack problems for beam-type structures [160]. Also in robotics is the BA with studies on robotic disassembly in remanufacturing [161]. The world of network applications in manufacturing also uses the BA method. Xu and his research team used the



technique for the middleware layer of the Quality of Services in manufacturing networks. In this application, the BA was tasked with finding the best parameters to optimise system performance [162,163]. In general, however, the role of the BA remains that of tool for function optimisation [164], and it is for this reason that it will be used in the following work, albeit with a new target. The goal is to use the search ability of the bee agents to delimit the contours of a tool's wear. Thus, calculate its value in terms of amplitude. As far as the annual scientific production is concerned, as it is possible to see from Fig. 32, there has been a remarkable increase of the production in little more than ten years, with peaks in the last years. The trend of the quotations sees the works of 2006 as the most cited ones. This is since these are the jobs in which BA introduced. In Fig. 33, it is possible to observe the trend of the quotations on Scopus indexed works.

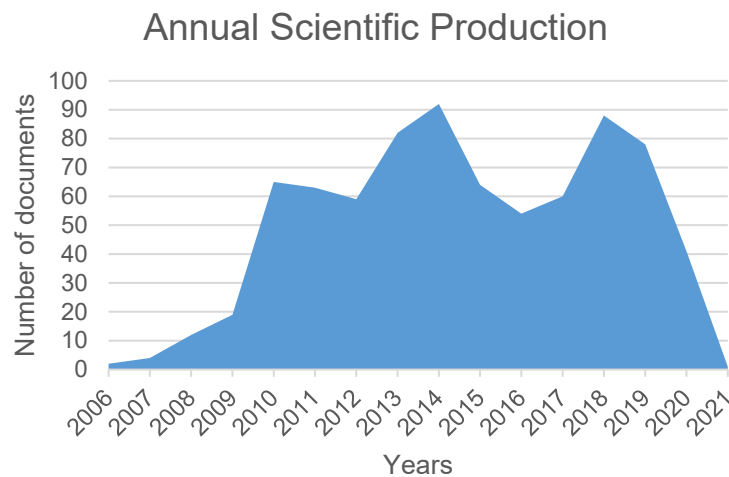


Fig. 32 - Annual scientific production realized with *Biblioshiny* using metadata for “Bees Algorithm” keyword  
 [source: SCOPUS]

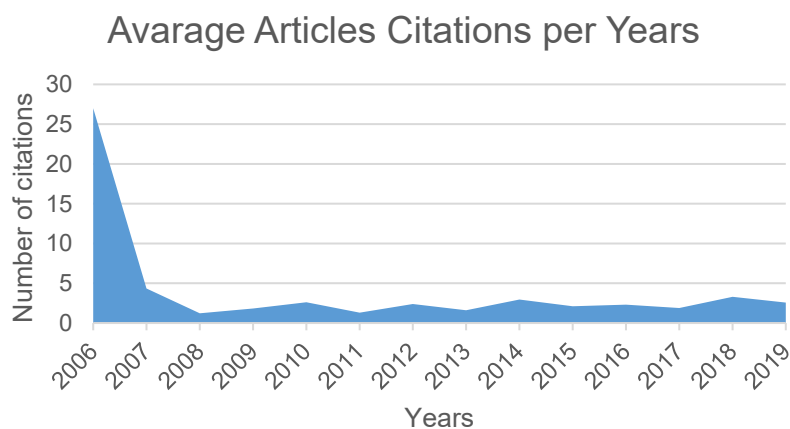


Fig. 33 - Average article citations per year realized with *Biblioshiny* using metadata for “Bees Algorithm” keyword  
 [source: SCOPUS]

The algorithm uses a population of agents, "a family of bees", to explore the whole space of possible solutions. A part of the population, "the exploratory bees", randomly searches around regions with high suitability of results, i.e. "global research". Exploratory bees that find areas with abundant availability of pollen, nectar or sugar secretions are the most successful agents. They recruit a variable number of inactive agents, the "foraging bees" to search for the most suitable solutions, i.e. "local research". The global and local search cycles are repeated until an acceptable solution is discovered, the equivalent of a zone in full bloom, or a certain number of iterations have passed, in nature the limit of interactions is sunset [148].

The bee algorithm requires specific parameters to define:

- number of exploratory bees;
- size of the search areas, including the sites and their immediate vicinity;
- number of sites selected from all the sites explored;
- number of the best sites, chosen among those selected;
- number of foraging bees recruited for the collection at the best sites among those selected;
- number of foraging bees recruited for collection from the remaining selected top sites;
- criteria to end the search [147].

Fig. 34 describes the flowchart of the BA. There is the random initialisation phase in which the scout bees are randomly positioned throughout the space. This landscape is a matrix of solutions, and each is associated with a position. This position is a site that evaluated using the fitness function. This stage known as Fitness Evaluation. The sites scored by the bee scouts ranked, and those with better values in relation to the research objective are the best sites. The local research phase then begins with foraging bees going to the area of the sites selected by the bee scouts. Communication between the scout bee and the foraging bee takes place through "waggle dance" [147,148]. The waggle dance is a term used to describe a particular dance in the shape of eight bees. By performing this dance, whose movements are correctly coded, the worker bee can communicate to her companion's valuable information about the nature, position and degree of interest of a resource she has discovered, such as nectar and pollen flowers, water springs or new nesting sites [165]. This dance is, therefore, the mechanism by which bees can recruit other bees from their hive to collect resources. The waggle dance consists of the repetition of a variable number of circuits, each of which consists of two phases: the oscillatory phase and the return phase. When a bee finds a source of food, it returns to the hive and, excited by the discovery, performs this dance among the other bees. The oscillatory phase indicates the call to the foraging bees to indicate the presence of food in the direction of the path made in this phase. The oscillatory phase corresponds to a straight line made by oscillating the abdomen.

Ing. Salvatore Conte

The return phase consists of a right turn to return to the starting point [166]. This dance repeated in the opposite direction. The length of the oscillatory phase then indicates the distance from the resource [167]. Fig. 35 shows the waggle dance.

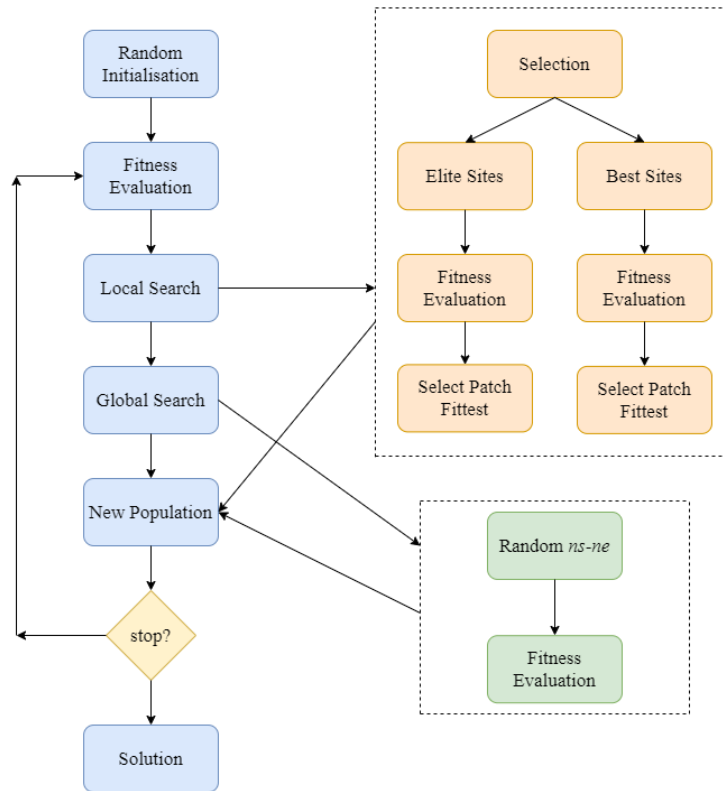


Fig. 34 - Bees algorithm flowchart [148]

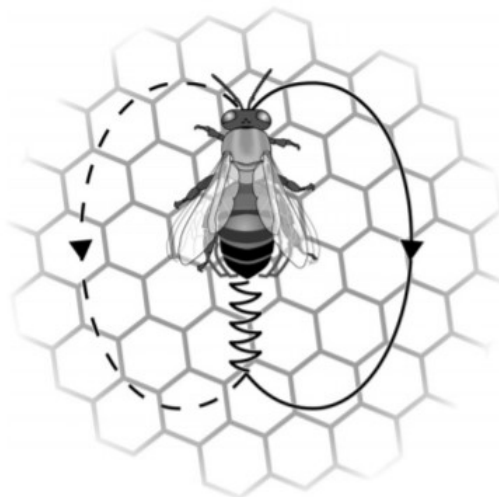


Fig. 35 - The waggle dance performed by a bee [166]

Some of the best sites named elite sites. Here the scout bees attract foragers to search around these sites. The remaining foraging bees are called by the other bees in the best sites to do a local search. The local search is intense near the elite sites where the largest number of foraging bees are concentrated. The fitness function regulates the determination of the sites may be better and worthy of being selected as elite [147]. The neighbourhood identified as flower patch. For each flower patch, the suitability evaluated. If a bee is in a position with better values than another is, the bee converted into a bee scout. This takes place until the end of the cycle and at that time the best solution found is used as a representative of the entire neighbourhood [148]. The next step after the local research phase is the global research phase. The remaining bee scouts compared to those who have identified the best sites placed randomly on the fitness landscape to find new flower patches. At the end of this phase, there will be two groups of new populations—one generated by local research and another generated by global research [147,148].

## 4. ACTIVITY ON GRINDING OPERATIONS

In this chapter, you will see the application of supervised and unsupervised neural networks to case studies related to grinding operations. The grinding process is a cutting process that affects the surface of the machined object. Grinding is, therefore, a surface finishing operation. The study linked to the optimisation of the process and a better understanding of it has produced countless research activities. In the SCOPUS database, in the last 100 years, i.e. since 1921, 58'165 documents have been produced, including scientific articles, conference proceedings, books, book chapters, reviews, etc. In Fig. 36, it is possible to see the progress up to 2021, considering the work in press on 10 November 2020.

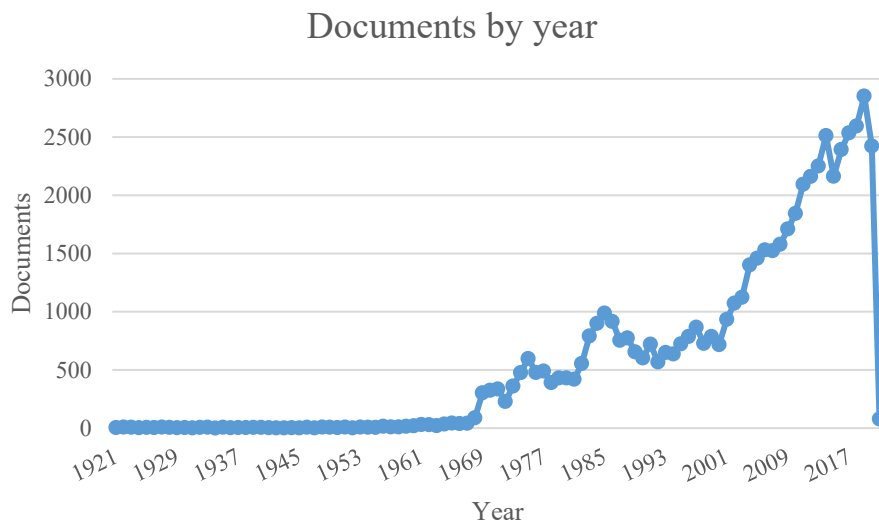


Fig. 36 - Trend in scientific production related to “Grinding” in the period 1921-2021 [source: SCOPUS]

From a technical point of view, the grinding operation involves the removal of part of the surface material of a workpiece utilizing a grinding wheel. The grinding wheel is the critical element of the operation. It is generally a wheel of ceramic matrix, which inside have abrasive grains dispersed. The nature of the grains may be different, as may the material have used for the grinding wheel matrix. As shown in Fig. 37, some of the grains are in contact with the material to process during the grinding operation. The grains called active grains, remove part of the material from the surface generating small pieces of the chip. The operation generates heat and the forces involved are very high. This leads to the breaking of these grains. It is evident how the grinding wheels tend to wear with machining. The removal of a layer of active grains promotes the release of new grains previously present within the grinding wheel matrix. This operation takes place automatically by exploiting the

wear of the wheel matrix itself. Very often, however, this regeneration of the grinding wheel is not efficient, mainly if it is not controlled. For this reason, there is a process known as dressing.

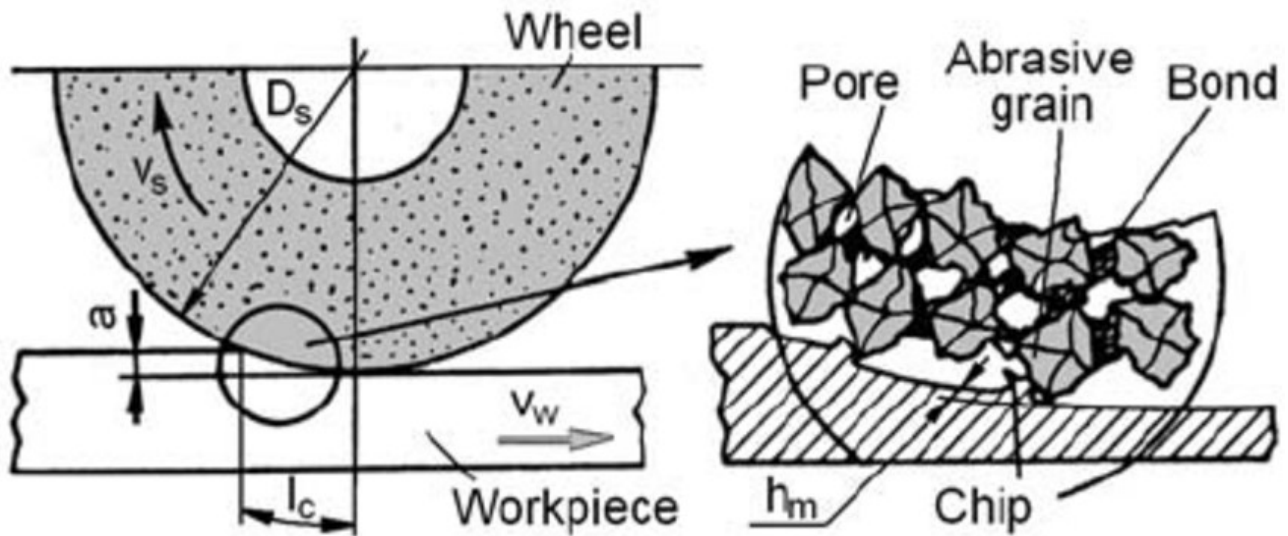


Fig. 37 - Mechanism of grinding process [168]

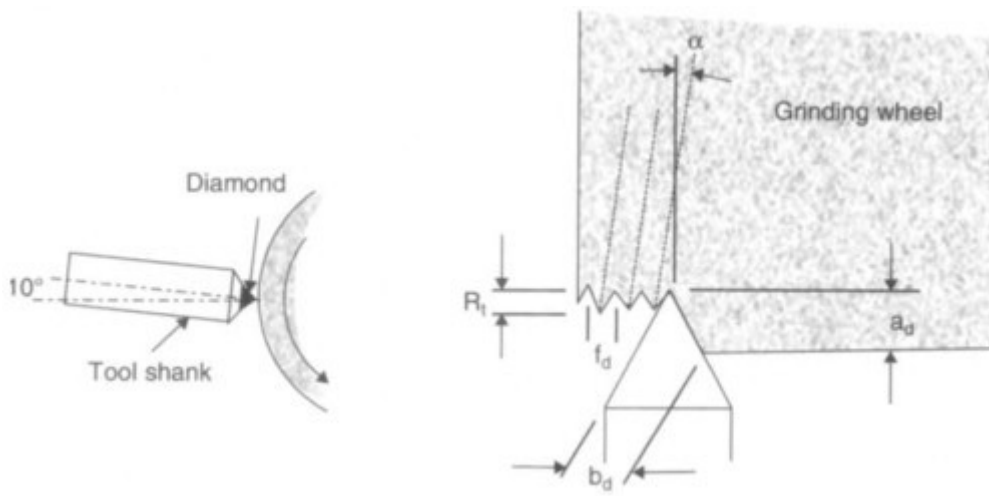


Fig. 38 - Single-point dressing with a stationary non-rotating dressing tool [169]

The dressing operation allows you to give the grinding wheel back its sharpness. It is, therefore, a fundamental operation to which the useful life of the grinding wheel is closely linked. The operation carried out thanks to a dresser, generally a diamond dresser. A dresser is a cylindrical tool whose end has a conical shape. This end is the one in contact with the abrasive wheel during the dressing operation. Fig. 38 shows an example of a single-point dressing. The finishing aspects include mechanical processing to eliminate changes in the specified shape or straightness, sharp cutting

surfaces, and evenly or evenly distributed cutting edges. Dressing removes the bond around the abrasive particles and forms a more open-wheel surface. This is especially important for super abrasive resin bonding and vitrified grinding wheels. Sometimes try to use cemented carbide or alumina abrasive rods for conditioning. Extensive use of grinding rods will abrade the abrasive in the grinding wheel and shorten the maintenance life. Another technique is to use a grinding wheel to perform the grinding process at a reduced cutting speed until it turned on. Clean to remove a layer of abrasive filled with workpiece material [169]. Stationary tools and rotary tools are the two basic types of dressing tool [170]. Fixed dressing tools include single-point diamond and impregnated diamond dressing tools, which mainly used to dress traditional abrasives. Such tools come in many shapes, including round and knife-shaped tools for trimming [169]. This thesis will only focus on single-point dressing as the operations performed with this tool. The single-point dresser is set in a tool holder that rotates regularly to provide different edges for dressing operations. If the handle does not rotate, the diamond will be worn severely on one edge, which will seriously reduce the dressing efficiency. If used correctly, single-point dresser can provide excellent trimming performance. For larger wheels, it is necessary to use a larger diamond to cope with the dressing action. For a wheel with a diameter of 500 mm, the smallest dressing tool is a 1-carat diamond. Single-point finishing tools are available in the form of 60 tapers for best sharpness or other shapes. Fig. 38 shows the dressing process parameters of the single-point dressing tool. For the sake of clarity, the point showed as sharp, although in practice, the included angle is usually much larger than the actual example shown, and the trim point is usually round. If you use a multipoint tool, the process is roughly the same. Large natural diamonds are most suitable for dressing large wheels. In order to ensure a vibration-free dressing, the tool holder allows the tool handle to be set to a drag angle of about 10 degrees. Moreover, the tool holder must be firmly installed in the tool holder. The resulting shape also depends on the width of the dressing tool  $b_d$  engaged with the grinding wheel. Due to the wear during the dressing process, the dressing diamond quickly forms a flat shape at its tip. This has the adverse effect of increasing the dressing force and decreasing the accuracy of the dressing process. The effect of diamond wear can reduce by rotating the diamond 90 around its axis at frequent intervals. Ideally, each skirt should be worn at most once. In practice, this ideal process may be challenging to maintain for a long time. Ideally, precision production grinders may be able to automate the diamond rotation process [169].

$$U_d = b_d / f_d \quad (\text{Eq. 9})$$

Eq. 9 shows the expression of overlap ratio, where  $b_d$  is the width of the dressing tool and  $f_d$  is the dressing feed per revolution of the grinding wheel. Fig. 38 shows these parameters. A higher overlap

ratio can make the surface of the grinding wheel smoother, but it will result in a higher grinding force and higher material removal energy. A lower overlap ratio value will make the cutting surface of the ground workpiece sharper and the surface roughness higher. The smoothness of the grinding wheel also depends on the sharpness of the dressing tool, which can be determined in the following ways:

$$\gamma_d = a_d/b_d \quad (\text{Eq. 10})$$

In Eq. 10,  $a_d$  is the dressing depth of cut [170]. A type of wheel wear is one that can have a catastrophic impact on grinding performance. This is wheel clogging or wheel loading. Clogging is a place where the workpiece material adheres to the tip of the abrasive grain and makes it repeatedly contact the material. If long workpiece chips fill the abrasive hole and remain there, clogging can also occur. The consequence of clogging is that the surface texture of the workpiece is inferior, the grinding force increases and the wear of the grinding wheel increases. Even a small amount of clogged material adheres to the tip of the die or remains in the surface of the grinding wheel, which will result in an inferior surface texture of the grinding workpiece. When the grain material and the working material have a chemical affinity, adhesion is a particular problem. When a fine-grained grinding wheel with low porosity used to grind soft, malleable materials, the problem of wheel clogging increases. To avoid clogging, it is essential to use sufficient coolant with useful lubricating properties. Other measures that can help solve the problem include increasing the wheel speed or reducing the depth of cut, choosing active slurry additives or replacing the abrasive [169,170].

In the next sub-paragraphs, the problems described above will be address using smart monitoring techniques and artificial intelligence techniques. The aim is to determine the correct timescales for dressing work on dressing tools. In real-time monitoring, supervised neural networks will be develop to determine the wear status of the grinding wheel. The techniques and experiments used to reach these determinations will be different, passing from data acquired via acoustic emission to data acquired through the pressure exerted on a low cost piezoelectric. All the tests carried out in collaboration with the Universidade de São Paulo, owner of the instruments used for the tests.



## 4.1. TOOL CONDITION MONITORING VIA ACOUSTIC EMISSION

Grinding processing are generally one of the last operations on the workpiece. These processes are not necessarily limited to surface finishing or removal of small quantities of material. They can use to remove large amounts of material and can compete in economic terms with processes such as milling and turning. The wear of the grinding wheel is more important because it adversely influence the shape and accuracy of the surfaces machined with this process [171]. A solution for this problem is the online monitoring of the grinding wheel conditions [172]. For the online monitoring of the grinding wheel, it is necessary to use sensors that acquire information about the performance of the grinding wheel. Such sensors can be sensors of force, vibration, current, acoustic emission (AE), etc. The sensors can control the dressing process. This is the process of grinding wheel surface restoring and it consists in eliminating worn grains in order to expose new sharp grains. Dressing is necessary when excessive friction wears the grinding wheel [171].

It is possible to correlate the AE produced by the dressing process to the exact point in which to stop the process. To do this, it is possible use Artificial Neural Networks (ANNs) to decisions making. ANN models have already been employed to predict the dressing wear of grinding operations on the basis of the measured AE signals and, furthermore, working parameters of cutting operations [173,174].

### 4.1.1. CASE STUDY

Numerous preliminary tests carried out to define the best parameters to used, according to the dressing conditions established for this test and considering the need to ensure the digital processing of the signals, analysis and discussion of the results. Therefore, an experimental test setup built and configured to allow process output variables to obtain with quality. In the exams, an aluminium oxide-grinding wheel used, from NORTON, model 38A150LVH, with dimensions of 355.6x25.4x127mm. It assembled on a surface tangential grinding machine; model RAPH 1055, from Sulmecânica. The acoustic emission (AE) sensor linked to a signal-processing module is the model Sensis DM-42. The AE sensor attached to the dresser holder, which specifically developed to perform dressing tests. The DM-42 module associated to an oscilloscope from the company Yokogawa is the model DL850. The module acquired an AE signals at a sampling frequency of two million samples per second. The dressing tool used was the CVD single-point diamond. The parameter  $b_d$  measured before the

beginning of each dressing test. The parameter is the width of action of the dresser for a given depth of dressing ( $a_d$ ).

To measure the sharpness of the grinding wheel, the method proposed by Nakayama et al. [175], Fig. 39, was used. This method provides for the use of a weight balance scale (an equipment similar to a seesaw) so that at one end is held fixed (without rotation) a cylindrical disc. The disc remains in constant contact with the cutting surface of the grinding wheel because of due to the force  $F_N$ , equal 1N, of known weights fixed on the opposite side of equipment. The movement of the grinding wheel generates wear on the disc, which consequently causes a displacement over a given contact time. A TESATRONIC recorded the displacement in time and collected by serial communication using MatLAB software. The TESATRONIC was a model TT60, from Tesa Technology. The sharpness of the grinding wheel is determined at different times of the test; at each time, four displacement curves generated as a function of time at 4 points along the cutting face of the grinding wheel. Eq. 11 determine the sharpness values ( $K$ ) for each displacement curve and the standard deviation. From these values, it is possible to calculate the average of the sharpness of the grinding wheel.

$$K = \frac{2b\sqrt{8r}}{3F_N} \cdot a^{\frac{2}{3}} \quad (\text{Eq. 11})$$

In Eq. 11  $b$  and  $r$  are the width and radius of the disc, respectively,  $F_N$  is the normal force applied on the opposite end of the disc, and  $a$  is the gradient of the regression line obtained from the characteristic of displacement curve versus  $(t)^{2/3}$ , and lastly  $t$  is the experiment time or contact time. The cylindrical discs used in the process of acquiring the sharpness curves was from a cylindrical bar of SAE 1020 steel. The measure was: external diameter was 24 mm; internal diameter was 7.8 mm; and with was 2 mm.

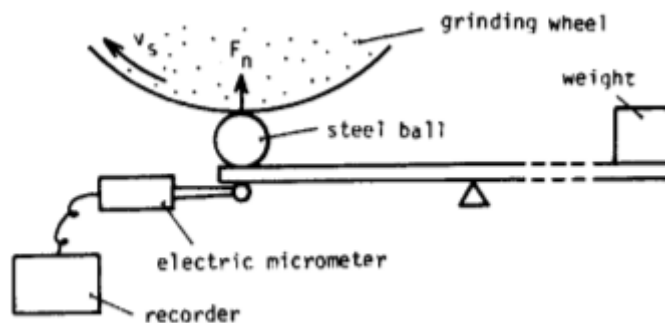


Fig. 39 - Scheme of Nakayama test [175]

Fig. 40 (a) shows the sharpness curves for two different grinding wheel conditions. Fig. 40 (b) is an amplification of the grey region of Fig. 40 (a). In that area, the sharpness of the grinding wheel computed. According to [176], sharpness is the measure of a body's capacity to remove material from another. Fig. 40 (a) shows that the sharpness curve for the undressed and uneven grinding wheel condition makes a small  $\alpha$  angle with the time axis. That happens because the grinding wheel has its sharpness degraded. Thus, its capacity to remove material from the workpiece is low. This occurs due to the clogging of the cutting face of the grinding wheel, caused by chips. In addition, the wear of the abrasive grains during the grinding process also contributes to a reduction in the material removal capacity of the grinding wheel. On the other hand, for a fully dressed and even grinding wheel, the sharpness curve forms a high  $\beta$  angle with the time axis. This indicates that the grinding wheel is sharp because of its high capacity to remove material.

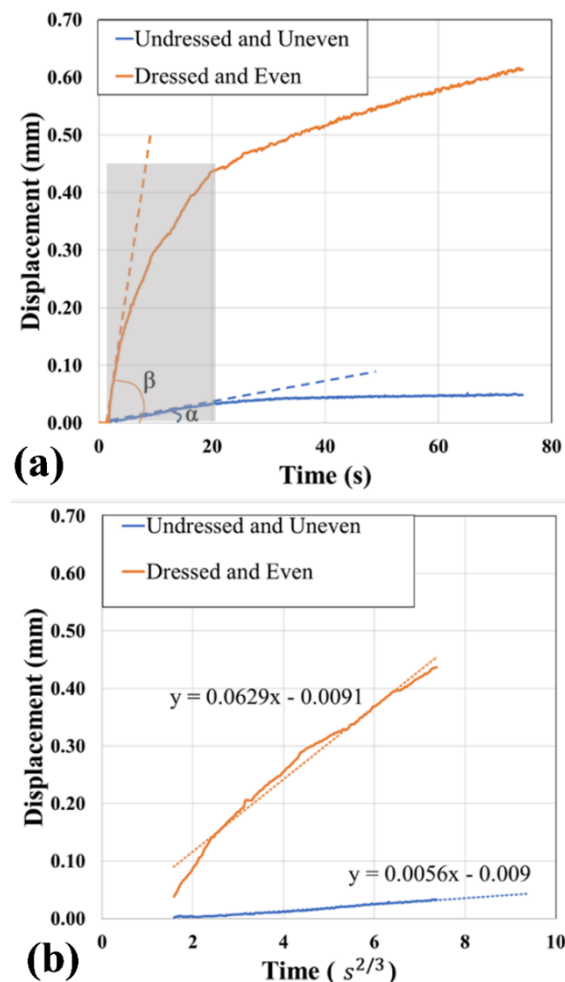


Fig. 40 - Displacement Curve vs  $T(2/3)$  [174]

There are three steps for the process of clogging and dressing of the grinding wheel:

- Dressing performed with an overlap ratio ( $U_d$ ) of 1.5 and  $a_d$  equals to 10  $\mu\text{m}$ , consisting of 10 consecutive passes from the moment when the wheel surface was already cleaned after the last pass, the sharpness was measured;
- Planning the clogging of the grinding wheel, it grinds an SAE 1020 steel workpiece, with dimensions of 150x48x12 mm. The grinding process provided 20 passes with cutting depths of 20  $\mu\text{m}$ , and constant peripheral speed of the grinding wheel equal to 33 m/s. The workpiece speed was equal 0.098 m/s. After the grinding, the sharpness of the grinding wheel was measured by the system described above;
- After the grinding operation, dressing performed on the wheel with  $U_d$  equals to 1.5 and  $a_d$  equals to 10  $\mu\text{m}$ , which consisted of 24 consecutive passes. The collected signals of raw AE come from the measurement during the test, and the sharpness measured after the last pass.

During the dressing and the grinding tests, there is not the cutting fluid. In Table 15 and Table 16 there are the parameters of each dressing test:  $v_d$  is the dressing speed;  $b_d$  is the width of action of the dresser;  $t_d$  is dressing time;  $K_0$  is the sharpness measured before the start of the dressing test;  $K_f$  is the sharpness at the end of the dressing test (last dressing pass). Table 17 shows the classifications of the different grinding wheel conditions achieved during the tests 15, 16 and 17.

Table 15. Parameters of dressing test [177]

N° TEST	Passes	$v_s$ (m/s)	$v_d$ (m/s)	$b_d$ ( $\mu\text{m}$ )	$t_d$ (s)	$U_d$
TEST I	24	33	0.0098	520	2.6	1.5
TEST II	10	33	0.0098	520	2.6	1.5
TEST III	17	33	0.0069	365	3.7	1.5

Table 16. Parameters of dressing test [177]

N° TEST	Passes	Sharpness ( $K_0$ ) ( $\text{mm}^3/\text{N}^* \text{s}$ )	Sharpness ( $K_f$ ) ( $\text{mm}^3/\text{N}^* \text{s}$ )
TEST I	24	0.569	2.854
TEST II	10	2.437	2.796
TEST III	17	1.987	2.695

Table 17. Classification of the different grinding wheel conditions [177]

Condition	TEST I	TEST II	TEST III
Undressed and Uneven	Passes 1-9	-	Passes 1-9
Dressed and Uneven	Passes 10-14	Passes 1-4	Passes 10-14
Dressed and Even	Passes 15-24	Passes 5-10	Passes 15-17

The raw AE signal was initially analysed to select only the period corresponding to the dressing process (dressing pass only). Then, there was the analysis of the signal in the frequency domain in order to identify specific frequency bands that best characterized the behaviour of the process. There were two spectrums for the different conditions of the grinding wheel (dressed and even; undressed and uneven). The discrete Fourier transform (DFT) derived from 9 points equidistant from the dressing pass. Using the fft command and the Hanning window, MatLAB processed nine vectors of 32'768 points and obtained the average of the spectra. This represents the spectral behaviour of the dressing pass. The analysis of the spectra referring to two conditions of the surface of the grinding wheel made it possible to select a band of frequencies using the criterion of non-overlap between the spectra. After analysing the signals, the selected band for study was that between 25 kHz and 40 kHz. A 2'048-point window, corresponding to 1 ms, as suggested by [174], was used. The ROP statistic was defining from the non-filtered signals, since this statistic uses a "self-filtering". For obtaining the Counts statistics, a Butterworth digital filter, bandpass of order 30, in the selected band of 25 to 40 kHz, filtered the raw AE signal. A threshold of 100 mV calculated the statistics Counts for all the tests [174].

The results from the digital processing of the AE signals show the changes of the spectral content. They depend by the shape and sharpening characteristics of the grinding wheel. In the spectrum of the Fig. 41, two different conditions of shape and sharpening of the grinding wheel presented are:

- undressed and uneven grinding wheel;
- dressed and even grinding wheel.

The spectrum of each condition of the grinding wheel express different energy levels, how show the Fig. 41. The grinding wheel without cutting capacity and uneven surface produces low energy levels over the entire significant frequency range (0-250 kHz). This is due to the low friction between the dressing tool and the grinding wheel. In that condition, the grinding wheel has its abrasive grains worn. On the other hand, the dressed and even grinding wheel generates higher energy levels, because the cutting edges of the grinding wheel exposed in this condition. Therefore, the contact between the dresser and the grinding wheel is full, and this causes a high friction and a higher level of AE. The Fig. 41 shows the characteristics for the 25-40 kHz band, in the zoomed area of the picture.

Fig. 42 and Fig. 43 present the results obtained from the application of the ROP and COUNTS statistics for the 25-40 kHz frequency band. The two figures show the results, respectively, for two different conditions of the grinding wheel: undressed and uneven, and dressed and even. There are great variations of peaks and valleys in the ROP and COUNTS values and an uneven behaviour of these signals for a worn and dull grinding wheel. It is possible see this in Fig. 42. The variations of peaks and valleys is a consequence of the clogging rate by chips. In addition to the uneven cutting

surface and the abrasive grain wear of the grinding wheel, directly influence on the acoustic activity generated during the dressing operation. On the other hand, the ROP and COUNTS values for the dressed and uneven grinding wheel are uniformly. This means that the statistics maintain a virtually constant energy level throughout the dressing pass. This occurs because at this stage, the grinding wheel is conditioned and its contact with the dresser is full and uniform. This generates more acoustic activity.

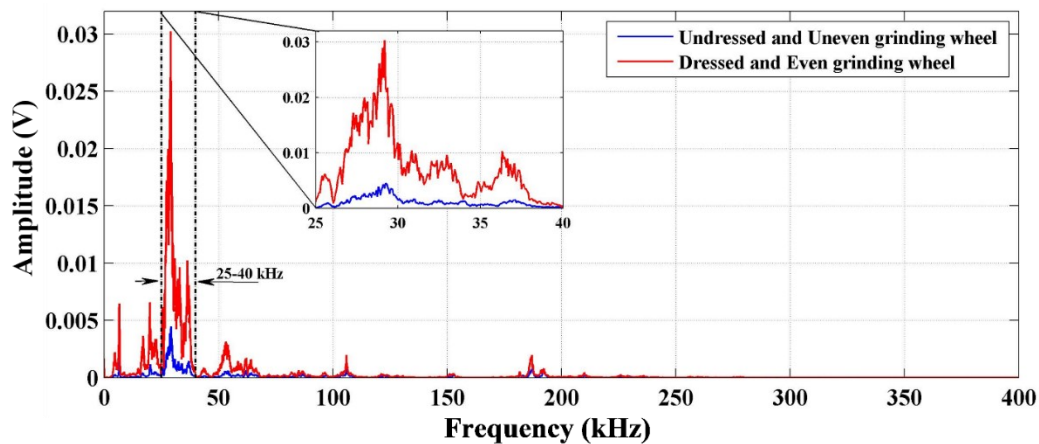


Fig. 41 - Spectrum of frequency for two conditions of the grinding wheel [174]

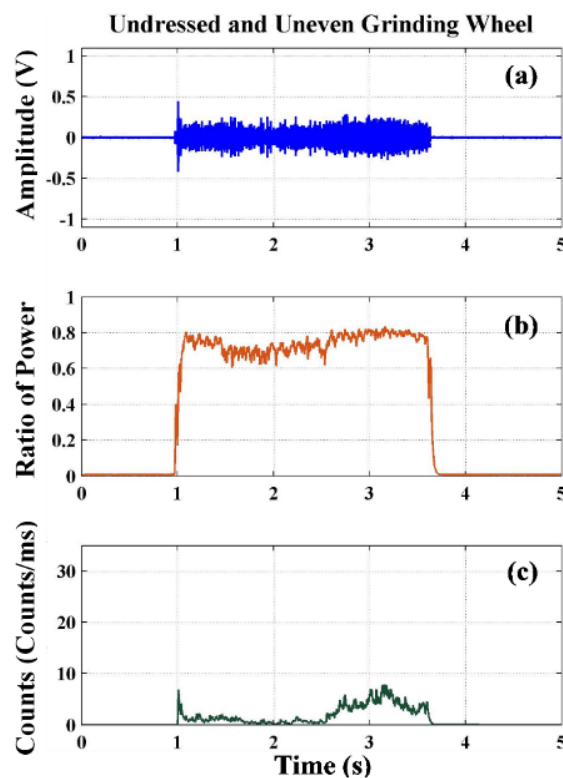


Fig. 42 - Undressed and uneven grinding wheel condition [174]

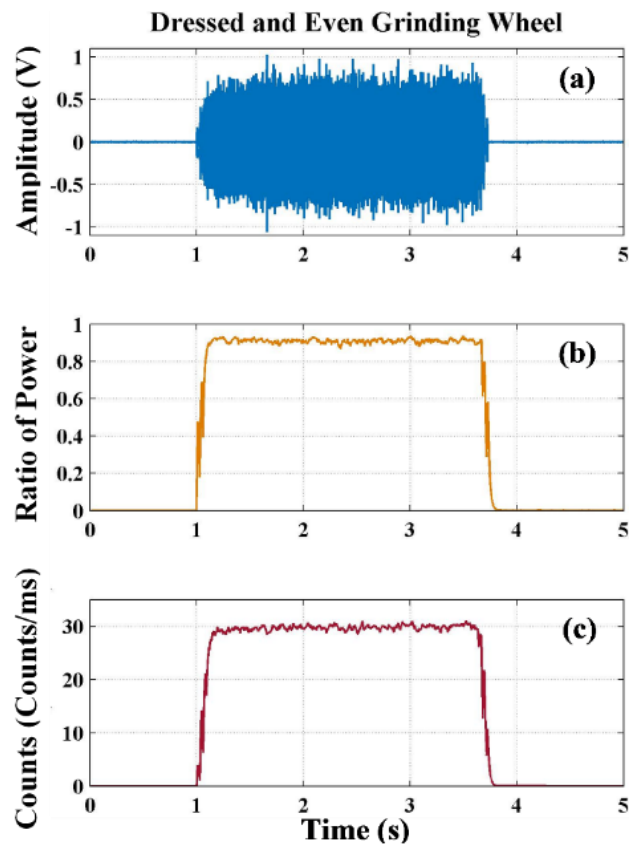


Fig. 43 - Dressed and even grinding wheel condition [174]

### 4.1.2. NEURAL NETWORK MODELS (SUPERVISED)

The performances of a neural network could sensibly change in function of the input parameters, network function, training function, number of nodes and epochs [172]. The ANN model based on every single points of AE waves and the passes number. MatLAB offers a specific tool for supervised Back Propagation neural network. This tool is called "Neural Net Pattern Recognition" and the user can use it by the application software's section or by the command "nctool" [174]. In order to work, the tool needs of an input matrix and a known output matrix or target matrix. These arrays must be in a specific way. Each AE wave data vector of a single pass compose the data from digital signal processing phase. Every single pass has a vector with COUNTS and ROP information. Neural Net Clustering APP needs to a matrix with all vectors of a test. In order to use the application, it is necessary to make two matrixes for every test: one matrix for COUNTS and one matrix for ROP. This is possible with a dedicated MatLAB script. This script uses *for loop* for open all vectors and saves them in a matrix. The script makes a folder in the main directory containing the vectors and it saves the generated matrix in this folder as .mat file. The generated matrices have passes as rows and the point's value of the wave of the passes as column, to design correctly the neural network. The first thing to do is to determine the number of hidden layers to include between the input layer and the output layer. In accordance with [172], the choice of the number of layers for the hidden layer is one. Once that is done, you need to determine the number of processing elements of each layer on the network. If the network is hetero-associative, the number of artificial neurons in the input layer coincides with the number of elements making up the characteristic input vector, excluding the desired outputs. If the network is self-associative, the desired outputs automatically identified with the input values and, therefore, the number of artificial neurons in the input level coincides with the number of elements constituting the input characteristic vector. In this case study, it is a self-associative network. In fact, the target matrix is characterised by the number of conditions as rows and the number of passes as a column. The conditions are Undressed and Uneven (UU), Dressed and Uneven (DU) and Dressed and Even (DE). Every condition in this matrix is indicated with 1 value. The reason for all this is related to a Boolean value (1 is true, and 0 is false). There is no valid theory for the choice of the number of processing elements in the hidden level; usually, this number obtained by trial and error. The number of neurons making up the hidden layer depends on the nature of the actual data entering the network. The information sent into an artificial neural network can be either behavioural or experimental. Behavioural information comes from different aspects of human behaviour, e.g. stock market index data is an indirect measure of human economic behaviour. The practical information comes directly from measurements made on physical quantities that characterise

Ing. Salvatore Conte



the phenomenon under observation. In this case study, it is dealing with practical information. In the case of experimental data, there are no restrictions on the number of neurons in the hidden level. It has been shown that by increasing the number of neurons in the hidden layer the performance of the network improves, this occurs until a limit value is reached above which the network operation declines [178–181]. Typically, it is necessary to test multiple networks with a different number of neurons in the hidden layer before reaching the operational neural network. Typically, you start with two neural networks with respectively 5 and 25 neurons in the hidden layer. They compared with each other; if the one with five neurons is better than the number of hidden neurons has been identified. If the network with 25 neurons is better, then the network with five neurons discarded and the network with 25 neurons compared with a new network with 50 neurons in the hidden layer. Repeat this in steps of 25, until you find the limit value above which it is useless to increase the number of neurons in the hidden layer, as this would only lead to a deterioration in performance. Suppose that this limit is 50, and then it knows that the number of neurons in the hidden level must be between 25 and 49. It then compares the net with 25 neurons with one with 37 neurons and repeat the above reasoning until we find the best value for the number of hidden neurons [180]. Once you have chosen an initial structure for the network, you must select the training rule and the type of transfer function used by the individual processing elements. Thanks to Eq. 12, it obtains Fig. 44 that describes the best number of neurons for hidden layers.

$$success\ rate = \frac{T_1 \cdot (sr_1^C + sr_1^R) + T_2 \cdot (sr_2^C + sr_2^R) + T_3 \cdot (sr_3^C + sr_3^R)}{2 \cdot (T_1 + T_2 + T_3)} \quad (Eq. 12)$$

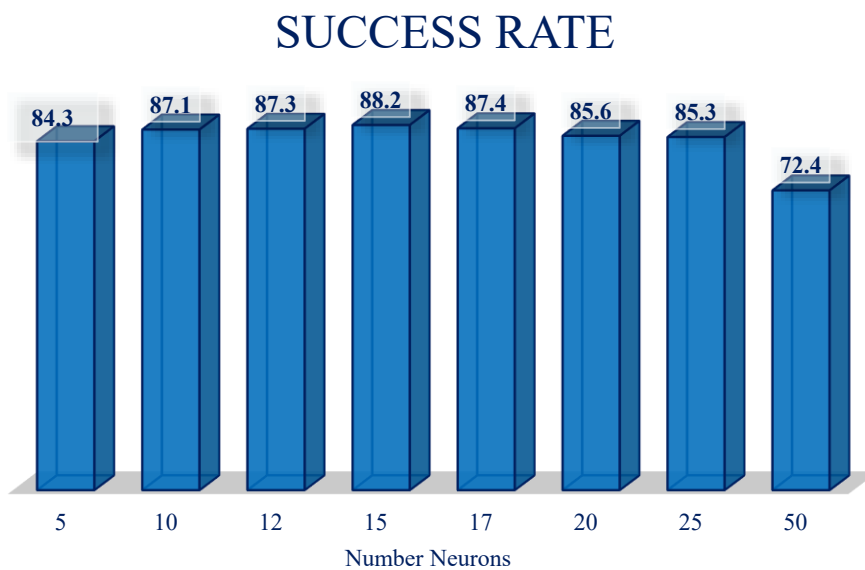


Fig. 44 - Histogram of the success rate relative to the number of neurons for the hidden layer

In Eq. 12,  $T_n$  is the number of rows for test  $n$ ,  $sr_n$  is the success rate for test  $n$ ,  $C$  is the number of COUNTS and  $R$  is the ratio of power. The best solution is 15 number neurons for hidden layer. The connection weights are changed only after the presentation of  $n$  training pairs, with a total number of incoming cases; the value of  $n$  is called epoch and is fixed in advance. The increments associated with each pair presented accumulated and then applied overall to the  $n$ -th presentation. If the epoch is not very big, the cumulative technique allows speeding up the learning phase, because if you update the weights regularly after each presentation of a pair, you reduce the error associated with it. However, it can increase that of the other pairs. Updating the weights cumulatively has the effect of reducing the overall error without favouring the particular pair. On the other hand, modifying a weight will require a more significant number of operations, so if the time is considerable, you may lose the advantage of a higher speed in the learning process. The surface of the global error is multi-dimensional compared to the connection weights; the trend in each dimension can be very different. In the training phase, an update can be appropriate for one weight, while it is not for another; this suggests that it is not correct to modify the connection weights of a network with the same value. Since the change in connection weights depends on the learning rate, the ideal would be to be able to assign a special learning rate for each change in a connection weight and to be able to control it as the learning progresses. Determining the optimum value of the learning rate and how it should be changed over time for the individual connection weights is very difficult and time-consuming. In recent years a heuristic technique has evolved, which suggests how to determine this value automatically; it based on the following considerations. Suppose for several consecutive training steps, the changes of a connection weight are of the opposite sign. In that case, the global error concerning this weight characterized by a graphic point of view by a considerable curvature. Therefore, the learning rate must decrease (Fig. 45a). If for several consecutive training steps, the changes of a connection weight are of the same sign, then the global error concerning that weight is graphically characterised by a small curvature. Therefore, the learning rate must increase (Fig. 45b). If we consider a network with only one output, the learning procedure synthesises a continuous function starting from discrete sets of input values. In other words, during the learning phase, the network configures itself to provide the desired output to a particular input. During the test phase, when an entirely new input is presented, the network performs a non-linear interpolation in order to provide good output [182–185]. According to [160], the chosen transfer function is the logistic (Table 10). After choosing the training rule and the transfer function, the training pairs must specify. If the same set of data were to use in the test phase and the network training phase, this would only show how well the network has stored the training set.

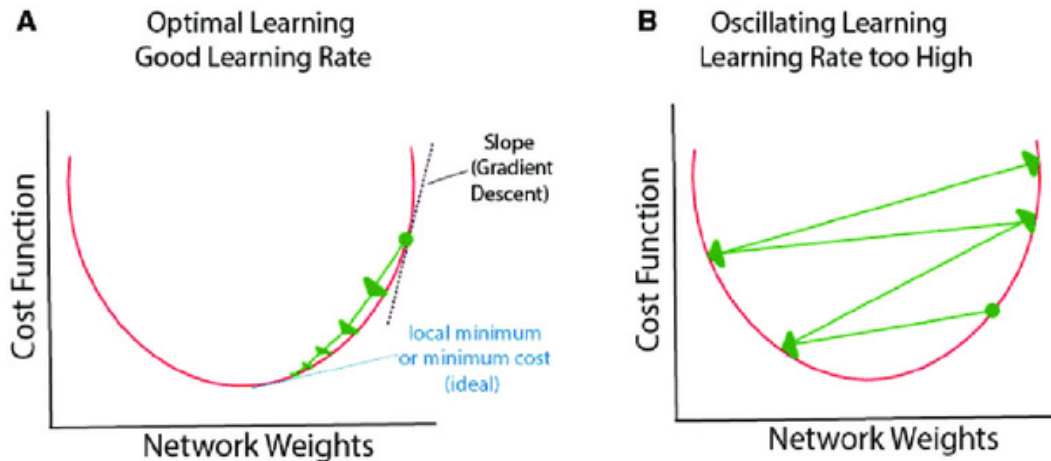


Fig. 45 - Learning rate: A) Efficient learning. The cost function (network error) gradually decreases ("gradient descent") to achieve an optimal point (called a local minimum) as a function of weight.

B) The learning rate is too high, so the cost function exceeds the minimum value and oscillates. For this problem, this network design may not be effectively trained. [186]

In most cases, one is interested in creating networks that generalize new input situations, which is why the complete set of data available divided generally into a training set and a test set. In cases where the number of cases available for training is high, a part of them used for the learning phase, the remaining part for the interrogation phase. In case the number of examples available for learning is low, the *leave-K-out* procedure is generally used [187,188]. If  $n$  is the total number of characteristic vectors, the leave-k-out procedure consists in training the network with  $n-k$  ( $k < n$ ) vectors and testing it with the remaining  $k$ ; this is repeated considering all the  $k$ -couple extractable from the training set. This technique makes it possible to evaluate the actual performance of the network; during the interrogation phase, the network, in practice, responds to stimuli never seen before. If  $n < 20$  it is advisable to choose  $k=1$  if  $n > 20$  the choice of  $k$  depends on the type of application and the designer. Assuming that  $n$  is divisible by  $k$ , it is necessary to modify the initial training set available to make proper use of the leave-k-out procedure, i.e. it is necessary to extract  $n/k$   $k$ -couple of characteristic vectors from it, to obtain  $n/k$  pairs of training and test sets [187].

Fig. 46 - 51 show respectively the confusion matrices for TEST 1 COUNTS, TEST 1 ROP, TEST 2 COUNTS, TEST 2 ROP, TEST 3 COUNTS and TEST 3 ROP. In the matrices, the green diagonal represents the classification success carried out by the neural network. In those cells, the superior number is the number of samples classified for each given class, and the inferior number is the percentage of those samples related to the total of samples. The red cells in the matrixes is the error of the ANN models and it might be considered (false positive or false negative) for each given class.

Table 18. Input ANN – COUNTS TEST 1

	Time (ms)								
<b>Passes</b>	<b>1</b>	<b>2</b>	<b>3</b>	<b>4</b>	<b>5</b>	<b>6</b>	<b>7</b>	<b>...</b>	<b>2570</b>
<b>1</b>	0	0	0	0	0	0	0	...	0
<b>2</b>	0	0	5	0	0	0	0	...	0
<b>3</b>	0	8	13	6	2	8	10	...	0
<b>4</b>	0	0	0	0	0	0	0	...	0
<b>...</b>	...	...	...	...	...	...	...	...	...
<b>24</b>	0	0	0	0	0	0	0	...	0

Table 19. Input ANN – COUNTS TEST 2

	Time (ms)								
<b>Passes</b>	<b>1</b>	<b>2</b>	<b>3</b>	<b>4</b>	<b>5</b>	<b>6</b>	<b>7</b>	<b>...</b>	<b>2570</b>
<b>1</b>	0	0	0	0	0	0	0	...	0
<b>2</b>	0	0	0	0	0	0	0	...	0
<b>3</b>	0	0	0	0	0	0	0	...	0
<b>4</b>	0	0	0	0	0	0	0	...	0
<b>...</b>	...	...	...	...	...	...	...	...	...
<b>10</b>	22	21	0	0	0	0	0	...	0

Table 20. Input ANN – COUNTS TEST 3

	Time (ms)								
<b>Passes</b>	<b>1</b>	<b>2</b>	<b>3</b>	<b>4</b>	<b>5</b>	<b>6</b>	<b>7</b>	<b>...</b>	<b>3680</b>
<b>1</b>	0	0	0	0	0	0	0	...	0
<b>2</b>	0	0	0	0	0	0	0	...	0
<b>3</b>	0	0	0	0	0	0	0	...	0
<b>4</b>	0	0	0	0	0	0	0	...	0
<b>...</b>	...	...	...	...	...	...	...	...	...
<b>17</b>	0	0	0	0	0	0	0	...	0

Table 21. Input ANN – ROP TEST 1

	ROP								
<b>Passes</b>	<b>1</b>	<b>2</b>	<b>3</b>	<b>4</b>	<b>5</b>	<b>6</b>	<b>7</b>	<b>...</b>	<b>9727</b>
<b>1</b>	0.008	0.006	0.010	0.009	0.006	0.006	0.009	...	0.008
<b>2</b>	0.010	0.008	0.005	0.012	0.006	0.012	0.009	...	0.932
<b>3</b>	0.009	0.006	0.013	0.005	0.011	0.015	0.004	...	0.010
<b>4</b>	0.005	0.007	0.005	0.006	0.011	0.008	0.009	...	0.007
<b>...</b>	...	...	...	...	...	...	...	...	...
<b>24</b>	0.001	0.001	0.002	0.003	0.002	0.002	0	...	0.003

Table 22. Input ANN – ROP TEST 2

	ROP								
<b>Passes</b>	<b>1</b>	<b>2</b>	<b>3</b>	<b>4</b>	<b>5</b>	<b>6</b>	<b>7</b>	<b>...</b>	<b>9727</b>
<b>1</b>	0.001	0.002	0.002	0.003	0.005	0.004	0.004	...	0.002
<b>2</b>	0.004	0.005	0.003	0.003	0.003	0.004	0.003	...	0.004
<b>3</b>	0.006	0.008	0.007	0.005	0.016	0.007	0.004	...	0.008
<b>4</b>	0.003	0.005	0.001	0.002	0.003	0.003	0.002	...	0.002
<b>...</b>	...	...	...	...	...	...	...	...	...
<b>10</b>	0.002	0.002	0.003	0.004	0.003	0.004	0.004	...	0.004

Table 23. Input ANN – ROP TEST 3

	ROP								
Passes	1	2	3	4	5	6	7	...	9727
1	0.001	0.001	0.002	0.002	0.001	0.002	0.002	...	0
2	0.002	0.001	0.001	0.001	0.002	0.002	0.002	...	0.002
3	0.002	0.001	0.002	0.003	0.002	0.002	0.002	...	0.002
4	0.002	0.001	0.001	0.002	0.002	0.002	0.001	...	0.001
...	...	...	...	...	...	...	...	...	...
17	0.002	0.003	0.001	0.002	0.001	0.002	0.001	...	0.001

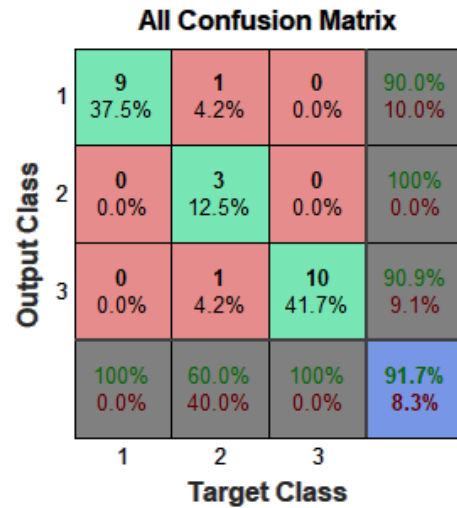


Fig. 46 - TEST 1 COUNTS confusion matrix [174]

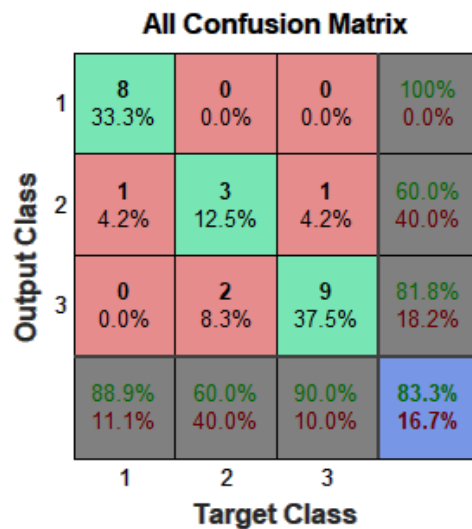


Fig. 47 - TEST 1 ROP confusion matrix [174]

**All Confusion Matrix**

Output Class	1	2	
	1	2	
	1	2	
1	2 20.0%	0 0.0%	100% 0.0%
2	2 20.0%	6 60.0%	75.0% 25.0%
	50.0% 50.0%	100% 0.0%	80.0% 20.0%
	1	2	
	Target Class		

Fig. 48 - TEST 2 COUNTS confusion matrix [174]

**All Confusion Matrix**

Output Class	1	2	
	1	2	
	1	2	
1	3 30.0%	1 10.0%	75.0% 25.0%
2	1 10.0%	5 50.0%	83.3% 16.7%
	75.0% 25.0%	83.3% 16.7%	80.0% 20.0%
	1	2	
	Target Class		

Fig. 49 - TEST 2 ROP confusion matrix [174]

**All Confusion Matrix**

Output Class	1	2	3	
	1	2	3	
	1	2	3	
	1	2	3	
1	9 52.9%	0 0.0%	0 0.0%	100% 0.0%
2	0 0.0%	5 29.4%	1 5.9%	83.3% 16.7%
3	0 0.0%	0 0.0%	2 11.8%	100% 0.0%
	100% 0.0%	100% 0.0%	66.7% 33.3%	94.1% 5.9%
	1	2	3	
	Target Class			

Fig. 50 - TEST 3 COUNTS confusion matrix [174]

**All Confusion Matrix**

<b>Output Class</b>	1	9 52.9%	0 0.0%	0 0.0%	100% 0.0%
	2	0 0.0%	5 29.4%	1 5.9%	83.3% 16.7%
	3	0 0.0%	0 0.0%	2 11.8%	100% 0.0%
		100% 0.0%	100% 0.0%	66.7% 33.3%	94.1% 5.9%
		1	2	3	
		<b>Target Class</b>			

Fig. 51 - TEST 3 ROP confusion matrix [174]

## 4.2. TOOL CONDITION MONITORING VIA IMPEDANCE

Different applications in civil, mechanical, and aerospace engineering projects often use structural health monitoring (SHM) systems. A SHM system offers important information on the structure condition in terms of damage occurrence, to ensure reliability and safety [189]. A typical SHM framework detects incipient damages and there are numerous approaches to reach this goal. Among them, there are non-destructive evaluation (NDE) methods. They focus mostly on vibration analysis and wave propagation. NDE are exalted because they are flexible in the application of various types of structures [190–192]. Recently, the electromechanical impedance (EMI) technique has become a promising tool within NDE methods. It uses smart piezoelectric devices and a low-cost methodology which identify small-sized damages [191,193]. The piezoelectric effect of lead zirconate and titanate (PZT) transducers coupled to monitoring structure is the basis of EMI technique [194]. The damage identification activities of EMI technique include:

- the excitation of the transducer in a suitable frequency range;
- the electrical impedance measurements of the transducer (response);
- the establishment of a relationship between the mechanical impedance of the structure and the electrical impedance of the transducer;
- the detection of possible damages through representative damage features;
- the diagnosis of the structure condition and its remaining useful life (cognitive systems can be used with this aim) [189,192,195,196].

Liang et al. [197] in 1994 were the first to develop the EMI technique based on the piezoelectric effect. From that data, a large number of experiments based on theoretical models were conducted by several researchers [198]. Many damage metrics or statistical indices [194] have been proposed to quantitatively identify structural damages based on EMI database. The root mean square deviation (RMSD) is the most common damage index. Furthermore, damage classification improvement methodologies based on EMI technique were developed. In this context there are previous studies on: wavelet transform [199], time-domain analysis [200], spectral element method (SEM) [201], numerical analysis (e.g.: finite element method (FEM) [202], and artificial intelligence [189]. The focus is to the damage classification enhancement methodology based on neural networks (NN). Many EMI-based SHM applications use multi-layer neural networks (MLNN) [203–205], probabilistic neural networks (NNP) [206], fuzzy ARTMAP networks [207], and more recently, convolutional neural networks (CNN) [208].



### 4.2.1. CASE STUDY N°1

Experimental dressing tests conducted in a surface grinding machine, model RAPH 1055 (Sulmecanica). It was equipped with an aluminium oxide-grinding wheel, model 38A150L6VH (specification of hardness, grain, flange and vitrification). Its dimensions were 355.6 x 25.4 x 127 mm. The researches of [209–211] are the basis of experimental tests. Fig. 52 shows a diagram of the proposed approach. The experiment used a synthetic diamond (chemical vapour deposition – CVD) single-point dressing tool. Each test consisted in dressing passes throughout the grinding wheel surface until the end of its lifespan. The main parameters were the constant dressing depth of 40  $\mu\text{m}$ , the constant dressing speed at 3.45 mm/s, the overlap ratio ( $U_d$ ) of 1 at the beginning of the test. The tests carried out without application of cutting fluid in order to cause a faster wear.

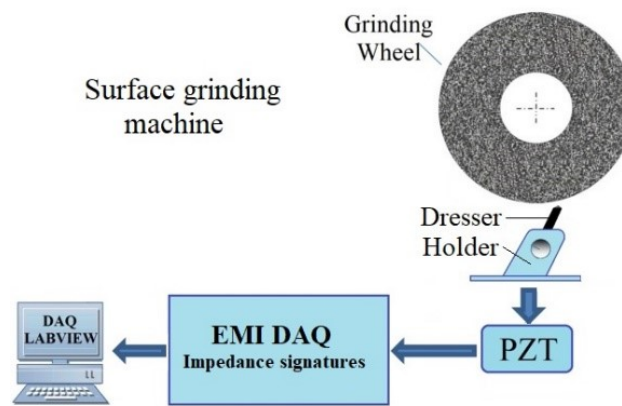


Fig. 52 - Experimental test bench and DAQ system [189]

Research [200] inspired the data acquisition system adopted. [200] considered the electromechanical impedance (EMI) technique, using the methodology proposed by [212]. Fig. 52 shows as the EMI data acquisition system. The DAQ device used was model NI USB-6221, from National Instruments. It acquired impedance signatures from a low-cost PZT transducer, mounted on the dressing tool holder, as shown in Fig. 52, at sampling rate of 250 kS/s. The PZT transducer was the model 7BB-20-6 low-cost diaphragm type, from MURATA [189]. It constructed of a circular bronze disc with a diameter of 20 mm and thickness of 0.20 mm. In the measurement system, a resistor of 2.2 k $\Omega$  by a chirp signal with magnitude of 1 V and frequency from 0 to 125 kHz excited this transducer. Based on the recommendations of [212–214], the mean value for three repetitions was calculated, ensuring a satisfactory accuracy. LABVIEW software acquired the impedance signatures from DAQ system. The impedance measurements were at 300 and 600 dressing passes, respectively, to the structural damage detection. The conditions of the grinding wheel were: healthy diamond dresser (H) was the baseline signal, damage 1 (D1) at 300 dressing passes, and damage 2 (D2) at 600 dressing passes. In

Fig. 53, there is the real part of impedance signatures for each one of the conditions. The healthy condition established for the dresser diamonds before the dressing passes. Otherwise, the calculation of the root mean square deviation (RMSD) allowed analysing the results. The RMSD is one of the most utilized metrics in SHM applications, according to [215], which is presented in Eq. 13. Fig. 54 show the results of RMSD index for defining dressing tool condition.

$$RMSD = \sum_{k=\omega_l}^{\omega_F} \sqrt{\frac{[Z_{E,D}(k) - Z_{E,H}(k)]^2}{Z_{E,H}^2(k)}} \quad (\text{Eq. 13})$$

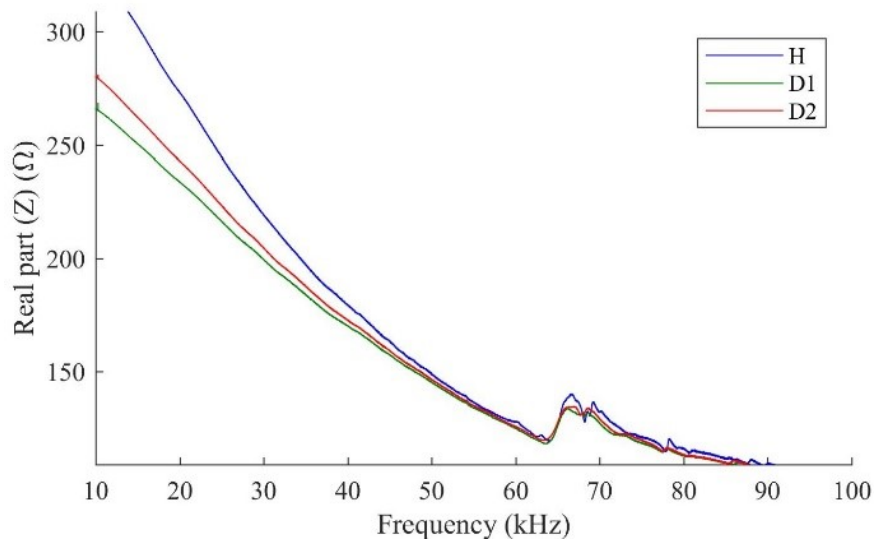


Fig. 53 - Real part of the impedance signature for dressing tool conditions [189]

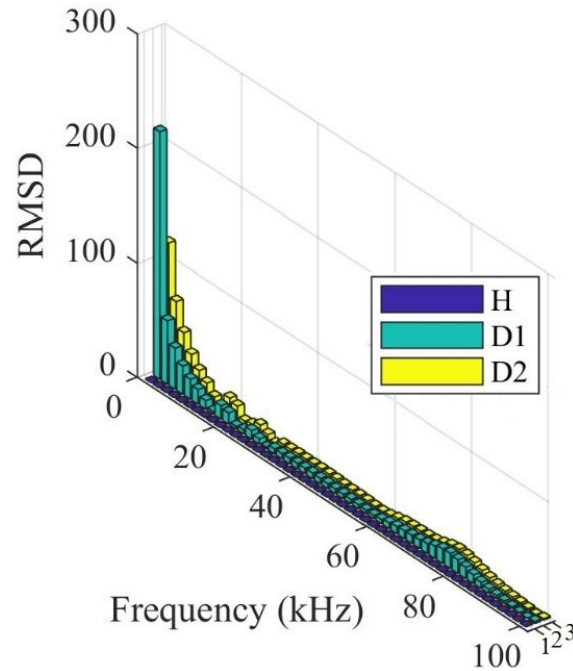


Fig. 54 - RMSD index for the defined dressing tool conditions [189]

## 4.2.2. NEURAL NETWORK MODELS FOR CASE STUDY N°1 (SUPERVISED)

The RMSD metric calculated for four sub-frequency bands, considering over a wide frequency of 0-100 kHz, with each frequency band spanning 25 kHz, according to Table 24. The frequency pass for damage indices calculation was 50 Hz. Therefore, neural models had 500 patterns as input for each frequency band. This approach was that of the sub-range of frequency most sensitive selection, presented by [203]. The multi-layer perceptron neural network (MLP), based on [211], selected the optimal frequency band to determine dressing tool damage pattern. The neural training process carried out by considering four inputs. They corresponding at each frequency band previously selected. For each chosen frequency bands, there are an input pattern for the neural model to obtain the best sub-frequency range, which is able to determine the dressing tool condition. The neural network trained in MATLAB by using the Levenberg-marquardt backpropagation algorithm. Experimental validation purpose use 10% of the input data. Confusion matrices and cross validation theory was the basis of the experimental validation step, reported by [189,216].

Table 24. Frequency bands defined [189]

Frequency bands	Range
#a	0-25 kHz
#b	25-50 kHz
#c	50-75 kHz
#d	75-100 kHz

Table 25. Mean features of the neural models [189]

Parameters	Specification			
Input pattern	#a	#b	#c	#d
Range	0-25 kHz	25-50 kHz	50-75 kHz	75-100 kHz
Structure	1-8-5-5-2	1-15-15-3	1-3-10-0-2	1-19-0-0-2
Algorithm	LVM Backpropagation			
Error	11.2 %	4.9 %	1.4 %	2.3 %

In Table 25, there are the mean features of the neural model. In Table 25, the first column shows the considered parameters in the training and in the feature extraction process, such as input patterns, neuronal model structure, training algorithm, and percentage errors of each input pattern. In the second column of Table 25, there are the respective specifications for those parameters. You can see that the input pattern #a, and, the input pattern #b, showed errors of 11.2 % and 4.9 %, respectively, by fixing the frequency bands of 0-25 kHz and 25-50 kHz. Consequently, this input pattern has not proved attractive for implementation because their percentage errors were too high when compared to the other input patterns of the neural model, such as pattern #c and pattern #d showed in Table 25.

Confusion matrices and region classifier graphics based on cross validation process are the best solution to verify the recognizing success of the proposed approach to achieve the optimal frequency band. Fig. 55a and Fig. 55b shows, respectively, the confusion matrix and region classifier graphic of the only results of the input pattern #c, which used the frequency band of 50-75 kHz. According to results of the confusion matrix showed in Fig. 55a, the network presented 97.8 % of prognostic capacity and 99.5 % of sensitivity for D1 condition, with incidence of false positive. In D2 condition, the prognostic capacity of the neural model was 99.4 % and the sensitivity was 97.7 %, corresponding to the incidence of only one false negative diagnostic. The overall correctness rate of the network for this input pattern was 98.3%, which is appealing for implementation. Fig. 55b shows the region graph based on pattern recognition system proposed. The data of both damage condition D1 and D2 are located and organized by regions in Fig. 55b. The points on the map of Fig. 55b correspond to location area of the values used in the model input. In the Fig. 55b, it is possible to see that the errors indicated by arrows occurred in the patterns located closer to the boundaries of the damage classes. Thus, with this representation, it is possible to check which models are misclassified. I.e., the model classified as D2 one pattern pertaining to D1 class, also some patterns relating to D2 class that were classified as D1. The pattern recognition system determines the frequency band most sensitive to damage, which was the range of 50-75 kHz. This approach presented a general average error of 1.4 % to define damage strictness D1, D2 in the single-point dressing tool.

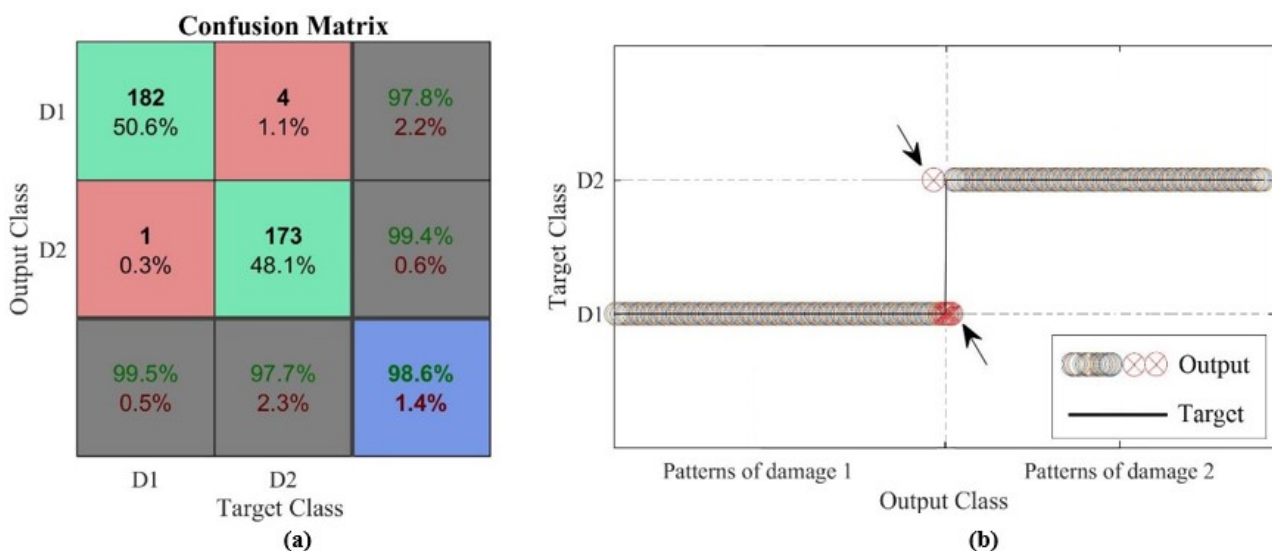


Fig. 55 - Confusion matrix for optimal frequency band achieved by neural (a) and region graph for the optimal frequency band achieved by neural model (b) [189]

### 4.2.3. CASE STUDY N°2

For the second case study, the structure had a multipoint dressing tool ( $20 \times 16 \times 5$  mm) mounted on an industrial stationary metal rod ( $30 \times 5$  mm). This type of tool is widely used in grinding operations. Seven chemical vapour deposition (CVD) diamond spikes ( $0.6 \times 10$  mm) constituted the dressing tool. The tool body have a model 7BB PZT diaphragm transducer manufactured from MURATA, which consist of a circular piezo ceramic of diameter 11 mm mounted on a circular brass disc of diameter 15 mm with a cyanoacrylate adhesive. Following the approach presented in [35], fixing holes at three different locations (H1, H2, and H3) created damages. An industrial drill with a diameter of 1 mm realized two 0.5 mm depth holes for each site. In Table 26 there are the total number of six holes drilled (damage#1 (D1), damage#2 (D2), damage#3 (D3), damage#4 (D4), damage#5(D5), and damage#6 (D6)). The six holes drilled helps to investigate the connection between the alterations in the impedance measurements against damaged dressing tool. Fig. 56 shows the experimental test bench. The approaches used for experiment are the following: [189,200,204,205]. Before (baseline) and after the damage, experimental measurements of electromechanical impedance performed. The used alternative EMI measurement system proposed by [214]. To achieve this purpose, the data acquisition system was a model 6'221 from National Instruments with a sampling frequency of 250 kHz. A 2.2 k $\Omega$  resistor and a one V amplitude chirp signal with a frequency range of 0-125 kHz (Fig. 57) excited the transducer.

Table 26. Description of experiments [196]

Experiment	Damage identification
Baseline	-
Damage#1	H1
Damage#2	H1
Damage#3	H2
Damage#4	H2
Damage#5	H3
Damage#6	H3

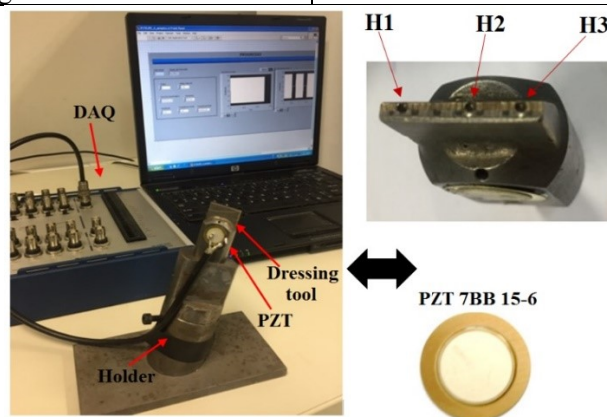


Fig. 56 - Experimental test bench [196]

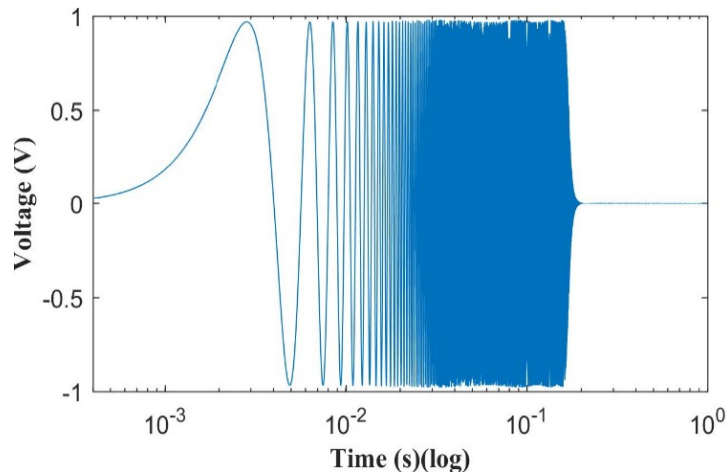


Fig. 57 - Chirp signal for excitation purpose [196]

The real part of the impedance ( $Re(Z)$ ) analysed with a broad sweep range from 10 kHz to 125 kHz confirmed a frequency range suitable for feature extraction. From SHM literature [209,214,215], the real part of the impedance has a significant relation to the resonance peaks corresponding to the structural damages. Instead, the imaginary part or impedance module do not have the same relation in comparison with the real part of impedance. Fig. 58 show the plot of the results. Fig. 58 shows, also, the impedance signatures, corresponding to the six damage levels, against a baseline signature. The changes in signatures there were in correspondence of damage levels. This means that the damage levels introduced sequentially at the structure. In this context, the damages altered the mechanical impedance of the structure because they influenced gradually the dressing tool. The increasing severity of the damage is the cause of the above. As a result, there is a clear difference between the signatures corresponding to the damage levels and the baseline signature. During the full frequency range of 10-90 kHz as compared to the frequency range of 90-110 kHz, there are only some slight and small variations between these signatures. This means that the frequency range of 90-110 kHz was most sensitive to detect structural damages.

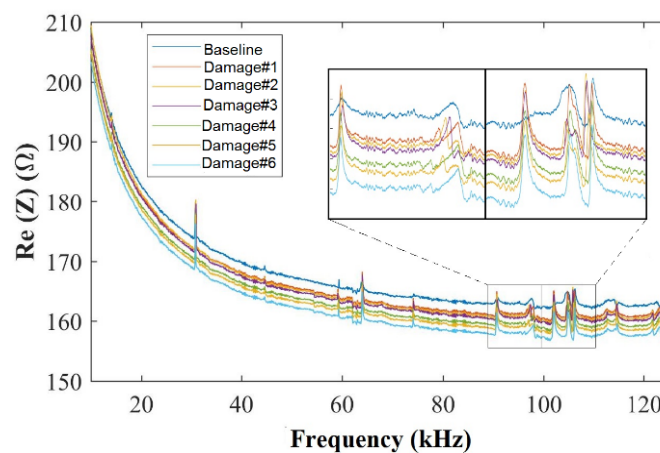


Fig. 58 - Real part of impedance signatures in different damage levels [196]

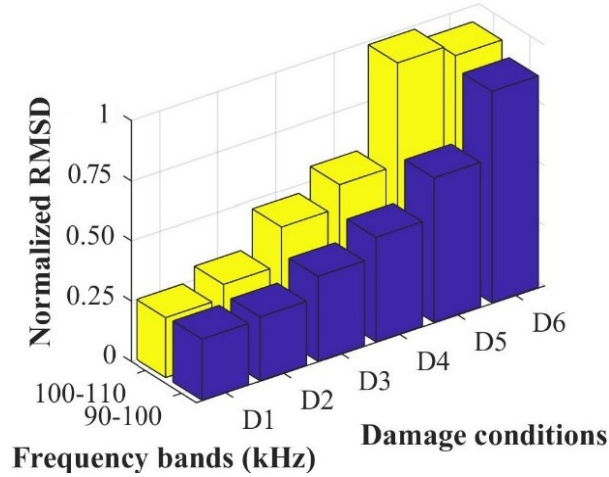


Fig. 59 - RMSD of the impedance signatures: 90-100 kHz and 100-110 kHz [196]

Trial and error method determined the best frequency range for a given structure in EMI technique. In literature, there are several analytical works on the subject of an optimal frequency range selection. Though, a frequency range with high density reveals higher sensitivity, since it generally overlays more structural dynamic information, according to [172,196]. For this reason, in this case study, the frequency ranges chosen for feature extraction were 90-100 kHz and 100-110 kHz. Fig. 59 shows the increase of these frequency ranges. The chosen RMSD index calculated the difference between the baseline signature and the signatures at the different damage levels. For this reason, the previously selected frequency ranges were 90-100 kHz and 100-110 kHz. Eq. 14 gives the calculation of the RMSD in terms of the real part of the impedance [214].

$$RMSD = \sum_{\omega_I}^{\omega_F} \sqrt{\frac{(Re(Z_2(\omega)) - Re(Z_1(\omega)))^2}{Re(Z_1(\omega))^2}} \quad (\text{Eq. 14})$$

In Eq. 14,  $Re(Z_1(\omega))$  is the real part of the signatures after possible damages, and RMSD is the index calculated in the range from initial to final frequency [214]. Fig. 59 shows the results of the RMSD calculation. The RMSD index clearly rises as the damage gradually influenced the dressing tool. Damage information extracted directly from RMSD values corresponding to the frequency ranges of 90-100 kHz and 100-110 kHz validated the proposed damage classification method.



#### 4.2.4. NEURAL NETWORK MODELS FOR CASE STUDY N°2 (UNSUPERVISED)

The EMI technique is sensitive to small changes in the nearby field of the PZT transducer. Tough, this technique cannot support a classification in terms of location and severity directly from the nature of the damage. Therefore, a method based on self-organizing features improves the impedance-based damage classification. The self-organizing maps is a type of unsupervised neural networks. They based on competitive learning. I.e., input and output layers connected between each other by nodes and neurons set up a SOM architecture. During the knowledge phase, the competition process established a distance between the input vector and the weight vector of the output neuron. During the training phase, the SOM examines the similar input data to pick the best neuron from the output layer, i.e. the best matching unit (BMU), and classifies it into cluster maps. Successively, the BMU adjusted the weight vector using a training algorithm. The most usual algorithms for training phase are batch and sequential (incremental). This means that a rule [196,217,218] give an update to the BMU and its neighbouring units have their weights. Based on the selection of those two frequency ranges of 90-100 kHz and 100-110 kHz, multiple set of measurements (for different damage levels) permit the training the neural networks. The implementation of the SOM toolbox for MATLAB makes it possible to carry out the project of using this type of neural network to classify dressing tool conditions. The input data contains the RMSD values of the real part of the impedance obtained previously. From each data set considered, i.e. two damage levels for each location ("H1", "H2" and "H3"), there are 100 consecutive values of the damage patterns (named N). The N-element vectors represents the number of damage patterns generated by RMSD indices for each frequency band [196]. The input matrix has a size of  $M \times N$ , where M is the number of damage levels. The training of numerous types of SOM networks achieved by implementing the batch algorithm and changing the grid and the number of neurons. A quantization error metrics permitted an inspection of the obtained maps in order to evaluate the quality of the results. The application of the leave-k-out method (l-k-o) [172,187,188] allowed the test SOM performance. The l-k-o method excluded a row from the dataset during the training phase. This means that  $k=1$ . This method creates a test variable, leaving the kth line of the input matrix and the output vector. Successively, the network trained with the remaining  $nk$  lines and eventually test the performance by evaluating the predicted output of NN with the test variable. After the training of numerous SOM topologies, the architecture selected was the two-dimensional hexagonal grid: 5 x 9. This topology has 64 neurons in the output layer and 3 nodes in the input layer (for the 3 ratios). The motivation behind this choice is related to the smallest quantization and typographic errors [196].



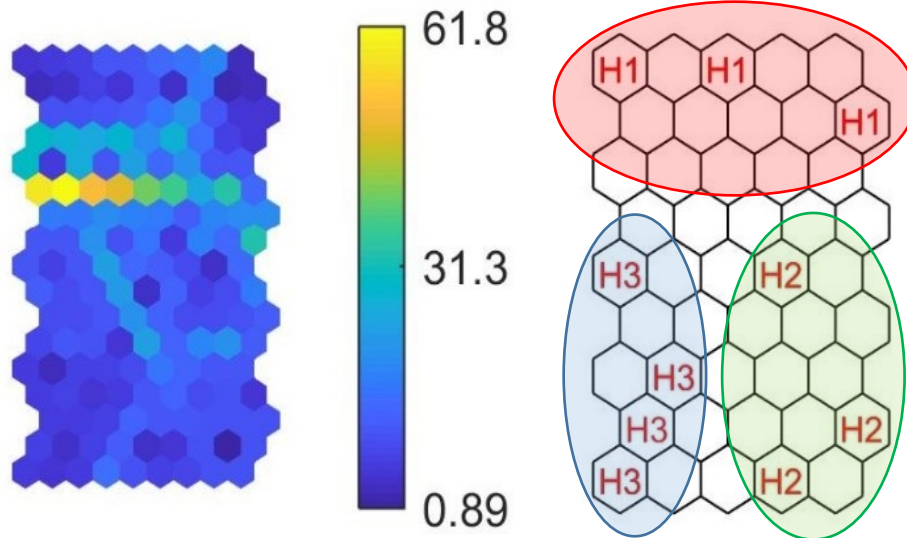


Fig. 60 - U-matrix and labels for damage classification [196]

Fig. 60 presents the representation of the U-matrix [219] and labels for the selected SOM architecture. The average distance between the vector of weights of the node and its closest neighbours provides the value of the U-matrix for a given node. The U-matrix makes it possible to distinguish the formation of three main clusters in the SOM. These clusters represent the six levels of damage caused in the dressing tool. In fact, there are three areas of groups H1, H2 and H3 in the label matrix. Each cluster contains samples of two types of damage in the frequency ranges of 90-100 kHz and 100-110 kHz. The U-matrix does not display a clear split-up between them, but it shows the formation of the clusters from the colour change. However, the labels show that clusters H2 and H3 are similar to each other but different from H1.

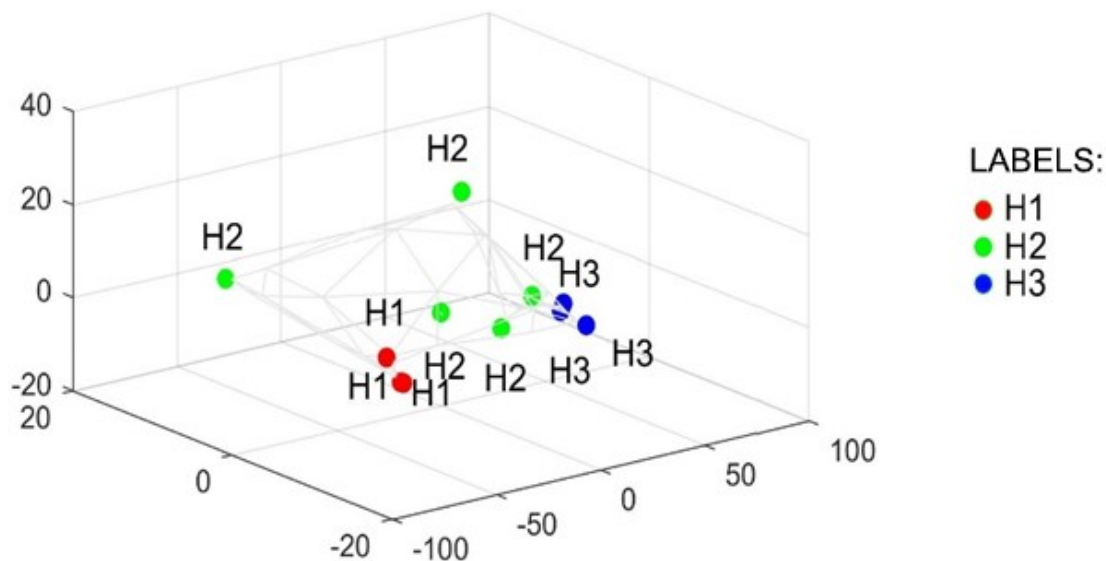


Fig. 61 - Projection of the dataset to the eigenvectors with greatest eigenvalues subspace [196]

Fig. 61 is only a three-dimensional projection, as shown in Fig. 62. To be precise, Fig. 61 is the projection of all damages in the subspace covered by its three eigenvectors with the largest eigenvalues. The SOM grid dataset has a tracking of different colours (green, blue and red). Lines join neighbouring map units. Labels show to which map clusters (H1, H2, H3) they correspond. The damage in the structure is obvious and distinguishable. This is because there has been a gradual degradation with the consecutive induction of holes.

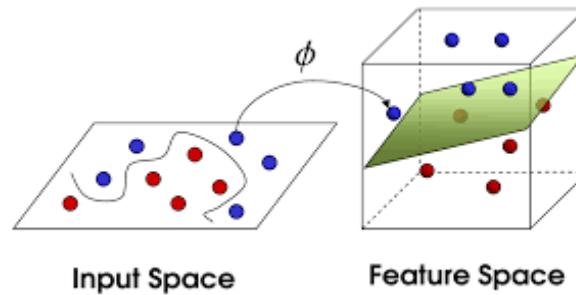


Fig. 62 - Function  $\Phi$  maps data from input space to feature space [220]

Fig. 60 and Fig. 61 show three map clusters: H1, H2 and H3. The reason for this is that the damages are located in three precise areas, as shown in Fig. 56. Another possible choice was to classify the six damages individually. Due to the extremely close position of the network, this could lead to confusion because the impedance signals were very close, as shown in Fig. 58. The classification into three map clusters allowed a better recognition of the groups.

Another very interesting aspect in the clusters assessment is the position of the groups in the three-dimensional space in Fig. 61. The three-dimensional reconstruction shows how the clusters placed in an ascending way. H1 is at the first position along the x-axis. It is ahead of H2 and the latter is in front of H3. Some of the points under examination between the groups are quite close, almost as if the clusters were touching. This is an expected result as the difference between some of the impedance values for individual damages is not large. This case study demonstrates how damage classification can be improved using the EMI technique combined with artificial intelligence [196].

## 5. ACTIVITY ON CUTTING TESTS

In this section of the thesis, it will deal with the analysis of images related to cutting tests. In the previous chapter, it has seen the use of artificial intelligence techniques associated with another material removal process: grinding. Grinding and cutting distinguished as operations in that the former is a surface finishing technique while the latter is a technique that shapes the geometry of the workpiece. As previously done, you will work to understand the wear state of the tool used. If previously, the tool was the dressing tool; in this case, it is the cutting tool. It is subject to various wear phenomena that compromise the useful life of the tool. Studying the wear trend and therefore determining the behaviour will undoubtedly improve the use of the tool and guarantee a longer life. Concerning this, the bibliography is rich in research on the study of the useful life of the cutting tool [221–224]. The following research activity can easily place in this area of scientific production. The ultimate aim is not to study the specific cutting tool life, but to provide a tool that can provide the operator with the wear conditions in real-time from images. The research work does images to calculate a specific parameter, in this case, wear, using the tool's images. However, the method used did not linked to graphics programs in which the operator goes to measure the required parameter. The method used uses an artificial intelligence technique known as bees algorithm [148]. This technique has been illustrating in the previous chapters and, as it has been possible to read, it is a technique that allows a search to be carried out in some outlines of a landscape consisting of an objective function. Starting from this principle, it decided to use this particular property of the bees' algorithm to study the image and determine the points of interest for the finalization of the target. The reason why it decided to work with this type of technique linked to the fact that the Particle Swarm Optimization (PSO) techniques are better suited to a detailed analysis of space than other artificial intelligence techniques such as neural networks. In fact, the objective was not the simple recognition of the wear area, but the precise calculation of the value.

In the first case, the machine learning techniques typical of neural networks would have gone very well. In this case, instead, an analysis that a PSO would have done better was necessary. Were it not that in literature, there are no works that use images as a fitness function for PSO. In fact, PSOs created to find local maximums and minimums from functions that describe the behaviour of a given problem. The idea, however, of finding local maximums and minimums is perfect if we consider images as matrices and, the differences in brightness, as numerical values. In this way, the wear edge would be easy to identify and, if the positions in the image known, the value of the required parameter could be obtained. The choice then fell on algorithm bees by virtue of direct contact with Prof. Pham, the creator of this technique. He supervised the progress made in this research activity.

Ing. Salvatore Conte

As far as the system and algorithm tuning phases are concerned, which will be shown in the next paragraph, work has begun on images of wear already cleaned up to ascertain the feasibility of the idea. These were then repertory images, in which the wear had been contoured and was used as Landscape associated with the algorithm developed by Prof. Pham and Dr Castellani [148]. Once the correct use had been verifying, it then moved on to work on images from new processes. The processes in question were almost orthogonal cutting tests, and the photos acquired during the tests processed without any previous work.

Starting from unprocessed images, the goal was to create an algorithm that would allow the user to know the required value quickly. The ultimate goal is, therefore not to know the wear trend during tests, but to understand the effectiveness of this method that can use in real-time during cutting tests. To do this, a comparison between data calculated by the algorithm and real values is necessary. This aspect will also be dealt with in the next paragraph.

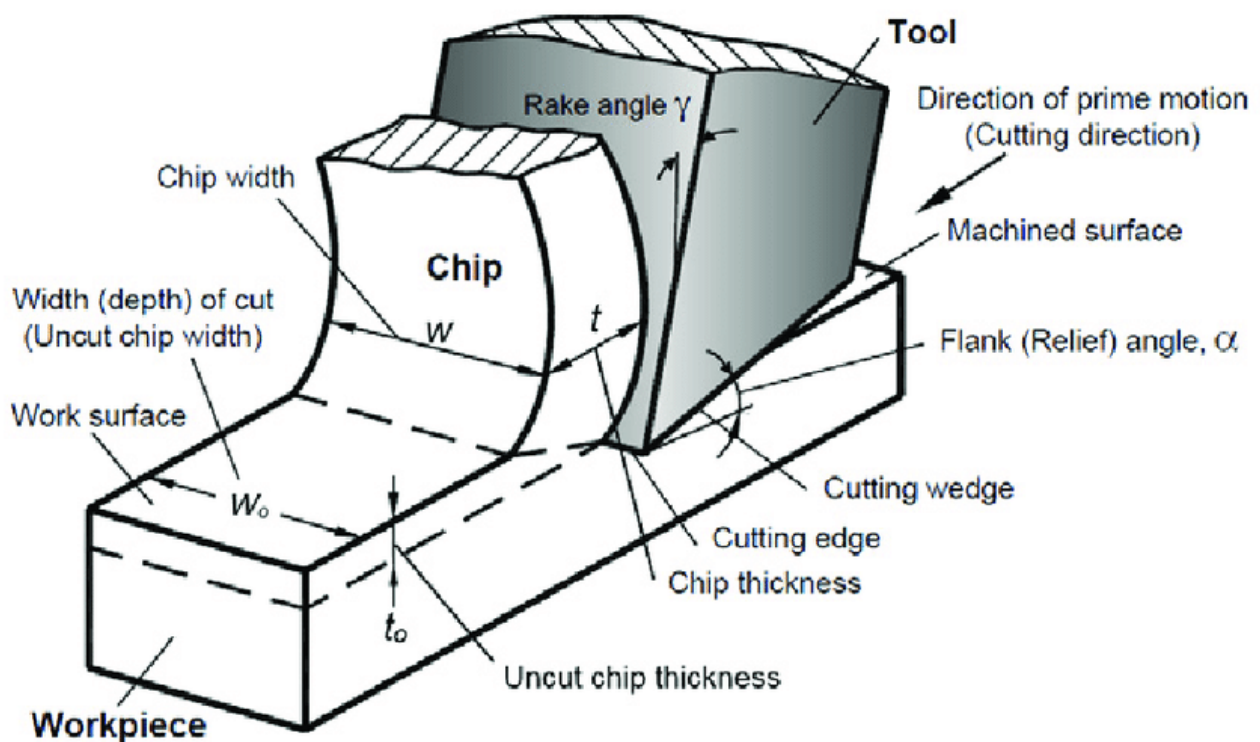


Fig. 63 - Basic terms in orthogonal cutting [225]

## 5.1. IMAGE ANALYSIS VIA BEES ALGORITHM

The BA is generally used for optimization problems [148,163,226–229] all related to functions defined from a mathematical point of view. In this work, the agents search capacity will be used to determine the extent of tool wear from images. The idea is to replace the fitness landscape with a landscape consisting of the image in a matrix version. Bees can find the characteristic points of wear and return the required value. In this case, the idea will be applying to a cutting tool, but in general, the method can also work with other types of images. The fundamental aspect is the choice of an objective function, which leads to a variety of steps compared to those shown in this work. The objective of the work is to obtain a curve with wear amplitude values calculated from the images collected between one test and another. The cutting work carried out was of the orthogonal type. Between some passes, images of the tool acquired. A copper wire with a diameter of 0.21 mm positioned near the tool. This will be the reference for the conversion between pixels and mm to verify the effectiveness of the BA method. Measurements made initially using image processing software. At the end of this work, there will be comparisons between the results obtained with the BA method and those obtained from photo analysis.

Fig. 64 shows the flowchart of the BA method for determining tool wear. The diagram shows all the steps taken to arrive at the result of the wear calculation in a single image. The process was possible by using MatLAB software with special scripts that performed the necessary steps.

The first step is image selection. The script allows the user to indicate the path and name of the image to be analysed. Once the image selected, MatLAB imports the RGB image as a three-dimensional matrix and shows the user the figure. If the figure did not correctly rotated, the script allows the user to rotate the image by entering the number of degrees required for counter clockwise rotation. This operation also rotates the matrix connected to the image accordingly. The next step is to determine the number of pixels to associate with the reference. To do this, the user can select the area of the image where the copper wire is present. The script will advise the user to click on two ends of the wire. After the selection of the two points, the script will calculate the distance between the two points according to Eq. 15. The result obtained will be save and use later.

$$\begin{cases} P_1(x_1, y_1) \\ P_2(x_2, y_2) \\ d(P_1, P_2) = \sqrt{(x_2 - x_1)^2 + (y_2 - y_1)^2} \end{cases} \quad (\text{Eq. 15})$$

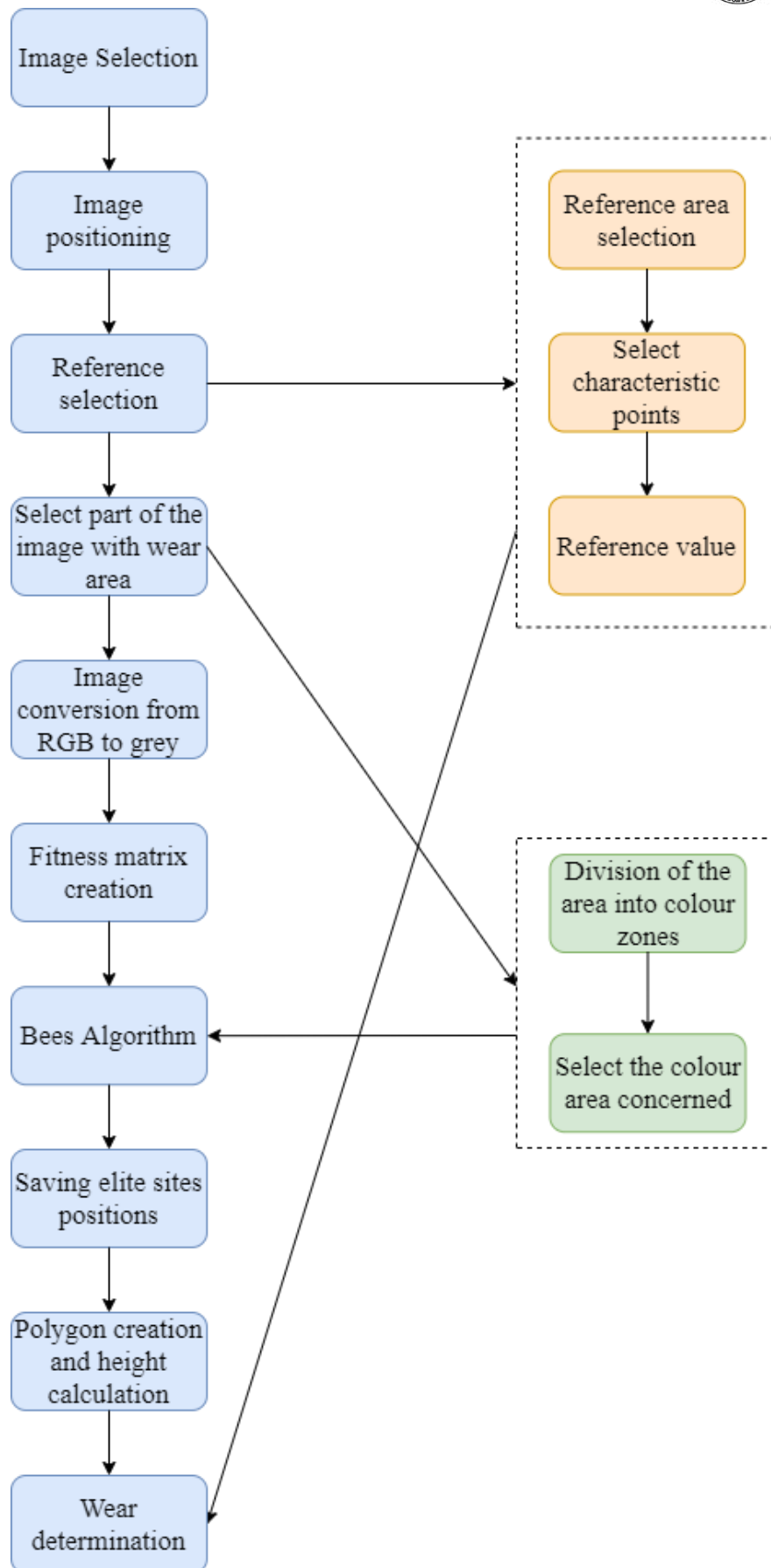


Fig. 64 - Bees algorithm for tool wear detection flowchart

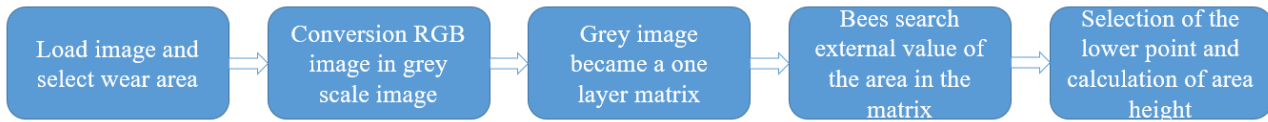


Fig. 65 - Simplified flowchart of the BA method for tool wear detection

The process continues with the return to the starting image and the selection of the image area where the wear is present. In this case, the user goes to cut the image, and the selected part will be the one that the script will keep in the form of a matrix. Anything outside the box will be delete. This will make the matrix smaller in size, which will help speed up the calculation, which will be slower. The remaining image will then be dividing into areas of colour thanks to the MatLAB function called *superpixels*. This function uses the information from an RGB image to create a label matrix referring to the colours in the source image. The label matrix created is a set of clusters, each characterised by the most common colour in a given region. This process is called *oversegmentation* [230]. Fig. 66 shows how the image changes because of this process. MatLAB then shows the user the effects of the *superpixels* function on the previously cut image. The user can click inside the wear to provide the script with information regarding the position of the wear. This step is of paramount importance because it reduces processing time and allows a more efficient search for bees. Each area is associated with a value that matches the colour shown on the image. The script searches the label matrix for the value selected by the user after clicking on the affected area. The rectangular area where the required values are present will be the actual scouting area for bees. This information is then saved and will be use later. The label matrix is no longer need, and the image will be visible again without the visual filter applied by the *superpixels* function. The image converted from RGB to grayscale. This conversion leads to the transformation of the original matrix from three-dimensional to one-dimensional. A one-dimensional matrix is a matrix of individual values. However, considering the information regarding the position of each value within the matrix, the matrix is a grayscale image that on MatLAB is visible in three dimensions with the mesh function. The grayscale image is the Fitness Landscape on which bees can move. The last step before starting the BA is the setting of the search parameters. Parameter optimisation will be show in the next chapter. Important information is the instructions given to the bees. In this case, you will not ask to search for a minimum point, but maximum points near a minimum area. The grey matrix has values ranging from 0 to 255. The minimum value corresponds to the black colour, while the white colour is associated with the maximum value. The wear zone is characterised by shadow and therefore a darker colour than the unused part of the tool. The edge of the wear area will have higher values than the area. For this reason, maxima will only search in areas where there are many minima. The risk of ending up outside the wear area has been avoid with the *superpixels* function. Without this operation, bees could roam

Ing. Salvatore Conte



the entire image area with the risk of identifying areas with characteristics similar to those of wear and tear and giving incorrect results. It then proceeds with the start-up of the BA whose operation remains unchanged with respect to what described in the previous chapter except for the changes just discussed. At the end of the search, the positions of the required values are saved.

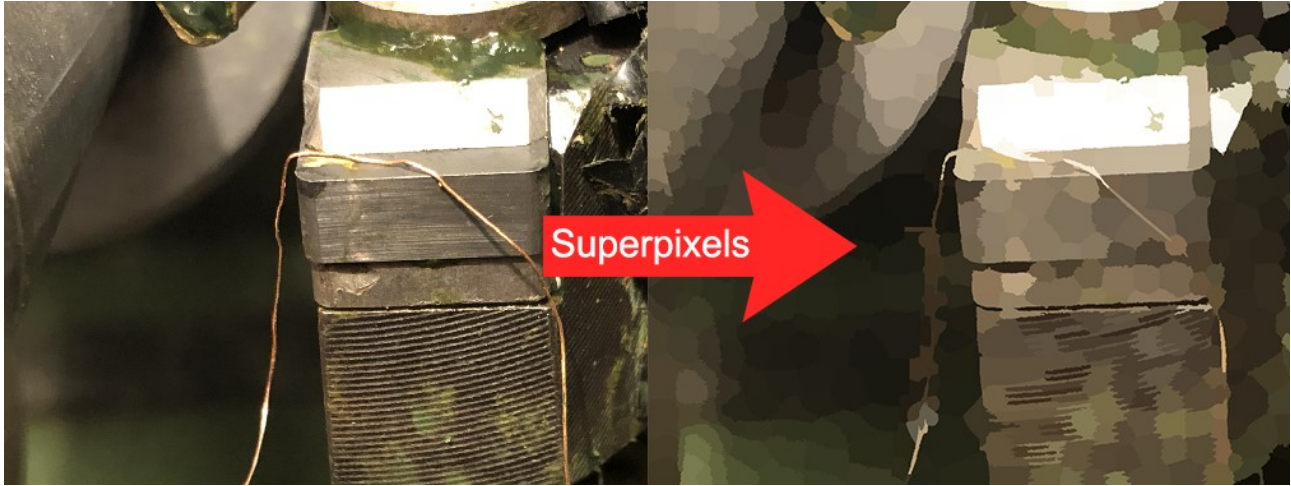


Fig. 66 - Oversegmentation realized by *superpixels* function in MatLAB

The positions are saved in two vectors for the coordinates of the abscissae and the ordinate respectively. MatLAB's *boundary* function creates a closed polygon with the newly saved vectors. The closed polygon represents the boundary of wear. By selecting the lowest point of the polygon, you can calculate the height with Eq. 15. The second point is the highest point. Since the image may be slightly oblique to the abscissa plane, the highest point searched in a range within which the abscissa value of the lowest point is present. Once the height  $h(px)$  is calculated, you get to the last step of this method. The height expressed in pixels and should be convert to mm. For conversion, you must have the data previously acquired from the reference available. The height  $h$  in mm calculated according to Eq. 16.

$$h(mm) = \frac{h(px) \cdot 0.21mm}{d(P_1, P_2)} \quad (Eq. 16)$$

Fig. 67 summarises the steps of the BA for tool wear detection method. The BA method for determining wear from images applied to figures of a cutting tool. The images came from orthogonal cutting tests and taken between several passes at irregular intervals. The tests are related to the works [231,232]. The aim of this work is not to investigate the quality of the tests carried out but rather the ability of the BA to determine the correct wear value from the images. The tests carried out are two made with different processing parameters. For each instant of time in which the wear value is present, a certain number of photos correspond. The wear value is not always precisely the same considering that the photos taken sometimes from different positions.



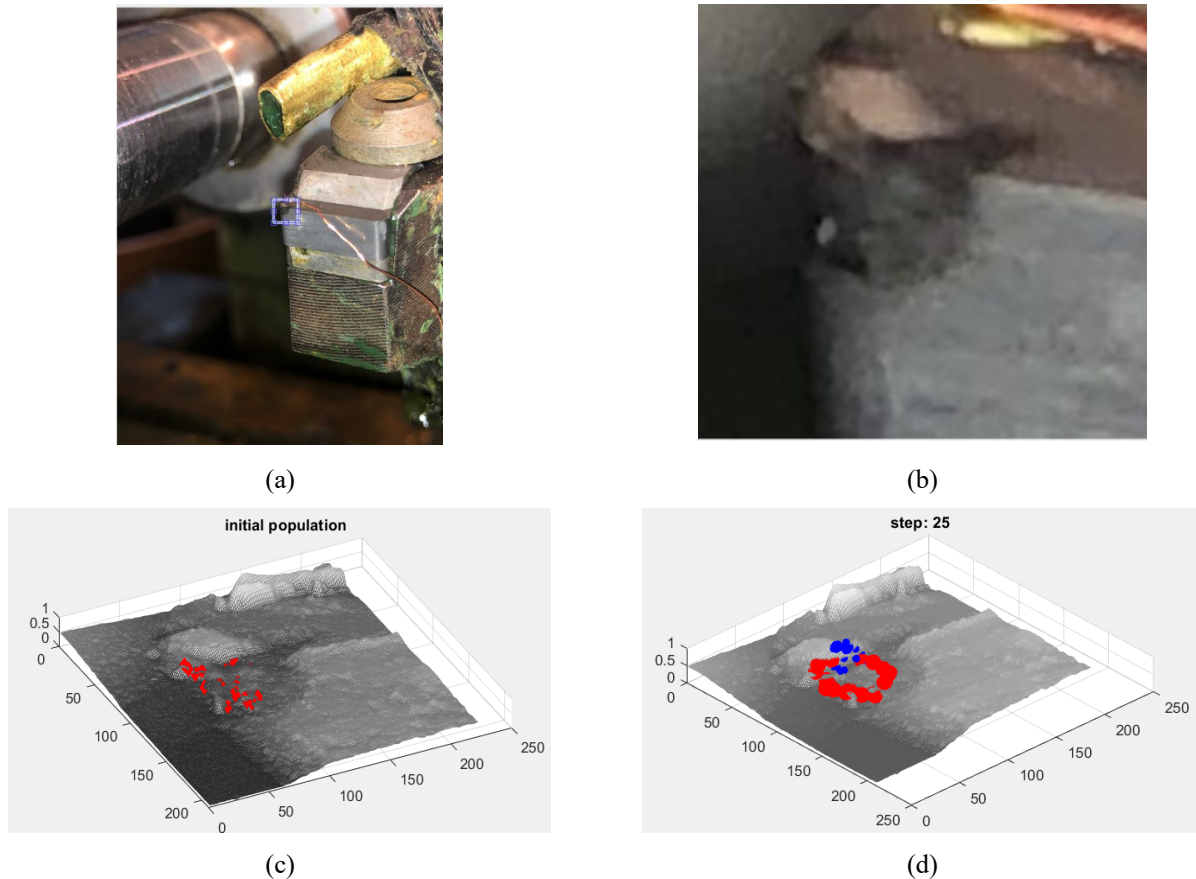


Fig. 67 - Steps of BA method for tool wear detection: in (a) the user selects the area of interest in the full image and obtain (b). After the conversion RGB to grey scale, the image become the fitness landscape (c). The Bees agents find the tool wear. His edge is shown in (d) with red circles.

The variation between the various measurements is in the order of hundredths of an mm. The average values will therefore be compared both for the survey taken directly on the photos and for the results provided by the BA. The objective of the following work is, in fact, to ascertain the effectiveness of the method by calculating how much it provides values different from those found with the direct measurement on the images. The comparison work begins with the selection of the best images for measurement. After that, measurements are recorded for each image. This is done by applying the BA method for tool wear detection. The application of the BA is not immediate, as it is necessary to choose the best parameters to optimise the results of the method. The parameters on which you can work are six: duration, random scouts, elite sites, best sites, foragers on elite sites and best sites. To optimise the process of determining the best parameters, the script sets the last three parameters, and the values of duration, random scouts and elite sites are varied. The results of these tests shown in Fig. 68, Fig. 69 and Fig. 70. The graphs show the test values and the percentage of error compared to the values determined by the measurement of the images. Once the parameters with the lowest error percentage have chosen, the remaining parameters chosen. Table 27 shows the various parameter configurations and Fig. 71 will show which configuration shows the best results.

Table 27. Configuration of parameters for BA method for tool wear detection

Conf.	Duration	Random Scouts	Elite Sites	Best Sites	Foragers on Elite Sites	Foragers on Best Sites
<i>a</i>	25	10	4	4	5	5
<i>b</i>	25	10	4	8	5	5
<i>c</i>	25	10	4	12	5	5
<i>d</i>	25	10	4	16	5	5
<i>e</i>	25	10	4	20	5	5
<i>f</i>	25	10	4	4	10	10
<i>g</i>	25	10	4	8	10	10
<i>h</i>	25	10	4	12	10	10
<i>i</i>	25	10	4	16	10	10
<i>j</i>	25	10	4	20	10	10

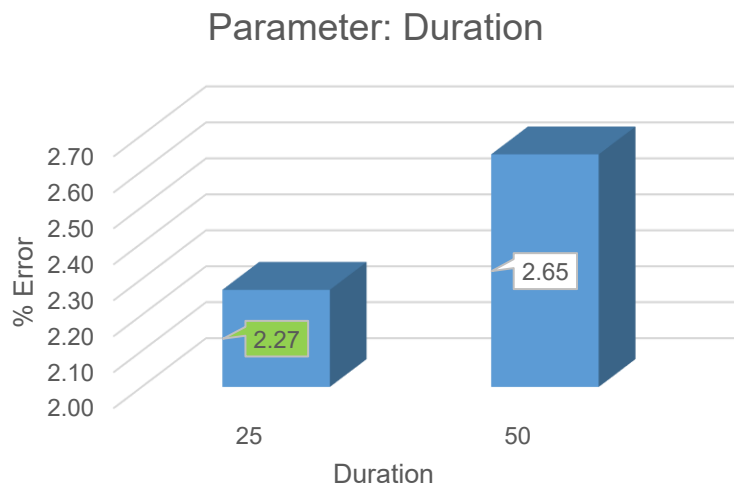


Fig. 68 - Comparison between different values of duration parameter

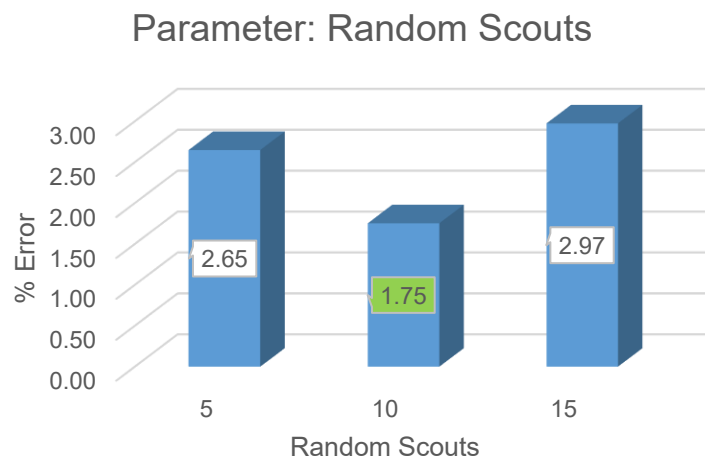


Fig. 69 - Comparison between different values of random scouts' parameter



Fig. 70 - Comparison between different values of elite sites parameter

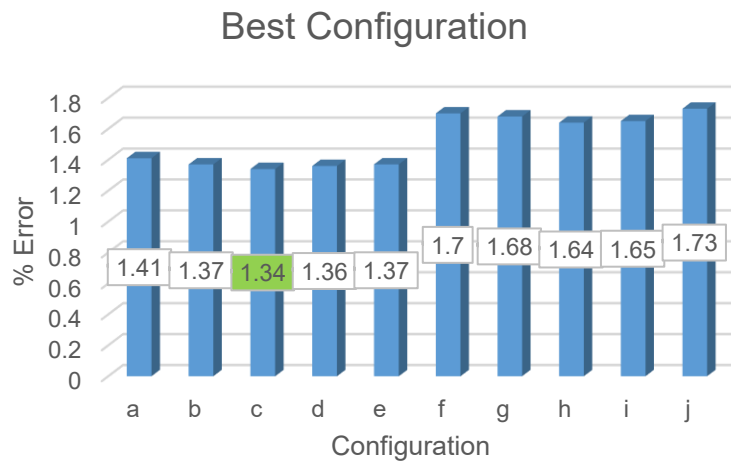


Fig. 71 - Comparison between different values of configurations

The best configuration is "c". The parameters are summarised in Table 27. The script that returns the matrices with all the results for each image shows the best configuration. Table 28 and Table 29 show the results for each instant in which the photos taken. The tables show the average value of both measured and BA-determined wear. Average value means the calculation of the average of the values of all images for each single photographed pass. For the first tool, the success rate of the BA is 98.64%. The success rate of the BA for the second tool is 98.69%. The graphs in Fig. 72 and Fig. 73 are the curves obtained using the values of the tables.

Table 28. Wear measured by photo and BA for first tool

First Tool		
Time (s)	Wear measured by photo (mm)	Wear measured by BA (mm)
90	0.659	0.659
180	1.012	1.043
220	1.104	1.124
260	1.301	1.296
300	1.820	1.813
333	1.879	1.865
453	2.538	2.522

Table 29. Wear measured by photo and BA for second tool

Second Tool		
Time (s)	Wear measured by photo (mm)	Wear measured by BA (mm)
76	0.554	0.548
210	0.705	0.710
309	0.963	0.950
407	1.290	1.272
505	1.453	1.476
572	1.562	1.576

Table 30. Mean error in wear determination for each tool

Mean Error			
Time (s)	First Tool	Time (s)	Second Tool
90	0.00 %	76	1.09 %
180	2.97 %	210	0.70 %
220	1.78 %	309	1.37 %
260	0.38 %	407	1.41 %
300	0.39 %	505	1.56 %
333	0.75 %	572	0.89 %
453	0.63 %	-	-
Mean Error First Tool		Mean Error Second Tool	
0.99 %		1.17 %	

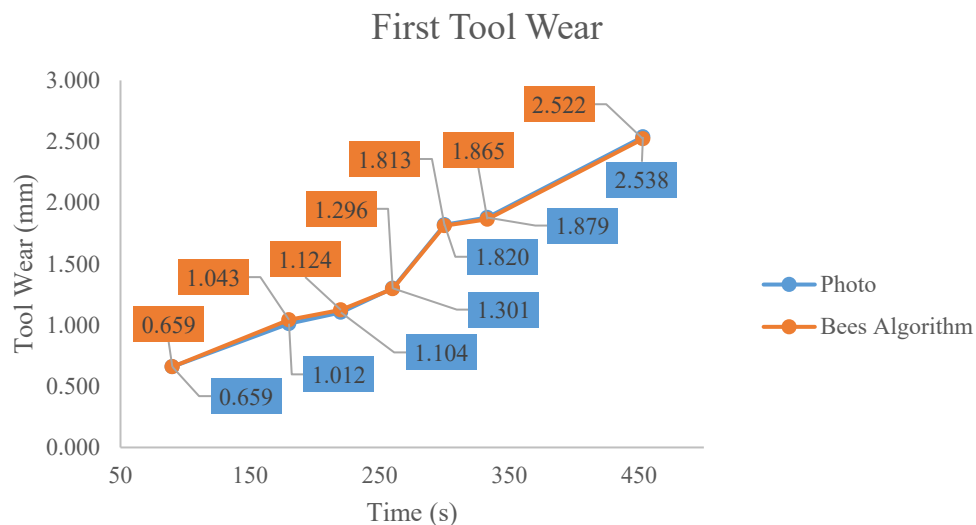


Fig. 72 - Tool wear vs time for first tool

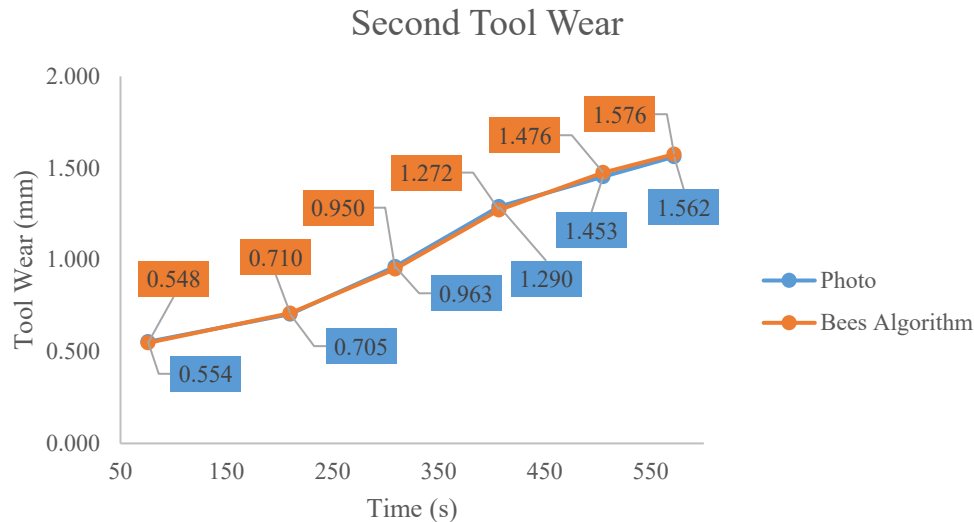


Fig. 73 - Tool wear vs time for second tool

An interesting aspect of this research is the computation time, i.e. the time taken by the bees to determine the boundary of the worn area. The response time is about 5 seconds. It can observe that the time can vary depending on the size of the images. When the images are small, as in the case of Fig. 66 (d), the computation times are lower. A photographic campaign that produces equal images can establish a direct correlation between the number of pixels, the resolution and the computational time. A lower image resolution affects the computation time, which will be lower. Conversely, a high-resolution lead to higher computation times. However, the resolution affects the accuracy of the wear measurement. A higher resolution image provides better accuracy already in the photographic analysis. The relationship between resolution and measurement accuracy is not directly observable in the analysis with the BA method. This non-observation occurs because the analysis tool based on the input image and the measurement made on the same image. If there is an inaccuracy in the wear measurement in the image due to a low resolution, the BA method cannot overcome the original problem and brings with it the same inaccuracy. Again, a photo campaign with images taken at the same distance but with a different resolution is necessary. A future development could be the realisation of an ad hoc campaign to highlight the correlation between computational time and image resolution. Other aspects that should not overlook are the characteristics of the computer on which the script runs. The capacity of the RAM memory and the capacity of the video card can affect the computational time. Leaving these aspects aside, the BA method developed in this thesis provides extremely interesting results. This is because the bees provided clearly with the area to be analysed with the oversegmentation technique. This is the reason for very low computational times.

## 6. CONCLUSIONS

The following thesis investigates the possibilities and potential of artificial intelligence techniques in manufacturing processes involving material removal. Supervised and unsupervised neural networks and bees algorithms show their ability to predict and measure specific parameters to optimise processing. Concerning dressing processes related to grinding wheels, neural networks could correctly classify grinding wheel conditions with 94.1%. This line of research belongs to the field of structural health monitoring (SHM). Recently, neural networks play a crucial role in this research field. Therefore, this study presented the SHM approach for the dressing operation monitoring. The work incorporates MLP neural models, in order to developing a damage pattern recognition system in dressing tools. To achieve this goal, a neural network model built considering as input the damage metric root mean square deviation (RMSD) by fixing different frequency bands. The intelligent system was an efficient technique to improve the damage diagnostic in the dressing operation. The pattern recognition system determined the most damage-sensitive frequency band, which was the range of 50-75 kHz. Thus, this work's objective achieved by confirming the potential of the developed neural network model. The proposed approach presented a general average error of 1.4% to determine the severity of damage D1, D2 in the single point dressing tool. Furthermore, this work offered a new approach to monitor the dressing operation, bringing improvements to the grinding process. The supervised neural network system offered an excellent classification and frequency range-finding tool. However, this work also lent itself well to the use of an unsupervised neural network system. The difference between the two types of networks lies in the information provided to them. The supervised neural network needs an output that controls its effectiveness. For problems of classification and realisation of patterns, an unsupervised system such as the maps of Kohonen (SOM) can also use to resolve this kind of problems. This artificial neural network typology can classify the various cases by studying the correlation present among the multiple inputs. For this reason, starting with a system that acquired electro-mechanical impedance signals, signals were collected during a dressing process with the aid of a low-cost piezoelectric. These signals used as input datasets for the self-organising maps. A SOM architecture was implemented whose characteristics derived from the RMSD values corresponding to the real part of the impedance in the frequency range of 90-100 kHz and 100-110 kHz. The improved self-organising characteristics showed a significant improvement in EMI-based damage classification, which is a promising and useful contribution to the field of rectification. The research work on SOMs carried out with a smaller dataset than the data collected due to an issue related to network stability and computer capabilities. A future upgrade of this work may further expand the dataset to confirm the proposed method's effectiveness and reliability for a

larger situation. In grinding, artificial intelligence techniques show enormous potential, particularly in the optimisation of dressing tests and the classification of grinding wheel status. There is still much room for improvement, and these techniques will likely use more and more for better process control. An operator can remotely control the process using a system that sends data in real-time to a smartphone display. The limitation of such a proposed approach is the data transfer technology, which contains a time delay by its nature. By bringing this value close to zero, it will be possible to know the grinding wheel's condition in real-time at all times, even remotely and during machining itself.

What about the bees' algorithm for determining wear in cutting processes? The BA method for determining tool wear works. The error rates are meagre, even those with non-optimised parameters as shown in Fig. 68, Fig. 69, Fig. 70 and Fig. 71. The method can also use for other types of analysis. The flowcharts in Fig. 64 and Fig. 65 have been develop for the specific case but can modify. The highlights of this method are:

- The ability to convert the image into a Fitness Landscape;
- The possibility of optimally addressing bees through over segmentation;
- The use of the position of the best sites for the realisation of a figure.

For the first of these points is fundamental to the conversion of the image in grayscale with the consequent realisation of the matrix to use as Fitness Landscape. Usually, in the BA, the Fitness Landscape generated by a function. This equation returns values in function of two variables. The variables are comparable to coordinates on a map and indexes in a matrix. The idea is, therefore, to supply the system directly with the matrix without the generating function. This is only possible in grayscale as this type of image only has information relating to the variation of one colour: grey. Its variation can only range from white (highest value) to black (lowest value). In the case of RGB images, the information is linked to 3 layers: red, green and blue. The combination of these three layers then provides the characteristic colour variation of the image. A matrix of this type is unusable for creating a Fitness Landscape. The conversion, on the other hand, allows the Fitness Landscape image to use and does not lose information compared to using only one of the three layers in the RGB encoding.

Another essential factor is over segmentation. In tests before those shown in this paper, over segmentation did not apply. For some repertory images, the system worked equally. The repertoire images, however, worked with only the interested party being highlighted. It was, therefore, easy for the bees to recognise the desired object. Without previous work on the photo, the recognition by the bees influenced by the elements in the photo. If the photo is simple and has only one characteristic

element, the recognition is significant. If there are other elements in the photo, not all bees will recognise the requested object, and this could be a problem for the investigation. With over segmentation bees have a more focused search box with lower processing time and a much higher recognition rate. In addition, over segmentation allows you to retain information about colours that would be lost with just the conversion from RGB to greyscale.

The last aspect underlined is that of the realization of a figure. In the specific case, the objective was the calculation of the height, but this does not mean that it is not possible to obtain other parameters such as the area. The position of the best sites is the element for the creation of the perimeter. The position of the best sites may not be optimal to create a homogeneous figure. Using the boundary function allows you to check the concavity and convexity of the built polygon with the position of the best sites. In this way, positions that are far from the group of the other positions did not consider excluding implausible forms for the object to identify.

The BA for tool wear detection method can also be used in real-time to obtain the required values by simply uploading the photos taken to the tool. The power of this method is to be able to identify any object. The ability to choose which section of the image to analyse is an excellent tool to speed up and optimise the process. One of the future developments of this method can be the automatic recognition of the area of the image where the object to be searched for is present. In this specific case, you could use deep learning and image recognition techniques to find the area where the object is present. To do this, the automatic division of the image into micro areas would be necessary. Now, the proposed system is faster, but it is not impossible to think that the proposed development could help to automate the process further.

In conclusion, it can say that the artificial intelligence techniques proposed and developed for the applications shown in this thesis work, do work. Both neural networks and bees algorithms have great potential, and the speed of the calculations demonstrate their attractiveness in an industrial sector that continues to evolve. It is now easy to imagine their use not only in academia but also in business and industry. Artificial intelligence techniques represent a fundamental step towards the automation and remote control that is so much in demand on the market. The very concept of Industry 4.0 is based on these principles and, to achieve its objectives, cannot do without artificial intelligence techniques. In the course of this thesis and demonstrating their effectiveness, it has analysed the various related research works and the benefits of using these techniques. In this futuristic momentum we are experiencing, it is also essential to consider the human being's role. The fear of many is: will artificial intelligence replace human beings? As the industry evolves, so do people's jobs. It will change the way work done. Some professions will disappear in favour of others that will emerge. Behind the



programming of artificial intelligence, there will always be a human being, even if artificial intelligence will learn on its own. Therefore, this evolution is not to greet with extreme fear. Technological development always has only one aim: to improve the quality of life of human beings.

## 7. REFERENCES

- Schwab, K. *The Fourth Industrial Revolution*; World Economic Forum: Cologne, 2016; ISBN 978-1-944835-01-9.
- European Commission 'A European strategy for Key Enabling Technologies – A bridge to growth and jobs.' **2012**, 1–18.
- Hellström, A.; Nilsson, S.; Andersson, M.; Håkanson, U. Intellectual property for generating value for start-up companies in key enabling technologies. *Biotechnol. Res. Innov.* **2019**, *3*, 80–90, doi:10.1016/j.biori.2019.01.001.
- Bag, S.; Gupta, S.; Kumar, S. Industry 4.0 adoption and 10R advance manufacturing capabilities for sustainable development. *Int. J. Prod. Econ.* **2021**, *231*, 107844, doi:10.1016/j.ijpe.2020.107844.
- Everton, S.K.; Hirsch, M.; Stavroulakis, P.I.; Leach, R.K.; Clare, A.T. Review of in-situ process monitoring and in-situ metrology for metal additive manufacturing. *Mater. Des.* **2016**, *95*, 431–445, doi:10.1016/j.matdes.2016.01.099.
- Evangelista, A.; Ardito, L.; Boccaccio, A.; Fiorentino, M.; Messeni Petruzzelli, A.; Uva, A.E. Unveiling the technological trends of augmented reality: A patent analysis. *Comput. Ind.* **2020**, *118*, 103221, doi:10.1016/j.compind.2020.103221.
- Yan, X.; Gu, P. A review of rapid prototyping technologies and systems. *CAD Comput. Aided Des.* **1996**, *28*, 307–318, doi:10.1016/0010-4485(95)00035-6.
- Rejeb, A.; Rejeb, K.; Zailani, S.; Treiblmaier, H.; Hand, K.J. Internet of Things Integrating the Internet of Things in the halal food supply chain : A systematic literature review and research agenda. *Internet of Things* **2021**, *13*, 100361, doi:10.1016/j.iot.2021.100361.
- Helali, L.; Omri, M.N. A survey of data center consolidation in cloud computing systems. *Comput. Sci. Rev.* **2021**, *39*, 100366, doi:10.1016/j.cosrev.2021.100366.
- Dixit, P.; Silakari, S. Deep Learning Algorithms for Cybersecurity Applications: A Technological and Status Review. *Comput. Sci. Rev.* **2021**, *39*, 100317, doi:10.1016/j.cosrev.2020.100317.
- Amanullah, M.A.; Habeeb, R.A.A.; Nasaruddin, F.H.; Gani, A.; Ahmed, E.; Nainar, A.S.M.; Akim, N.M.; Imran, M. Deep learning and big data technologies for IoT security. *Comput. Commun.* **2020**, *151*, 495–517, doi:10.1016/j.comcom.2020.01.016.
- Ullah, Z.; Al-Turjman, F.; Mostarda, L.; Gagliardi, R. Applications of Artificial Intelligence and Machine learning in smart cities. *Comput. Commun.* **2020**, *154*, 313–323, doi:10.1016/j.comcom.2020.02.069.
- Dalzochio, J.; Kunst, R.; Pignaton, E.; Binotto, A.; Sanyal, S.; Favilla, J.; Barbosa, J. Machine learning and reasoning for predictive maintenance in Industry 4.0: Current status and challenges. *Comput. Ind.* **2020**, *123*, 103298, doi:10.1016/j.compind.2020.103298.
- Johansson, D.; Lindvall, R.; Windmark, C.; M'Saoubi, R.; Can, A.; Bushlya, V.; Ståhl, J.-E. Assessment of Metal Cutting Tools using Cost Performance Ratio and Tool Life Analyses. *Procedia Manuf.* **2019**, *38*, 816–823, doi:10.1016/j.promfg.2020.01.114.
- Behera, B.C.; Ghosh, S.; Rao, P.V. Modeling of cutting force in MQL machining environment considering chip tool contact friction. *Tribol. Int.* **2018**, *117*, 283–295, doi:10.1016/j.triboint.2017.09.015.
- Zhou, G.; Lu, Q.; Xiao, Z.; Zhou, C.; Tian, C. Cutting parameter optimization for machining operations considering carbon emissions. *J. Clean. Prod.* **2019**, *208*, 937–950, doi:10.1016/j.jclepro.2018.10.191.
- Luoke, H.; Renzhong, T.; Wei, C.; Yixiong, F.; Xiang, M. Optimisation of cutting parameters for improving energy efficiency in machining process. *Robot. Comput. Integr. Manuf.* **2019**, *59*, 406–416, doi:10.1016/j.rcim.2019.04.015.
- Antsev, A. V Cutting tool life prediction in case of rough machining by the fracture model. *Mater. Today Proc.* **2019**, *19*, 2148–2151, doi:10.1016/j.matpr.2019.07.229.
- Johansson, D.; Akujarvi, V.; Hagglund, S.; Bushlya, V.; Ståhl, J.-E. Selecting Cutting Data Tests for Cutting Data Modeling Using the Colding Tool Life Model. *Procedia CIRP* **2018**, *72*, 197–201, doi:10.1016/j.procir.2018.03.035.
- Brenner, D.; Kleinert, F.; Imiela, J.; Westkämper, E. Life Cycle Management of Cutting Tools: Comprehensive Acquisition and Aggregation of Tool Life Data. *Procedia CIRP* **2017**, *61*, 311–316, doi:10.1016/j.procir.2016.11.168.
- Jamwal, A.; Agrawal, R.; Sharma, M.; Dangayach, G.S.; Gupta, S. Application of optimization techniques in metal cutting operations: A bibliometric analysis. *Mater. Today Proc. J.* **2020**, doi:10.1016/j.matpr.2020.07.425.
- Du Preez, A.; Oosthuizen, G.A. Machine learning in cutting processes as enabler for smart sustainable manufacturing. *Procedia Manuf.* **2019**, *33*, 810–817, doi:10.1016/j.promfg.2019.04.102.
- Xie, Y.; Lian, K.; Liu, Q.; Zhang, C.; Liu, H. Digital twin for cutting tool: Modeling, application and service strategy. *J. Manuf. Syst.* **2020**, doi:10.1016/j.jmsy.2020.08.007.
- Brettel, M.; Friederichsen, N.; Keller, M.; Rosenberg, M. How Virtualization, Decentralization and Network Building Change the Manufacturing Landscape: An Industry 4.0 Perspective. *Int. J. Inf. Commun. Eng.* **2014**, *8*, 37–44, doi:10.5281/zenodo.1336426.

25. Okolie, S.O.; Kuyoro, S.O.; Ohwo, O.B. Emerging Cyber-Physical Systems : An Overview. *Int. J. Sci. Res. Comput. Sci. Eng. Inf. Technol.* **2018**, *3*, 306–316, doi:10.32628/CSEIT183862.
26. Echchakouia, S.; Barka, N. Industry 4.0 and its impact in plastics industry: A literature review. *J. Ind. Inf. Integr.* **2020**, *20*, 1–14, doi:10.1016/j.jii.2020.100172.
27. Kagermann, H. Change Through Digitization---Value Creation in the Age of Industry 4.0. *Manag. Perm. Chang.* **2015**, 23–45, doi:10.1007/978-3-658-05014-6-2.
28. Gisbert, J.R.; Palau, C.; Uriarte, M.; Prieto, G.; Palazón, J.A.; Esteve, M.; López, O.; Correas, J.; Lucas-Estañ, M.C.; Giménez, P.; et al. Integrated system for control and monitoring industrial wireless networks for labor risk prevention. *J. Netw. Comput. Appl.* **2014**, *39*, 233–252, doi:10.1016/j.jnca.2013.07.014.
29. Schuh, G.; Potente, T.; Varandani, R.; Hausberg, C.; Fränken, B. Collaboration Moves Productivity to the Next Level. *Procedia CIRP* **2014**, *17*, 3–8, doi:10.1016/j.procir.2014.02.037.
30. Khaitan, S.K.; McCalley, J.D. Design Techniques and Applications of Cyberphysical Systems: A Survey. *IEEE Syst. J.* **2014**, *9*, 350–365, doi:10.1109/JSYST.2014.2322503.
31. Toro, R.; Correa, J.E.; Ferreira, P.M. A Cloud-Monitoring Service for Manufacturing Environments. *Procedia Manuf.* **2018**, *26*, 1330–1339, doi:10.1016/j.promfg.2018.07.128.
32. Oztemel, E.; Gursev, S. Literature review of Industry 4.0 and related technologies. *J. Intell. Manuf.* **2020**, *31*, 127–182, doi:10.1007/s10845-018-1433-8.
33. Ghobakhloo, M.; Fathi, M. Corporate survival in Industry 4.0 era: the enabling role of lean-digitized manufacturing. *J. Manuf. Technol. Manag.* **2020**, *31*, 1–30, doi:10.1108/JMTM-11-2018-0417.
34. Rosa, P.; Sassanelli, C.; Urbinati, A.; Chiaroni, D.; Terzi, S. Assessing relations between Circular Economy and Industry 4.0: a systematic literature review. *Int. J. Prod. Res.* **2020**, *58*, 1662–1687, doi:10.1080/00207543.2019.1680896.
35. Teti, R.; Jemielniak, K.; O'Donnell, G.; Dornfeld, D. Advanced monitoring of machining operations. *CIRP Ann.* **2010**, *59*, 717–739, doi:10.1016/j.cirp.2010.05.010.
36. Byrne, G.; Dornfeld, D.; Inasaki, I.; Ketteler, G.; König, W.; Teti, R. Tool Condition Monitoring (TCM) --- The Status of Research and Industrial Application. *CIRP Ann.* **1995**, *44*, 541–567, doi:10.1016/S0007-8506(07)60503-4.
37. Rangwala, S.; Dornfeld, D. Sensor Integration Using Neural Networks for Intelligent Tool Condition Monitoring. *J. Eng. Ind.* **1990**, *112*, 219–228, doi:10.1115/1.2899578.
38. Berman, D. Nonideal behavior of rotating gravitational mass sensors. *AIAA J.* **1967**, *5*, 1000–1008, doi:10.2514/3.4114.
39. Nevins, J.L.; Whitney, D.E. Information and control issues of adaptable, programmable assembly systems for manufacturing and teleoperator applications. *Mech. Mach. Theory* **1977**, *12*, 27–43, doi:10.1016/0094-114X(77)90054-4.
40. Quittner, G.F. Sensors in Automation. *IEEE Trans. Ind. Electron. Control Instrum.* **1974**, *IECI-21*, 3–12, doi:10.1109/TIECI.1974.351171.
41. Quaranta, A.A. Sensors And Transducers. *IEEE Trans. Ind. Electron. Control Instrum.* **1976**, *IECI-23*, 319–324, doi:10.1109/TIECI.1976.351400.
42. Nitzan; Rosen Programmable Industrial Automation. *IEEE Trans. Comput.* **1976**, *C-25*, 1259–1270, doi:10.1109/TC.1976.1674593.
43. Gregory, R.L. Seeing as thinking: an active theory of perception. *Times Lit. Suppl.* **1972**, 707–708.
44. Gregory, R.L. Knowledge in perception and illusion. *Philos. Trans. R. Soc. Lond. B. Biol. Sci.* **1997**, *352*, 1121–1127, doi:10.1098/rstb.1997.0095.
45. Bajcsy, R. From Active Perception to Active Cooperation Fundamental Process of Intelligent Behavior. *Vis. Atten. Cogn.* **1995**, 309–321.
46. Teti, R. Advanced IT Methods of Signal Processing and Decision Making for Zero Defect Manufacturing in Machining. *Procedia CIRP* **2015**, *28*, 3–15, doi:10.1016/j.procir.2015.04.003.
47. Wang, L.; Gao, R.X. *Condition monitoring and control for intelligent manufacturing*; Springer series in advanced manufacturing; Springer: London, 2006; ISBN 9781846282683.
48. Axinte, D.A.; Gindy, N. Tool condition monitoring in broaching. *Wear* **2003**, *254*, 370–382, doi:10.1016/S0043-1648(03)00003-6.
49. Axinte, D.; Gindy, N. Assessment of the effectiveness of a spindle power signal for tool condition monitoring in machining processes. *Int. J. Prod. Res.* **2004**, *42*, 2679–2691, doi:10.1080/00207540410001671642.
50. Teti, R.; Baciú, I.L. Neural Network Processing of Audible Sound Signal Parameters for Sensor Monitoring of Tool Conditions. *4th CIRP Int. Sem. ICME, Sorrento* **2004**, 385–390.
51. Lee, J.M.; Choi, D.K.; Kim, J.; Chu, C.N. Real-Time Tool Breakage Monitoring for NC Milling Process. *CIRP Ann.* **1995**, *44*, 59–62, doi:10.1016/S0007-8506(07)62275-6.
52. Ryabov, O.; Mori, K.; Kasashima, N.; Uehara, K. An In-Process Direct Monitoring Method for Milling Tool Failures Using a Laser Sensor. *CIRP Ann.* **1996**, *45*, 97–100, doi:10.1016/S0007-8506(07)63024-8.
53. Lee, D.J.; Kim, S.H.; Ahn, J.H. Breakage detection of small-diameter tap using vision system in high-speed tapping machine with open architecture controller. *KSME Int. J.* **2004**, *18*, 1055–1061.

54. Kim, H.Y.; Ahn, J.H.; Kim, S.H.; Takata, S. Real-time drill wear estimation based on spindle motor power. *J. Mater. Process. Technol.* **2002**, *124*, 267–273, doi:10.1016/S0924-0136(02)00111-5.
55. Gandarias, E.; Dimov, S.; Pham, D.T.; Ivanov, A.; Popov, K.; Lizarralde, R.; Arrazola, P.J. New Methods for Tool Failure Detection in Micromilling. *Proc. Inst. Mech. Eng. Part B J. Eng. Manuf.* **2006**, *220*, 137–144, doi:10.1243/095440506X77562.
56. Govekar, E.; Gradišek, J.; Grabec, I. Analysis of acoustic emission signals and monitoring of machining processes. *Ultrasonics* **2000**, *38*, 598–603, doi:10.1016/S0041-624X(99)00126-2.
57. Teti, R.; Jawahir, I.S.; Jemielniak, K.; Segreto, T.; Chen, S.; Kossakowska, J. Chip Form Monitoring through Advanced Processing of Cutting Force Sensor Signals. *CIRP Ann.* **2006**, *55*, 75–80, doi:10.1016/S0007-8506(07)60370-9.
58. Venuvinod, P.K.; Djordjevic, A. Towards Active Chip Control. *CIRP Ann.* **1996**, *45*, 83–86, doi:10.1016/S0007-8506(07)63021-2.
59. Andreasen, J.L.; de Chiffre, L. An Automatic System for Elaboration of Chip Breaking Diagrams. *CIRP Ann.* **1998**, *47*, 35–40, doi:10.1016/S0007-8506(07)62780-2.
60. Azouzi, R.; Guillot, M. On-line prediction of surface finish and dimensional deviation in turning using neural network based sensor fusion. *Int. J. Mach. Tools Manuf.* **1997**, *37*, 1201–1217, doi:10.1016/S0890-6955(97)00013-8.
61. Chen, J.C.; Huang, B. An In-Process Neural Network-Based Surface Roughness Prediction (INN-SRP) System Using a Dynamometer in End Milling Operations. *Int. J. Adv. Manuf. Technol.* **2003**, *21*, 339–347, doi:10.1007/s001700300039.
62. Abouelatta, O.B.; Mádl, J. Surface roughness prediction based on cutting parameters and tool vibrations in turning operations. *J. Mater. Process. Technol.* **2001**, *118*, 269–277, doi:10.1016/S0924-0136(01)00959-1.
63. Salgado, D.R.; Alonso, F.J.; Cambero, I.; Marcelo, A. In-process surface roughness prediction system using cutting vibrations in turning. *Int. J. Adv. Manuf. Technol.* **2009**, *43*, 40–51, doi:10.1007/s00170-008-1698-8.
64. Axinte, D.A.; Gindy, N.; Fox, K.; Unanue, I. Process monitoring to assist the workpiece surface quality in machining. *Int. J. Mach. Tools Manuf.* **2004**, *44*, 1091–1108, doi:10.1016/j.ijmachtools.2004.02.020.
65. Kwak, J.-S.; Song, J.-B. Trouble diagnosis of the grinding process by using acoustic emission signals. *Int. J. Mach. Tools Manuf.* **2001**, *41*, 899–913, doi:10.1016/S0890-6955(00)00082-1.
66. Zhou, Z.D.; Chen, Y.P.; Fuh, J.Y.H.; Nee, A.Y.C. Integrated Condition Monitoring and Fault Diagnosis for Modern Manufacturing Systems. *CIRP Ann.* **2000**, *49*, 387–390, doi:10.1016/S0007-8506(07)62971-0.
67. Ojstersek, R.; Brezocnik, M.; Buchmeister, B. Multi-objective optimization of production scheduling with evolutionary computation: A review. *Int. J. Ind. Eng. Comput.* **2020**, 359–376, doi:10.5267/j.ijiec.2020.1.003.
68. Yang, W.; Takakuwa, S. Simulation-based dynamic shop floor scheduling for a flexible manufacturing system in the industry 4.0 environment. *Winter Simul. Conf.* **2017**, 3908–3916, doi:10.1109/WSC.2017.8248101.
69. Rivera, L.; Frank Chen, F. Measuring the impact of Lean tools on the cost–time investment of a product using cost–time profiles. *Robot. Comput. Integr. Manuf.* **2007**, *23*, 684–689, doi:10.1016/j.rcim.2007.02.013.
70. Ojstersek, R.; Buchmeister, B. Use of Simulation Software Environments for the Purpose of Production Optimization. *28TH DAAAM Int. Symp. Intell. Manuf. Autom.* **2017**, *1*, 750–758, doi:10.2507/28th.daaam.proceedings.106.
71. Bartodziej, C.J. *The concept industry 4.0*; Springer Berlin Heidelberg: New York NY, 2016; ISBN 978-3-658-16501-7.
72. Sule, D.R. *Manufacturing facilities: Location, planning, and design / Dileep R. Sule*; 3rd ed.; CRC Press: Place of publication not identified, 2008; ISBN 1420044230.
73. Pinedo, M. *Scheduling: Theory, algorithms, and systems*; Prentice-Hall International Series in Industrial and Systems Engineering; 4th ed.; Springer: New York, 2012; ISBN 1461419867.
74. Altıok, T. *Performance Analysis of Manufacturing Systems*; Springer Series in Operations Research; Springer New York: New York, NY, 1997; ISBN 978-1-4612-1924-8.
75. Fetene Adane, T.; Bianchi, M.F.; Archenti, A.; Nicolescu, M. Application of system dynamics for analysis of performance of manufacturing systems. *J. Manuf. Syst.* **2019**, *53*, 212–233, doi:10.1016/j.jmsy.2019.10.004.
76. Hon, K.K.B. Performance and Evaluation of Manufacturing Systems. *CIRP Ann.* **2005**, *54*, 139–154, doi:10.1016/S0007-8506(07)60023-7.
77. Jain, S.; Smith, J.M. Open finite queueing networks with M/M/C/K parallel servers. *Comput. Oper. Res.* **1994**, *21*, 297–317, doi:10.1016/0305-0548(94)90092-2.
78. Patchong, A.; Willayes, D. Modeling and analysis of an unreliable flow line composed of parallel-machine stages. *IIE Trans.* **2001**, *33*, 559–568, doi:10.1080/07408170108936854.
79. Cao, X.R.; Ho, Y.C. Sensitivity analysis and optimization of throughput in a production line with blocking. *IEEE Trans Auto Cont* **1987**, *32*, 959–967.
80. Peralta Álvarez, M.E.; Marcos Bárcena, M.; Aguayo González, F. A Review of Sustainable Machining Engineering: Optimization Process Through Triple Bottom Line. *J. Manuf. Sci. Eng.* **2016**, *138*, doi:10.1115/1.4034277.
81. Prinsloo, J.; Sinha, S.; von Solms, B. A Review of Industry 4.0 Manufacturing Process Security Risks. *Appl. Sci.*

**2019**, 9, 5105, doi:10.3390/app9235105.

82. Feng, C.; Huang, S. The Analysis of Key Technologies for Sustainable Machine Tools Design. *Appl. Sci.* **2020**, *10*, 731, doi:10.3390/app10030731.
83. Moderato, P.; Rovetto, F. *Psicologo: Verso la professione : dall'esame di Stato al mondo del lavoro*; Psicologia / [McGraw-Hill]; 4. ed.; McGraw-Hill: Milano [etc.], 2016; ISBN 9788838639852.
84. von Neumann, J.; Morgenstern, O. *Theory of games and economic behavior*; Princeton classic editions; 60th anniv.; Princeton University Press: Princeton N.J. and Woodstock, 2007; ISBN 9780691130613.
85. Tversky, A.; Kahneman, D. Judgment under Uncertainty: Heuristics and Biases. *Science* **1974**, *185*, 1124–1131, doi:10.1126/science.185.4157.1124.
86. Tversky, A.; Kahneman, D. The framing of decisions and the psychology of choice. *Science* **1981**, *211*, 453–458, doi:10.1126/science.7455683.
87. Lu, H. *Cognitive internet of things: Frameworks, tools and applications*; Studies in computational intelligence; Springer: Cham, 2019; Vol. volume 810; ISBN 978-3-030-04945-4.
88. Hoffmann Souza, M.L.; da Costa, C.A.; de Oliveira Ramos, G.; da Rosa Righi, R. A survey on decision-making based on system reliability in the context of Industry 4.0. *J. Manuf. Syst.* **2020**, *56*, 133–156, doi:10.1016/j.jmsy.2020.05.016.
89. Lee, C.K.M.; Zhang, S.Z.; Ng, K.K.H. Development of an industrial Internet of things suite for smart factory towards re-industrialization. *Adv. Manuf.* **2017**, *5*, 335–343, doi:10.1007/s40436-017-0197-2.
90. Burggräf, P.; Wagner, J.; Koke, B.; Bamberg, M. Performance assessment methodology for AI-supported decision-making in production management. *Procedia CIRP* **2020**, *93*, 891–896, doi:10.1016/j.procir.2020.03.047.
91. Han, S.; Chang, T.-W.; Hong, Y.S.; Park, J. Reconfiguration Decision-Making of IoT based Reconfigurable Manufacturing Systems. *Appl. Sci.* **2020**, *10*, 4807, doi:10.3390/app10144807.
92. Lv, L.; Deng, Z.; Meng, H.; Liu, T.; Wan, L. A multi-objective decision-making method for machining process plan and an application. *J. Clean. Prod.* **2020**, *260*, 121072, doi:10.1016/j.jclepro.2020.121072.
93. Yu, J.; Gu, S.; Wang, J.; Jia, Z.; Zhao, Y. The Intelligent Decision-making based on Multisource Heterogeneous Data Fusion in Manufacturing. *12th Int. Conf. Adv. Comput. Intell.* **2020**, 155–159, doi:10.1109/ICACI49185.2020.9177661.
94. Tran, Q.-P.; Nguyen, V.-N.; Huang, S.-C. Drilling Process on CFRP: Multi-Criteria Decision-Making with Entropy Weight Using Grey-TOPSIS Method. *Appl. Sci.* **2020**, *10*, 7207, doi:10.3390/app10207207.
95. Zheng, P.; Liu, D.; Guo, J.; Zhi, Z. A new method for optimizing process parameters of active measurement grinding based on grey target decision making. *Proc. Inst. Mech. Eng. Part C J. Mech. Eng. Sci.* **2020**, *234*, 4645–4658, doi:10.1177/0954406220927052.
96. Yurdakul, M. AHP as a strategic decision-making tool to justify machine tool selection. *J. Mater. Process. Technol.* **2004**, *146*, 365–376, doi:10.1016/j.jmatprotec.2003.11.026.
97. Bozdağ, C.E.; Kahraman, C.; Ruan, D. Fuzzy group decision making for selection among computer integrated manufacturing systems. *Comput. Ind.* **2003**, *51*, 13–29, doi:10.1016/S0166-3615(03)00029-0.
98. Kannan, D.; Khodaverdi, R.; Olfat, L.; Jafarian, A.; Diabat, A. Integrated fuzzy multi criteria decision making method and multi-objective programming approach for supplier selection and order allocation in a green supply chain. *J. Clean. Prod.* **2013**, *47*, 355–367, doi:10.1016/j.jclepro.2013.02.010.
99. Dietmair, A.; Verl, A. A generic energy consumption model for decision making and energy efficiency optimisation in manufacturing. *Int. J. Sustain. Eng.* **2009**, *2*, 123–133, doi:10.1080/19397030902947041.
100. Chakraborty, S. Applications of the MOORA method for decision making in manufacturing environment. *Int. J. Adv. Manuf. Technol.* **2011**, *54*, 1155–1166, doi:10.1007/s00170-010-2972-0.
101. Russell, S.J.; Norvig, P.; Davis, E. *Artificial intelligence: A modern approach*; Prentice Hall series in artificial intelligence; 3rd ed.; Prentice Hall: Upper Saddle River, 2010; ISBN 9780136042594.
102. Guida, G.; Somalvico, M. Interacting in natural language with artificial systems: The donau project. *Inf. Syst.* **1980**, *5*, 333–344, doi:10.1016/0306-4379(80)90079-4.
103. McCarthy, J. *A Basis for a mathematical theory of computation*; North-Holland Publishing Company Amsterdam, 1959; Vol. 26;.
104. Livshin, I. *Artificial Neural Networks with Java*; 2019; ISBN 9781484244203.
105. Fogelman Soulié, F. *Algorithms, Architectures and Applications*; Springer-Verlag & NATO Scientific Affairs Division: Les Arcs, France, 1990; ISBN 9783642761553.
106. Hertz, J.; Krogh, A.; Palmer, R.G. *Introduction to the theory of Neural Computation*; CRC Press: Santa Fe Institute Studies, 2018; ISBN 9780201515602.
107. McCulloch, W.S.; Pitts, W. A logical calculus of the ideas immanent in nervous activity. *Bull. Math. Biophys.* **1943**, *5*, 115–133, doi:10.1007/BF02478259.
108. Rosenblatt, F. The perceptron: A probabilistic model for information storage and organization in the brain. *Psychol. Rev.* **1958**, *65*, 386–408, doi:10.1037/h0042519.
109. Freund, Y.; Schapire, R.E. Large Margin Classification Using the Perceptron Algorithm. *Mach. Learn.* **1999**, *37*, 277–296, doi:https://doi.org/10.1023/A:1007662407062.

110. Petkar, P.M.; Gaitonde, V.N.; Karnik, S.R.; Kulkarni, V.N.; Raju, T.K.G.; Paulo Davim, J. Analysis of forming behavior in cold forging of aisi 1010 steel using artificial neural network. *Metals (Basel)*. **2020**, *10*, 1–24, doi:10.3390/met10111431.
111. Kalombo, R.B.; Pestana, M.S.; Freire Júnior, R.C.S.; Ferreira, J.L.A.; Silva, C.R.M.; Veloso, L.A.C.M.; Câmara, E.C.B.; Araújo, J.A. Fatigue life estimation of an all aluminium alloy 1055 MCM conductor for different mean stresses using an artificial neural network. *Int. J. Fatigue* **2020**, *140*, 105814, doi:10.1016/j.ijfatigue.2020.105814.
112. Khorasani, A.M.; Yazdi, M.R.S. Development of a dynamic surface roughness monitoring system based on artificial neural networks (ANN) in milling operation. *Int. J. Adv. Manuf. Technol.* **2017**, *93*, 141–151, doi:10.1007/s00170-015-7922-4.
113. Zhao, D.; Ren, D.; Zhao, K.; Pan, S.; Guo, X. Effect of welding parameters on tensile strength of ultrasonic spot welded joints of aluminum to steel – By experimentation and artificial neural network. *J. Manuf. Process.* **2017**, *30*, 63–74, doi:10.1016/j.jmapro.2017.08.009.
114. Hanief, M.; Wani, M.F.; Charoo, M.S. Modeling and prediction of cutting forces during the turning of red brass (C23000) using ANN and regression analysis. *Eng. Sci. Technol. an Int. J.* **2017**, *20*, 1220–1226, doi:10.1016/j.jestch.2016.10.019.
115. Wiciak-Pikuła, M.; Felusiak-Czyryca, A.; Twardowski, P. Tool Wear Prediction Based on Artificial Neural Network during Aluminum Matrix Composite Milling. *Sensors* **2020**, *20*, 5798, doi:10.3390/s20205798.
116. Saoudi, A.; Fellah, M.; Hezil, N.; Lerari, D.; Khamouli, F.; Atoui, L.; Bachari, K.; Morozova, J.; Obrosof, A.; Abdul Samad, M. Prediction of mechanical properties of welded steel X70 pipeline using neural network modelling. *Int. J. Press. Vessel. Pip.* **2020**, *186*, 104153, doi:10.1016/j.ijpvp.2020.104153.
117. Chowdhury, S.; Mhapsekar, K.; Anand, S. Part Build Orientation Optimization and Neural Network-Based Geometry Compensation for Additive Manufacturing Process. *J. Manuf. Sci. Eng. Trans. ASME* **2018**, *140*, doi:10.1115/1.4038293.
118. Hesser, D.F.; Markert, B. Tool wear monitoring of a retrofitted CNC milling machine using artificial neural networks. *Manuf. Lett.* **2019**, *19*, 1–4, doi:10.1016/j.mfglet.2018.11.001.
119. Mikołajczyk, T.; Nowicki, K.; Bustillo, A.; Pimenov, D.Y. Predicting tool life in turning operations using neural networks and image processing. *Mech. Syst. Signal Process.* **2018**, *104*, 503–513, doi:10.1016/j.ymssp.2017.11.022.
120. D’Addona, D.M.; Ullah, A.M.M.S.; Matarazzo, D. Tool-wear prediction and pattern-recognition using artificial neural network and DNA-based computing. *J. Intell. Manuf.* **2017**, *28*, 1285–1301, doi:10.1007/s10845-015-1155-0.
121. Zerti, A.; Yallese, M.A.; Zerti, O.; Nouioua, M.; Khettabi, R. Prediction of machining performance using RSM and ANN models in hard turning of martensitic stainless steel AISI 420. *Proc. Inst. Mech. Eng. Part C J. Mech. Eng. Sci.* **2019**, *233*, 4439–4462, doi:10.1177/0954406218820557.
122. Laouissi, A.; Yallese, M.A.; Belbah, A.; Belhadi, S.; Haddad, A. Investigation, modeling, and optimization of cutting parameters in turning of gray cast iron using coated and uncoated silicon nitride ceramic tools. Based on ANN, RSM, and GA optimization. *Int. J. Adv. Manuf. Technol.* **2019**, *101*, 523–548, doi:10.1007/s00170-018-2931-8.
123. Ghosh, G.; Mandal, P.; Mondal, S.C. Modeling and optimization of surface roughness in keyway milling using ANN, genetic algorithm, and particle swarm optimization. *Int. J. Adv. Manuf. Technol.* **2019**, *100*, 1223–1242, doi:10.1007/s00170-017-1417-4.
124. Bensingh, R.J.; Machavaram, R.; Boopathy, S.R.; Jebaraj, C. Injection molding process optimization of a bi-aspheric lens using hybrid artificial neural networks (ANNs) and particle swarm optimization (PSO). *Meas. J. Int. Meas. Confed.* **2019**, *134*, 359–374, doi:10.1016/j.measurement.2018.10.066.
125. Venkata Rao, K.; Murthy, P.B.G.S.N. Modeling and optimization of tool vibration and surface roughness in boring of steel using RSM, ANN and SVM. *J. Intell. Manuf.* **2018**, *29*, 1533–1543, doi:10.1007/s10845-016-1197-y.
126. Patra, K.; Jha, A.K.; Szalay, T.; Ranjan, J.; Monostori, L. *Artificial neural network based tool condition monitoring in micro mechanical peck drilling using thrust force signals*; Elsevier Inc., 2017; Vol. 48; ISBN 0141635916.
127. Mikołajczyk, T.; Nowicki, K.; Kłodowski, A.; Pimenov, D.Y. Neural network approach for automatic image analysis of cutting edge wear. *Mech. Syst. Signal Process.* **2017**, *88*, 100–110, doi:10.1016/j.ymssp.2016.11.026.
128. Maynard, M. *Neural Networks: Introduction to Artificial Neurons, Backpropagation and Multilayer Feedforward Neural Networks with Real-World Applications*; 2020; ISBN 9788578110796.
129. Mitchell, T.M. *Machine Learning*; McGraw-Hill, 1997; ISBN 9780070428072.
130. Dike, H.U.; Zhou, Y.; Deveerasetty, K.K.; Wu, Q. Unsupervised Learning Based On Artificial Neural Network: A Review. *2018 IEEE Int. Conf. Cyborg Bionic Syst. CBS 2018* **2019**, 322–327, doi:10.1109/CBS.2018.8612259.
131. Hush, D.R.; Horne, B.G. Progress in supervised neural networks. *Signal Process. Mag. IEEE* **1993**, *10*, 8–39.
132. Yusof, Y.; Mansor, H.M.A.H.; Ahmad, A. Utilizing unsupervised weightless neural network as autonomous states classifier in reinforcement learning algorithm. *Proc. - 2017 IEEE 13th Int. Colloq. Signal Process. its Appl. CSPA 2017* **2017**, 264–269, doi:10.1109/CSPA.2017.8064963.

133. Bailey, K.D. Typologies and Taxonomies: An Introduction to Classification Techniques (Sage University Paper series on Quantitative Applications in the Social Sciences, series no. 07-102). *Sage Univ. Pap. Ser. Quant. Appl. Soc. Sci. no 07 102* 1994, 90.
134. Hodge, V.J.; Austin, J. A Survey of Outlier Detection Methodologies. *Artif. Intell. Rev.* **2004**, *22*, 85–126, doi:10.4324/9781315744988-22.
135. Tomek, I. Experiment With the Edited Nearest-Neighbor Rule. *IEEE Trans. Syst. Man Cybern.* **1976**, *SMC-6*, 448–452, doi:10.1109/TSMC.1976.4309523.
136. Bengio, Y. *Learning deep architectures for AI*; 2009; Vol. 2; ISBN 2200000006.
137. Hecht-Nielsen, R. Theory of the backpropagation neural network. **1989**, 593–605, doi:10.1109/ijcnn.1989.118638.
138. Wu, H.; Ji, Z.; Li, M. Non-invasive continuous blood-pressure monitoring models based on photoplethysmography and electrocardiography. *Sensors (Switzerland)* **2019**, *19*, doi:10.3390/s19245543.
139. Aritonang, M.; Sihombing, D.J.C. An Application of Backpropagation Neural Network for Sales Forecasting Rice Milling Unit. *2019 Int. Conf. Comput. Sci. Inf. Technol. ICoSNIKOM 2019* **2019**, 7–10, doi:10.1109/ICoSNIKOM48755.2019.9111612.
140. Effendi, M.K.; Soepangkat, B.O.P.; Pramujati, B.; Norcahyo, R.; Nurullah, F.P. The combined methodology of backpropagation neural network with genetic algorithm to optimize delamination factor and surface roughness in end-milling of carbon fiber reinforced polymer composites. *AIP Conf. Proc.* **2019**, *2187*, 1–7, doi:10.1063/1.5138310.
141. Sovia, R.; Yanto, M.; Budiman, A.; Mayola, L.; Saputra, D. Backpropagation neural network prediction for cryptocurrency bitcoin prices. *J. Phys. Conf. Ser.* **2019**, *1339*, doi:10.1088/1742-6596/1339/1/012060.
142. Negrov, D.; Karandashev, I.; Shakirov, V.; Matveyev, Y.; Dunin-Barkowski, W.; Zenkevich, A. An approximate backpropagation learning rule for memristor based neural networks using synaptic plasticity. *Neurocomputing* **2017**, *237*, 193–199, doi:10.1016/j.neucom.2016.10.061.
143. Kohonen, T. Self-organized formation of topologically correct feature maps. *Biol. Cybern.* **1982**, *43*, 59–69, doi:10.1007/BF00337288.
144. Kohonen, T. Self-organizing maps, 3rd ed. 2001, 501.
145. Chifu, E.S.; Letia, T.S.; Chifu, V.R. Unsupervised Aspect Level Sentiment Analysis Using Self-Organizing Maps. *Proc. - 17th Int. Symp. Symb. Numer. Algorithms Sci. Comput. SYNASC 2015* **2016**, 468–475, doi:10.1109/SYNASC.2015.75.
146. Hammer, B.; Gisbrecht, A.; Hasenfuss, A.; Mokbel, B. *Advances in Self-Organizing Maps: 8th International Workshop, WSOM 2011, Espoo, Finland, June 13-15, 2011. Proceedings*; Springer-Verlag Berlin Heidelberg, 2011; ISBN 9783642215667.
147. Pham, D.T.; Eldukhri, E.E.; Soroka, A.J.; Ghanbarzadeh, A.; Kog, E.; Otri, S.; Rahim, S.; Zaidi, M. Intelligent Production Machines and Systems The Bees Algorithm-A Novel Tool for Complex Optimisation Problems. **2006**, 454–459.
148. Pham, D.T.; Castellani, M. The bees algorithm: Modelling foraging behaviour to solve continuous optimization problems. *Proc. Inst. Mech. Eng. Part C J. Mech. Eng. Sci.* **2009**, *223*, 2919–2938, doi:10.1243/09544062JMES1494.
149. Aria, M.; Cuccurullo, C. bibliometrix: An R-tool for comprehensive science mapping analysis. *J. Informetr.* **2017**, *11*, 959–975, doi:10.1016/j.joi.2017.08.007.
150. Packianather, M.S.; Kapoor, B. A wrapper-based feature selection approach using Bees Algorithm for a wood defect classification system. *2015 10th Syst. Syst. Eng. Conf. SoSE 2015* **2015**, 498–503, doi:10.1109/SYSESE.2015.7151902.
151. Pham, D.T.; Soroka, A.J.; Ghanbarzadeh, A.; Koc, E.; Otri, S.; Packianather, M. Optimising neural networks for identification of wood defects using the bees algorithm. *2006 IEEE Int. Conf. Ind. Informatics, INDIN'06* **2006**, 1346–1351, doi:10.1109/INDIN.2006.275855.
152. Sundararaj, V. Optimal Task Assignment in Mobile Cloud Computing by Queue Based Ant-Bee Algorithm. *Wirel. Pers. Commun.* **2019**, *104*, 173–197, doi:10.1007/s11277-018-6014-9.
153. Guney, K.; Babayigit, B. Amplitude-only pattern nulling of linear antenna arrays with the use of an immune algorithm. *Int. J. RF Microw. Comput. Eng.* **2008**, *18*, 397–409, doi:10.1002/mmce.20298.
154. Saeidian, B.; Mesgari, M.S.; Ghodousi, M. Evaluation and comparison of Genetic Algorithm and Bees Algorithm for location-allocation of earthquake relief centers. *Int. J. Disaster Risk Reduct.* **2016**, *15*, 94–107, doi:10.1016/j.ijdr.2016.01.002.
155. Liu, J.; Zhou, Z.; Pham, D.T.; Xu, W.; Ji, C.; Liu, Q. Robotic disassembly sequence planning using enhanced discrete bees algorithm in remanufacturing. *Int. J. Prod. Res.* **2018**, *56*, 3134–3151, doi:10.1080/00207543.2017.1412527.
156. Addeh, J.; Ebrahimzadeh, A. Breast Cancer Recognition Using a Novel Hybrid Intelligent Method. *J. Med. Signals Sens.* **2012**, *2*, 95–102, doi:10.4103/2228-7477.110446.
157. Pham, D.T.; Koç, E.; Lee, J.Y.; Phrueksanant, J. Using the bees algorithm to schedule jobs for a machine. *Laser Metrol. Mach. Perform. VIII - 8th Int. Conf. Exhib. Laser Metrol. Mach. Tool, C. Robot. Performance*,

LAMDAMAP 2007 **2007**, 430–439.

158. Phrueksanant, J. Machine Scheduling Using The Bees Algorithm. **2013**.
159. Pham, D.T.; Castellani, M.; Ghanbarzadeh, A. Preliminary design using the bees algorithm. *Laser Metrol. Mach. Perform. VIII - 8th Int. Conf. Exhib. Laser Metrol. Mach. Tool, C. Robot. Performance, LAMDAMAP 2007* **2007**, 420–429.
160. Moradi, S.; Razi, P.; Fatahi, L. On the application of bees algorithm to the problem of crack detection of beam-type structures. *Comput. Struct.* **2011**, *89*, 2169–2175, doi:10.1016/j.compstruc.2011.08.020.
161. Zheng, Z.; Xu, W.; Zhou, Z.; Pham, D.T.; Qu, Y.; Zhou, J. Dynamic Modeling of Manufacturing Capability for Robotic Disassembly in Remanufacturing. *Procedia Manuf.* **2017**, *10*, 15–25, doi:10.1016/j.promfg.2017.07.005.
162. Xu, W.; Zhou, Z.; Pham, D.T.; Liu, Q.; Ji, C.; Meng, W. Quality of service in manufacturing networks: A service framework and its implementation. *Int. J. Adv. Manuf. Technol.* **2012**, *63*, 1227–1237, doi:10.1007/s00170-012-3965-y.
163. Xu, W.; Tian, S.; Liu, Q.; Xie, Y.; Zhou, Z.; Pham, D.T. An improved discrete bees algorithm for correlation-aware service aggregation optimization in cloud manufacturing. *Int. J. Adv. Manuf. Technol.* **2016**, *84*, 17–28, doi:10.1007/s00170-015-7738-2.
164. Pham, D.T.; Castellani, M. A comparative study of the Bees Algorithm as a tool for function optimisation. *Cogent Eng.* **2015**, *2*, 1–28, doi:10.1080/23311916.2015.1091540.
165. Seeley, T.D. Honey bee foragers as sensory units of their colonies. *Behav. Ecol. Sociobiol.* **1994**, *34*, 51–62, doi:10.1007/s002650050018.
166. Gardner, K.E.; Seeley, T.D.; Calderone, N.W. Do honeybees have two discrete dances to advertise food sources? *Anim. Behav.* **2008**, *75*, 1291–1300, doi:10.1016/j.anbehav.2007.09.032.
167. Seeley, T.D.; Mikheyev, A.S.; Pagano, G.J. Dancing bees tune both duration and rate of waggle-run production in relation to nectar-source profitability. *J. Comp. Physiol. - A Sensory, Neural, Behav. Physiol.* **2000**, *186*, 813–819, doi:10.1007/s003590000134.
168. Gostimirović, M.; Rodić, D.; Kovač, P.; Jesić, D.; Kulundžic, N. Investigation of the Cutting Forces in Creep-Feed Surface Grinding Process. *J. Prod. Eng.* **2015**, *18*, 21–24.
169. Rowe, W.B. *Principles of modern grinding technology*; 2013; ISBN 9780323242714.
170. Marinescu, I.D.; Rowe, W.B.; Dimitrov, B.; Inasaki, I. *TRIBOLOGY OF ABRASIVE MACHINING PROCESSES*; 2005; ISBN 9780815519386.
171. Kalpakjian, S.; Schmid, S.R. *Manufacturing Processes for Engineering Materials - Solution Manual*. Prentice Hall **2008**, 1–281.
172. D'Addona, D.M.; Matarazzo, D.; De Aguiar, P.R.; Bianchi, E.C.; Martins, C.H.R. Neural Networks Tool Condition Monitoring in Single-point Dressing Operations. *Procedia CIRP* **2016**, *41*, 431–436, doi:10.1016/j.procir.2016.01.001.
173. D'Addona, D.M.; Teti, R. Image data processing via neural networks for tool wear prediction. *Procedia CIRP* **2013**, *12*, 252–257, doi:10.1016/j.procir.2013.09.044.
174. Daddona, D.M.; Conte, S.; Lopes, W.N.; De Aguiar, P.R.; Bianchi, E.C.; Teti, R. Tool Condition Monitoring of Single-point Dressing Operation by Digital Signal Processing of AE and AI. *Procedia CIRP* **2018**, *67*, 307–312, doi:10.1016/j.procir.2017.12.218.
175. Nakayama, K.; Takagi, J. ichiro; Irie, E.; Okuno, K. Sharpness Evaluation of Grinding Wheel Face by the Grinding of Steel Ball. *CIRP Ann. - Manuf. Technol.* **1980**, *29*, 227–231, doi:10.1016/S0007-8506(07)61327-4.
176. De Pellegrin, D. V.; Stachowiak, G.W. Sharpness of abrasive particles and surfaces. *Wear* **2004**, *256*, 614–622, doi:10.1016/j.wear.2003.10.004.
177. Daddona, D.M.; Conte, S.; Lopes, W.N.; De Aguiar, P.R.; Bianchi, E.C.; Teti, R. Tool Condition Monitoring of Single-point Dressing Operation by Digital Signal Processing of AE and AI. In *Proceedings of the Procedia CIRP*; 2018; Vol. 67.
178. Xu, S.; Chen, L. A novel approach for determining the optimal number of hidden layer neurons for FNN's and its application in data mining. *5th Int. Conf. Inf. Technol. Appl. ICITA 2008* **2008**, 683–686.
179. Teoh, E.; Tan, K.; Xiang, C. Estimating the Number of Hidden Neurons Singular Value Decomposition. *IEEE transactions neural networks* **2006**, *17*, 1623–1629.
180. Tetko, I. V.; Livingstone, D.J.; Luik, A.I. Neural Network Studies. 1. Comparison of Overfitting and Overtraining. *J. Chem. Inf. Comput. Sci.* **1995**, *35*, 826–833, doi:10.1021/ci00027a006.
181. Karsoliya, S. Approximating Number of Hidden layer neurons in Multiple Hidden Layer BPNN Architecture. *Int. J. Eng. Trends Technol.* **2012**, *3*, 714–717.
182. Wen Jin; Zhao Jia Li; Luo Si Wei; Han Zhen The improvements of BP neural network learning algorithm. **2002**, 1647–1649, doi:10.1109/icosp.2000.893417.
183. Barreto, J.M. Neural network learning: A new programming paradigm? *Proc. 1990 ACM SIGBDP Conf. Trends Dir. Expert Syst. SIGBDP 1990* **1990**, 434–446, doi:10.1145/97709.97740.
184. Bond, W.E.; St. Clair, D.C.; Amirfathi, M.M.; Merz, C.J.; Aylward, S. Neural network analysis of nondestructive evaluation patterns. *Appl. Comput. Technol. Challenges 1990's* **1992**, 643–650, doi:10.1145/130069.130071.
185. Nasereddin, M.; Mansoorreh, M. THE DEVELOPMENT OF A METHODOLOGY FOR THE USE OF NEURAL



NETWORKS AND SIMULATION MODELING IN SYSTEM DESIGN. *Proc. 1999 Winter Simul. Conf.* **1999**, 537–542, doi:10.5860/choice.41-2927.14.

186. Krittanawong, C.; Johnson, K.W.; Rosenson, R.S.; Wang, Z.; Aydar, M.; Baber, U.; Min, J.K.; Wilson Tang, W.H.; Halperin, J.L.; Narayan, S.M. Deep learning for cardiovascular medicine: A practical primer. *Eur. Heart J.* **2019**, *40*, 2058–2069C, doi:10.1093/eurheartj/ehz056.
187. Cawley, G.C.; Talbot, N.L.C. Efficient leave-one-out cross-validation of kernel fisher discriminant classifiers. *Pattern Recognit.* **2003**, *36*, 2585–2592, doi:10.1016/S0031-3203(03)00136-5.
188. Leisch, F. Error-Dependent Resampling for Artificial Neural Network Classifiers. **1997**, 1–13.
189. Junior, P.O.C.; Conte, S.; D’Addona, D.M.; Aguiar, P.R.; Baptista, F.G.; Bianchi, E.C.; Teti, R. Damage patterns recognition in dressing tools using PZT-based SHM and MLP networks. *Procedia CIRP* **2019**, *79*, 303–307, doi:10.1016/j.procir.2019.02.071.
190. Selva, P.; Cherrier, O.; Budinger, V.; Lachaud, F.; Morlier, J. Smart monitoring of aeronautical composites plates based on electromechanical impedance measurements and artificial neural networks. *Eng. Struct.* **2013**, *56*, 794–804, doi:10.1016/j.engstruct.2013.05.025.
191. Kim, J.; Wang, K.W. An enhanced impedance-based damage identification method using adaptive piezoelectric circuitry. *Smart Mater. Struct.* **2014**, *23*, doi:10.1088/0964-1726/23/9/095041.
192. Budoya, D.E.; Baptista, F.G. A Comparative Study of Impedance Measurement Techniques for Structural Health Monitoring Applications. *IEEE Trans. Instrum. Meas.* **2018**, *67*, 912–924, doi:10.1109/TIM.2018.2792854.
193. Na, W.S.; Baek, J. A review of the piezoelectric electromechanical impedance based structural health monitoring technique for engineering structures. *Sensors (Switzerland)* **2018**, *18*, doi:10.3390/s18051307.
194. Fan, S.; Zhao, S.; Qi, B.; Kong, Q. Damage evaluation of concrete column under impact load using a piezoelectric-based EMI technique. *Sensors (Switzerland)* **2018**, *18*, doi:10.3390/s18051591.
195. Baptista, F.G.; Filho, J.V.; Inman, D.J. Influence of excitation signal on impedance-based structural health monitoring. *J. Intell. Mater. Syst. Struct.* **2010**, *21*, 1409–1416, doi:10.1177/1045389X10385032.
196. Junior, P.O.; Conte, S.; D’Addona, D.M.; Aguiar, P.; Baptista, F. An improved impedance-based damage classification using self-organizing maps. *Procedia CIRP* **2020**, *88*, 330–334, doi:10.1016/j.procir.2020.05.057.
197. Liang, C.; Sun, F.P.; Rogers, C.A. Coupled Electro-Mechanical Analysis of Adaptive Material Systems — Determination of the Actuator Power Consumption and System Energy Transfer. *J. Intell. Mater. Syst. Struct.* **1994**, *5*, 12–20, doi:10.1177/1045389X9400500102.
198. Park, G.; Sohn, H.; Farrar, C.R.; Inman, D.J. Overview of piezoelectric impedance-based health monitoring and path forward. *Shock Vib. Dig.* **2003**, *35*, 451–463, doi:10.1177/05831024030356001.
199. He, C.; Yang, S.; Liu, Z.; Wu, B. Damage localization and quantification of truss structure based on electromechanical impedance technique and neural network. *Shock Vib.* **2014**, *2014*, doi:10.1155/2014/727404.
200. Da Conceição Junior, P.O.; Ferreira, F.I.; De Aguiar, P.R.; Batista, F.G.; Bianchi, E.C.; Daddona, D.M. Time-domain Analysis Based on the Electromechanical Impedance Method for Monitoring of the Dressing Operation. *Procedia CIRP* **2018**, *67*, 319–324, doi:10.1016/j.procir.2017.12.220.
201. Pears, D.M.; Inman, D.J.; Park, G. Circuit analysis of impedance-based health monitoring of beams using spectral elements. *Struct. Heal. Monit.* **2007**, *6*, 81–94, doi:10.1177/1475921707072621.
202. Fairweather, J.A.; Craig, K.C. Incorporating finite element techniques to simplify the impedance modeling of active structure. *5th Annu. Int. Symp. Smart Struct. Mater.* **1998**, *3323*, 602–613.
203. Min, J.; Park, S.; Yun, C.B. Impedance-based structural health monitoring using neural networks for autonomous frequency range selection. *Smart Mater. Struct.* **2010**, *19*, doi:10.1088/0964-1726/19/12/125011.
204. Junior, P.; D’addona, D.M.; Aguiar, P.R.; Teti, R. Dressing tool condition monitoring through impedance-based sensors: Part 1—pzt diaphragm transducer response and emi sensing technique. *Sensors (Switzerland)* **2018**, *18*, doi:10.3390/s18124455.
205. Junior, P.; D’Addona, D.M.; Aguiar, P.; Teti, R. Dressing tool condition monitoring through impedance-based sensors: Part 2—neural networks and K-nearest neighbor classifier approach. *Sensors (Switzerland)* **2018**, *18*, doi:10.3390/s18124453.
206. Na, S.; Lee, H.K. Neural network approach for damaged area location prediction of a composite plate using electromechanical impedance technique. *Compos. Sci. Technol.* **2013**, *88*, 62–68, doi:10.1016/j.compscitech.2013.08.019.
207. De Oliveira, M.A.; Inman, D.J. Simplified fuzzy ARTMAP network-based method for assessment of structural damage applied to composite structures. *J. Compos. Mater.* **2016**, *50*, 3501–3514, doi:10.1177/0021998315621964.
208. de Oliveira, M.A.; Monteiro, A. V.; Filho, J.V. A new structural health monitoring strategy based on PZT sensors and convolutional neural network. *Sensors (Switzerland)* **2018**, *18*, doi:10.3390/s18092955.
209. Marchi, M.; Baptista, F.G.; De Aguiar, P.R.; Bianchi, E.C. Grinding process monitoring based on electromechanical impedance measurements. *Meas. Sci. Technol.* **2015**, *26*, doi:10.1088/0957-0233/26/4/045601.
210. Conceição Junior, P.D.O.; Ruzzi, R.D.S.; Lopes, W.N.; Alexandre, F.A.; Baptista, F.G.; De Aguiar, P.R.; Bianchi, E.C. A New Approach For Dressing Operation Monitoring Using Voltage Signals Via Impedance-Based Structural Health Monitoring. *KnE Eng.* **2018**, *3*, 942, doi:10.18502/keg.v3i1.1514.

211. Martins, C.H.R.; Aguiar, P.R.; Frech, A.; Bianchi, E.C. Tool condition monitoring of single-point dresser using acoustic emission and neural networks models. *IEEE Trans. Instrum. Meas.* **2014**, *63*, 667–679, doi:10.1109/TIM.2013.2281576.
212. Baptista, F.G.; Vieira, J.F. A new impedance measurement system for PZT based structural health monitoring. *IEEE Trans. Instrum. Meas.* **2009**, *58*.
213. Baptista, F.G.; Budoya, D.; Almeida, V.A.D.; Ulson, J.A.C. An experimental study on the effect of temperature on piezoelectric sensors for impedance-based structural health monitoring. *Sensors* **2014**, *14*.
214. da Silveira, R.Z.M.; Campeiro, L.M.; Baptista, F.G. Performance of three transducer mounting methods in impedance-based structural health monitoring applications. *J. Intell. Mater. Syst. Struct.* **2017**, *28*, 2349–2362, doi:10.1177/1045389X17689942.
215. Sun, F.P.; Chaudhry, Z.; Liang, C.; Rogers, C.A. Truss Structure Integrity Identification Using PZT Sensor-Actuator. *J. Intell. Mater. Syst. Struct.* **1995**, *6*, 134–139, doi:10.1177/1045389X9500600117.
216. Franc, V.; Hlavac, V. Toolbox for Matlab Statistical Pattern Recognition. *Computer (Long. Beach. Calif.)*. **2004**, *48*, 1003–10.
217. Da Silva, A.C.M.E.; Garcez Castro, A.R.; Miranda, V. Transformer failure diagnosis by means of fuzzy rules extracted from Kohonen Self-Organizing Map. *Int. J. Electr. Power Energy Syst.* **2012**, *43*, 1034–1042, doi:10.1016/j.ijepes.2012.06.027.
218. Katunin, A.; Amarowicz, M.; Chrzanowski, P. Faults diagnosis using self-organizing maps: A case study on the DAMADICS Benchmark problem. *Proc. 2015 Fed. Conf. Comput. Sci. Inf. Syst. FedCSIS 2015* **2015**, *5*, 1673–1681, doi:10.15439/2015F26.
219. Kaski, S.; Lagus, K. Comparing Self-Organizing Maps.
220. Kordon, A.K. *Applying Computational Intelligence: How to Create Value*; Springer, 2010; Vol. 53; ISBN 9783540699132.
221. Kumar, A.; Chinnam, R.B.; Tseng, F. An HMM and polynomial regression based approach for remaining useful life and health state estimation of cutting tools. *Comput. Ind. Eng.* **2019**, *128*, 1008–1014, doi:10.1016/j.cie.2018.05.017.
222. Gaddafee, M.; Chinchani, S. An Experimental Investigation of Cutting Tool Reliability and its Prediction Using Weibull and Gamma Models: A Comparative Assessment. *Mater. Today Proc.* **2020**, *24*, 1478–1487, doi:10.1016/j.matpr.2020.04.467.
223. Sun, H.; Liu, Y.; Pan, J.; Zhang, J.; Ji, W. Enhancing cutting tool sustainability based on remaining useful life prediction. *J. Clean. Prod.* **2020**, *244*, doi:10.1016/j.jclepro.2019.118794.
224. Hopkins, C.; Hosseini, A. A Review of Developments in the Fields of the Design of Smart Cutting Tools, Wear Monitoring, and Sensor Innovation. *IFAC-PapersOnLine* **2019**, *52*, 352–357, doi:10.1016/j.ifacol.2019.10.056.
225. Liu, R.; Eaton, E.; Yu, M.; Kuang, J. An Investigation of Side Flow during Chip Formation in Orthogonal Cutting. *Procedia Manuf.* **2017**, *10*, 568–577, doi:10.1016/j.promfg.2017.07.053.
226. Mastrocinque, E.; Yuce, B.; Lambiase, A.; Packianather, M.S. A multi-objective optimization for supply chain network using the bees algorithm. *Int. J. Eng. Bus. Manag.* **2013**, *5*, 1–11, doi:10.5772/56754.
227. Moradi, A.; Mirzakhani Nafchi, A.; Ghanbarzadeh, A. Multi-objective optimization of truss structures using the bee algorithm. *Sci. Iran.* **2015**, *22*, 1789–1800.
228. Tsai, H.C. Integrating the artificial bee colony and bees algorithm to face constrained optimization problems. *Inf. Sci. (Ny)*. **2014**, *258*, 80–93, doi:10.1016/j.ins.2013.09.015.
229. Yuce, B.; Packianather, M.S.; Mastrocinque, E.; Pham, D.T.; Lambiase, A. Honey bees inspired optimization method: The bees algorithm. *Insects* **2013**, *4*, 646–662, doi:10.3390/insects4040646.
230. Thilagamani, S.; Shanthi, N.; Technology, K.S.R.C. Object Recognition Based on Image Segmentation and Clustering Department of Information Technology , M . Kumarasamy College of Engineering , Department of Information Technology ,. **2011**, *7*, 1741–1748.
231. D’Addona, D.M.; Conte, S.; Teti, R.; Marzocchella, A.; Raganati, F. Feasibility study of using microorganisms as lubricant component in cutting fluids. *Procedia CIRP* **2020**, *88*, 606–611, doi:10.1016/j.procir.2020.05.106.
232. Teti, R.; D’Addona, D.M.; Segreto, T. Microbial-based cutting fluids as bio-integration manufacturing solution for green and sustainable machining. *CIRP J. Manuf. Sci. Technol.* **2021**, *32*, 16–25, doi:10.1016/j.cirpj.2020.09.016.